INVESTIGATING THE DISTRIBUTION AND BIOSYNTHESIS OF MODIFIED F_{430} COFACTORS IN METHANOGENIC AND METHANOTROPHIC ARCHAEA

KALEB STORM BOSWINKLE

Thesis submitted to the faculty of the Virginia Polytechnic Institute and State University in partial fulfillment of the requirements for the degree of

Master of Science

In

Biochemistry

Kylie Allen, Chair

Biswarup Mukhopadhyay

Emily Mevers

May 3rd 2022

Blacksburg, VA

Keywords: methanogenesis, Archaea, radical SAM

Investigating the distribution and biosynthesis of modified F_{430} cofactors in methanogenicand methanotrophic archaea

Kaleb Boswinkle

ABSTRACT

Methanogenesis is the biological production of methane and is utilized by methanogenic archaea (methanogens) to generate energy. This process is responsible for 70% of total atmospheric methane, a potent greenhouse gas and an important energy source (natural gas). In the future, reversing methanogenesis in an engineered methanogenic strain could be realized to efficiently convert natural gas into liquid fuels.

Methyl coenzyme M reductase (Mcr) catalyzes the final reaction of methanogenesis in methanogens and the first reaction in the anaerobic oxidation of methane (AOM) carried out by the anaerobic methanotrophs (ANME). Cofactor F_{430}, a unique nickel-containing tetrapyrrole, serves as the prosthetic group and catalytic component of Mcr. Recently, multiple F_{430} variants have been discovered in several methanogenic species, including *Methanococcus maripaludis*, *Methanosarcina acetivorans*, and *Methanocaldococcus jannaschii*. A novel variant reported herehas an exact mass of 1008.3478, a similar absorption spectrum as unmodified F_{430}, and associates with purified Mcr from *M. acetivorans*. Based on the exact mass, this molecule is likely modified with a mercaptopropamide moiety. In some conditions, this modified F_{430} comprises 30-50% of the total F_{430} pool.

We also report upon our work to identify the sulfur insertion enzyme required to produce methylthio-F_{430} that functions with Mcr in ANME-1. We hypothesized that the insertion of the methylthio moiety is likely catalyzed by a methylthiotransferase (MTTase) homolog present in ANME. However, purified ANME MTTase does not appear to catalyze this reaction, and insteadcatalyzes the methylthiolation of N^6-threonylcarbamoyladenosine (t^6A) in tRNA.

Investigating the distribution and biosynthesis of modified F_{430} cofactors in methanogenic and methanotrophic archaea

Kaleb Boswinkle

GENERAL AUDIENCE ABSTRACT

Methanogens are a unique but diverse group of microorganisms that produce methane to generate their energetic needs. The byproduct of their metabolism is methane gas, most of which escapes into the atmosphere. Methanogens produce 70% of Earth's atmospheric methane, which is a gas that has contributed to 20% of global warming since the start of the industrial era. However, methane, which makes up the majority of natural gas, is also an important source of energy, and natural gas generates 40% of the United States' electricity. An issue with natural gas is, as a gas, it readily leaks out in the extraction and transport process. A solution to this is to convert the gas into liquids, which do not display these negatives. It is possible, through a better understanding of how methanogens work, we could produce a methanogen strain that can efficiently convert methane into liquid fuels.

The last methane-generating step in methanogenic metabolism uses a protein known as methyl-coenzyme M reductase (Mcr). To do this, Mcr uses a small molecule known as cofactor F_{430}. Recently, variants of the standard F_{430} structure have been described, in both methanogens as well as another microbial group known as the anaerobic methanotrophs (ANME). ANME generate their energy through reversing methanogenic metabolism. The work here involves studying why and how methanogens and ANME make F_{430} variants. The hope is this work will reveal either different functionalities of cofactor F_{430} not previously known, or that they influence Mcr catalysis, potentially in the reverse (methane degradation) direction.

Dedication

To my mom, Joan Boswinkle, and my dad, Bill Boswinkle, whose love and endless support have helped me at every step.

Acknowledgement

Dr. Kylie Allen has been an outstanding mentor. When I first joined her lab, I had no background in science, and she taught me the most basic skills, starting with pipetting and conducting literature reviews. She is ridiculously intelligent and always there to help guide me through my projects, but also patient and kind, and a constant source of inspiration. She has opened doors that I never knew existed, and I am proud to call her my mentor.

I would also like to thank my committee members, Dr. Mukhopadhyay, and Dr. Mevers for their helpful comments and edits, as well as future ideas. I am grateful for Christian Heryakusuma and Bela Khairunisa, two PhD members of Dr. Mukhopadhyay's lab, who provided us with methanogen pellets from organisms our lab does not have experience culturing. We hope to continue with Dr. Mukhopadhyay and his students in the future.

I would also like to thank the Virginia Tech Department of Biochemistry as a whole, and especially the great friends I have made, for their support. Spenser Stone, a fellow graduate student of Dr. Allen's lab, has been a kind friend. Ashylnn VanWinkle, Paul Kavanaugh, and Kayla Kester, also all fellow graduate students, have been great friends as well. Thank you!

Table of contents

Chapter I: Introduction

1.1 Methanogenic and methanotrophic archaea

A brief history and overview. Methanogenic archaea ("methanogens") are a group of obligate anaerobic Archaea that generate energy by performing methanogenesis, the reduction of simple carbon compounds to methane. Methanogenesis evolved at least 3.5 billion years ago, and has been handed down vertically since then, making it one of the oldest metabolisms on Earth.[1] Methanogenesis is found in eight orders of the Euryarchaeota phylum: *Methanococcales*, *Methanopyrales*, *Methanobacteriales*, *Methanomicrobiales*, *Methanocellales*, *Methanomassiliicoccales*, *Methanosarcinales,* and *Methanonatronarchaeales*.[2] More recently, the potential of methanogenesis has been described in the *Archaeoglobi* class of Euryarchaeota, as well as the *Bathyarchaeota* and *Verstraeteoarchaeota* phyla.[3,4] As the major contributor to atmospheric methane on Earth, methanogenesis has sculpted Earth's climate, natural history, and the carbon cycle for billions of years.[1]

In 1868, Béchamp was the first to demonstrate the ability of microbial life to synthesize methane.[5] However, isolating and characterizing the responsible agents proved to be challenging. Barker's lab pioneered early efforts that resulted in what was thought to be the first pure methanogenic culture, of *Methanobacillus omelianskii*, in 1940.[6] However, it was discovered two decades later this consisted of a mixed culture of two microorganisms, and the first true axenic culture was established in 1947.[7, 8] It took the foundational work of Hungate to develop robust and reproducible techniques to prepare anoxic media and for the anoxic and aseptic transfer of culture.[9, 10] These techniques were expanded in the laboratory of Ralph Wolfe to enable growth in pressurized atmospheres with tubes stoppered and crimped with aluminum seals.[11] The mastery of these techniques led to kilogram-scale growth of a methanogen for the first time in 1967.[12] This

was essential in enabling subsequent biochemical investigations, including investigation into the enzymes and coenzymes of methanogenesis.[13-16] By 1998, all of the enzymes involved in the reduction of CO_2 to methane had been characterized, but even today scientists still make exciting and fundamental discoveries regarding methanogenic enzymology.[17] Fortuitously, Wolfe's lab and that of a Carl Woese were founded in connected buildings, enabling a close relationship that led to the discovery of the archaeal domain of life. Specifically, the methanogenic cells Wolfe provided to Woese for 16S rRNA analyses led to the discovery that methanogenic "bacteria" were not, in fact, bacteria, and were in fact just as distantly related to eubacteria as eukaryotes.[18, 19]

Related to methanogens are the anaerobic methanotrophic archaea (ANME), organisms that are capable of oxidizing methane in the absence of oxygen using a reverse methanogenic pathway.[20] It was a curious observation in the 1960's that, despite their immense surface area and known methane production, net methane emissions from Earth's oceans are remarkably low.[21] Another early observation, in 1974, was that methane production does not occur in regions with significant sulfate reduction, but that methane production is active in regions of low sulfate reduction.[22] This "concave up" curve representing a steep rise in methane production in depths below the sulfate-reducing zone was the first evidence of methane oxidation under anoxic conditions. It was hypothesized that sulfate reduction and methanogenesis are mutually exclusive metabolisms.[22] However, it was later demonstrated that sulfate-reducing bacteria (SRB) and methanogens can co-exist, and are found in freshwater sediment with overlapping distribution.[23] Later, evidence in 1976 that methane consumption was active in the sulfate-reducing zone was described, and it was hypothesized that the methane produced by methanogens below the sulfate-reducing zone diffuses upwards, where SRB are able to oxidize the gas in a thermodynamically favorable net reaction.[24] However, it was shown later that SRB conduct rates of AOM of only

0.2% of the sulfate reduction rate.[25, 26] Thus, while it was shown SRB themselves cannot conduct AOM in isolation, a link between sulfate reduction with AOM was strongly supported by co-incidence of sulfate reduction and methane oxidation in marine sediments.[27] And, in 1980, radiotracer experiments with marine sediment cores unequivocally demonstrated AOM rates throughout the sulfate-reducing zone.[28] Therefore, there was strong evidence, collected from multiple decades, for AOM with a link to sulfate-reduction. However, biochemical studies probing the basic underlying mechanism proved difficult due to the inability to isolate one organism capable of AOM. In 1994, it was first postulated that AOM is performed by a syntrophic consortium of methanogens performing methanogenesis in reverse, supplying SRB with H_2 as an intermediate for sulfate reduction.[26] Finally, in 1999, through a combination of ^{13}C-depleted lipid analysis and 16S rRNA sequencing, the identity of an agent performing AOM was elucidated.[29] It was found that these are archaea phylogenetically distinct from known methanogenic orders, and thus were named ANME.[29] It was postulated that the most likely scenario is that ANME are obligate methanotrophs.[29] Lipid analysis showed that SRB also contain ^{13}C-depleted fatty acids, possible only by the transfer of carbon between ANME and SRB, evincing a close relationship between these partner cells.[30] Presumably, direct contact between cells mediated the transfer of intermediates. This close relationship between ANME and specific SRB was further corroborated by fluorescent *in-situ* hybridization experiments with organism-specific 16S rRNA probes.[30, 31] The hypothesis of AOM as reverse methanogenesis was supported by subsequent metagenomic studies in the following five years after the discovery of ANME.[32, 33] During AOM, ANME carry out the oxidation reactions and reducing equivalents generated throughout methane oxidation to CO_2 are transferred to SRB for use in sulfate reduction.[34, 35]

Importance of studying methanogenesis and AOM. There are three major reasons to study methanogenesis and AOM: (a) methanogenesis has been extant on Earth for at least 3.5 billion years, and its study provides an exciting window into ancient life that has informed the study of life on exoplanets; (b) methanogens are the primary methane-producers on Earth, an abundant and terrifically potent greenhouse gas; and (c) methane, as the main component of natural gas, is an increasingly vital fuel source.

Methanogenesis and AOM play critical roles in Earth's carbon cycle. The former is the last step in the anaerobic decomposition of organic matter in sulfate-, nitrate-, Mn(IV)- and Fe(III)-poor environments and is responsible for 74% of total atmospheric methane.[36, 37] In contrast, AOM, consumes an estimated 90% of the 85-300 Tg of methane released in marine sediments annually.[38] Thus, AOM is an important process mitigating methane emissions from oceans. More recently, AOM has been ascribed to constraining methane emissions in freshwater wetlands.[39, 40] And, as the ecology of AOM and alkane oxidation is a rapidly developing field, we likely currently greatly underestimate the importance of AOM in the carbon, sulfate, and metal cycles.

Methanogens are found in virtually every anaerobic environment in which organic matter is decayed. This includes natural environments such as wetlands, glacial ice, hydrothermal vents, oceans, the GI tract of animals, and anthropogenic environments such as the rumen of livestock, rice fields, landfills, and sewage systems.[40, 41] Methanogenesis is necessary to keep other anaerobic metabolisms energetically favorable by removing their products. The net production of methane by methanogenesis is an estimated 1,000 Tg annually, or roughly 2% of the net CO_2 fixed by photosynthesis into biomass.[36] Methanogenesis results in the eventual recycling of organic carbon, since the released methane is either oxidized to CO_2 enzymatically by ANME or aerobic methanotrophs, or abiotically in the atmosphere via reactions with hydroxyl radicals, where it can

be fixed back into organic compounds.[42] However, methane is also an extraordinarily potent greenhouse gas, and is second only to carbon dioxide in driving global warming. Alarmingly, methane surface concentrations have increased from 772 ppb in 1750 ("pre-industrial") to 1886 ppb in 2019.[43] Global temperatures rose faster from 1970 to 2020 than in any other 50-year period over at least the last 2000 years.[43] While methane has a short lifetime of only about 9 years, and is far less abundant than carbon dioxide (1.87 ppm compared to 410 ppm), it contributed a radiative forcing of 0.97 W m^{-2} against carbon dioxide's 1.68 W m^{-2} since 1750 (total forcing since 1750 is 2.29 W m^{-2}).[44, 45] Thus, relative to CO_2, methane contributes roughly 60% radiative forcing while present in concentrations less than 1% relative to CO_2. Therefore, it will be of the utmost importance to limit methane emissions to combat global warming; however, an unfortunate fact is as temperatures rise and precipitation increases due to global warming, methane emissions from methanogenesis, for example from wetlands and tundra, will only increase, contributing to a deadly feedback loop.[46, 47] Due to its short life-span and high warming potential, control over methane presents an opportunity to slow global warming quickly.

Methane is the main component of natural gas, an important source of energy that in 2020 in the US generated more electricity than any other energy source, and encompasses 34% of all primary energy (second only to petroleum).[48, 49] This has been fueled by advances in horizontal drilling technology over just the past few decades, resulting in an explosion in shale gas (gas trapped in tight rock formations) extraction.[50] Shale gas accounted for just 1.6% of natural gas production in the United States, but 40.4% by 2013 and 79% in 2021.[51, 52] Shale gas may drive global demand for natural gas up 50% by 2035 relative to 2010 levels.[53] Further, methane hydrates, produced both biotically by methanogens and abiotically, are one of Earth's largest reservoirs of methane and remain a largely untapped resource.[54] Methane is attractive mainly due to its low cost

of extraction and great abundance, but its combustion is also cleaner relative to other fossil fuels, producing 40-45% less CO_2 and 25-30% less than oil.[55] However, methane is a potent greenhouse gas and tiny leaks into the atmosphere in extraction and transport negate this benefit. It was estimated in 2015 that in the US, accidental leakage of methane in the domestic production, processing, and transport of oil and natural gas is about 13 Tg methane per year.[56] This figure results in radiative forcing comparable to natural gas combustion over a 20-year period.[56] Therefore, strategies to mitigate methane leaks must be expanded upon. One such strategy currently employed is gas-to-liquid technology to convert gases to liquids fuels that do not present leak concerns. The chemical Fisher-Tropsch process, in which methane can be used as a feedstock, has been implemented for this purpose for decades, but is limited in practice due to its exorbitant multi-billion dollar capital cost and the requirement of large plants with complex machinery.[57] Therefore, this process is not amenable for most of the *ca.* 500,000 current gas-producing wells in the US.[58] A biological alternative, such as using a methanogenic strain capable of converting methane to liquid fuels such as methanol could be an attractive alternative. While trace methane oxidation has been observed in several methanogens, engineering a strain capable of efficiently oxidizing methane into specific liquid fuels will require further understanding and mastery over methanogenesis and AOM.[59] As a proof-of-concept, one methanogen, *Methanosarcina acetivorans*, has been engineered to be capable of oxidizing about 9% of methane provided over a six-week period into acetate.[60] *M. acetivorans* also has potential for metabolic engineering, and has been engineered to produce lactate, as well as electricity through reversing methanogenesis.[61] In addition to these applications, methanogenesis can be harnessed in bioreactors for the digestion of organic waste to generate methane, transforming waste to an energy source.[62]

Methanogenic metabolism. Four major methanogenic pathways exist: hydrogenotrophic, acetotrophic, methylotrophic, and methyl reduction. The central methanogenic pathway is the 7-step reduction of carbon dioxide to methane with electrons supplied by H_2 or formate (Figure 1.1).[63] This "hydrogenotrophic" pathway is the most widespread and likely primordial methanogenic pathway, present in all known methanogenic orders with the exception of the more recently described *Methanomassiliicoccales, Methanonatronarchaeales* and *Ca.* Methanofastidiosa.[64, 65] Further, this metabolism has recently been ascribed through metagenomics to a non-Euryarchaeote for the first time: *Ca.* Methanohydrogenales of the *Verstraetearchaeota*.[3] In hydrogenotrophic methanogenesis, CO_2 is reduced to methane using electrons usually derived from H_2. First, CO_2 is reduced to a formyl group by formylmethanofuran dehydrogenase (FwdA-DFHG or FwdA/FmdBCE) through reaction with a reduced ferredoxin to generate formyl-methanofuran.[66] The reduction of ferredoxin with hydrogen is endergonic, and the strategies methanogens use to produce reduced ferredoxin are discussed below. A common reductant that serves as an alternative to H_2 is formate.[67] Formate is oxidized to carbon dioxide by formate dehydrogenase and this is coupled to the reduction of cofactor F_{420}.[67] In this case, formate is used both as the source of reducing equivalents and carbon source for methanogenesis.[67] Other known possible electron sources for

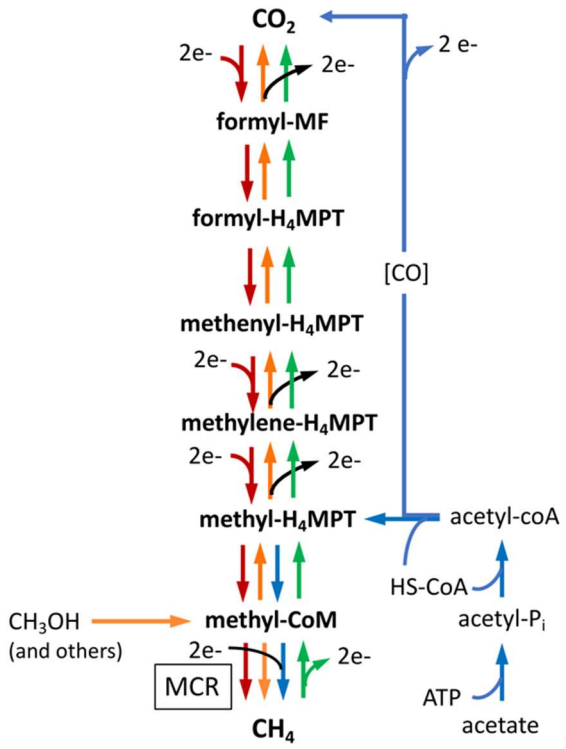

Figure 1.1. Methanogenic and methanotrophic pathways. Hydrogenotrophic (red), methylotrophic (yellow), acetotrophic (blue), and AOM (green).

methanogenesis include CO, ethanol, and secondary alcohols.[68] In any case, the formyl group of formyl-methanofuran is transferred to tetrahydromethanopterin (H_4MPT) or tetrahydrosarcinapterin (H_4SPT) by formylmethanofuran:H_4MPT formyltransferase (Ftr), and is subsequently converted to a methenyl group by methenyl-H_4MPT cyclohydrolase (Mch).[63] Methenyl-H_4MPT is subsequently reduced to the methylene then methyl level by, respectively, methylene-H_4MPT dehydrogenase (Mtd) and methylene-H_4MPT reductase (Mer).[63] Both reduction steps are coupled to $F_{420}H_2$ oxidation, produced from the F_{420}-reducing hydrogenase (FrhAGB) in all methanogens on growth with H_2. However, since formate oxidation directly produces $F_{420}H_2$, bypassing the need for hydrogenases, hydrogenases are not essential for growth on formate.[67] The methyl group of methyl-H_4MPT is subsequently transferred to coenzyme M by N^5-methyl-tetrahydromethanopterin:coenzyme M methyltransferase (MtrA-H), an exergonic reaction coupled to the translocation of Na^+ ions across the plasma membrane.[69] The sodium-ion-motive force is used to power the phosphorylation of ADP via an A_1A_0-ATP synthase.[70] Finally, methyl-coenzyme M (CH_3-S-CoM) is reduced to methane by methyl-coenzyme M reductase (Mcr or Mrt) to methane with coenzyme B (HS-CoB), generating the mixed heterodisulfide CoM-S-S-CoB.[71] The exergonic reduction of the heterodisulfide product is linked to flavin-based electron bifurcation in methanogens that lack an electron transport chain.[72] Electrons derived from H_2 (from the Vhu or Mvh hydrogenase) or formate (from formate dehydrogenase) are bifurcated to the heterodisulfide and to oxidized ferredoxin, concomitantly regenerating HS-CoB, HS-CoM, and reduced ferredoxin that then reduces CO_2 to the formyl level. Thus, here, the first and last steps of the process are directly linked.[72] Members of the *Methanosarcinales*, which contain a membrane-soluble electron carrier, methanophenazine, a membrane-bound heterodisulfide reductase

(HdrDE), instead reduce the heterodisulfide with electrons derived from H_2 oxidation by the Vht hydrogenase using methanophenazine as electron carrier.[73]

The acetotrophic pathway is limited to the cytochrome- and methanophenazine- containing *Methanosarcina* and *Methanothrix* within the *Methanosarcinales*.[74] Here, acetate must first be transported into the cell, and this is facilitated by the AceP transporter.[75] Then, acetate must be activated to acetyl-CoA, a step that differs between *Methanosarcina* and *Methanothrix*. In *Methanosarcina*, acetate is first activated to acetyl-CoA with ATP and CoA by acetate kinase (AckA) and phosphate transacetylase (Pta).[76] These genes were laterally acquired from bacteria in a single horizontal gene transfer event.[77] In contrast, acetyl-CoA is produced in one step in *Methanothrix* with the action of acetyl-CoA synthetase (ACS) with ATP and CoA, necessitating two high-energy phosphate bonds to generate AMP.[76] Overall, acetoclastic methanogenesis is the most energetically unfavorable form of methanogenesis, and the single-step ACS-catalyzed reaction is more costly than the two-step AckA/Pta pathway. The more efficient AckA/Pta pathway is much younger relative to methanogenesis as a whole, evolving around 240 million years ago.[77, 78] Despite its phylogenetic limitation, this process mediates the production of two-thirds of total methane generated from methanogenesis, and its evolution perturbed the natural world to the extent that it abetted one of Earth's greatest extinction events.[78, 79] Acetyl-CoA is cleaved by the 2.4 MDa five-subunit $(\alpha_2\varepsilon_2)_4\beta_8(\gamma\delta)_8$ acetyl-CoA decarbonylase/synthase (CdhABCDE) complex into a methyl group, a carbonyl group, and CoA.[80, 81] The overall reaction, which is reversible, of acetyl-CoA cleavage and synthesis can be separated into three partial reactions: (1) acetyl-CoA cleavage to enzyme-bound CO and CH_3 groups, and a HS-CoA, (2) methyl transfer to H_4SPT, and (3) CO oxidation to CO_2 coupled to ferredoxin reduction.[80] The A cluster, found at the β subunit, consists of a [4Fe-4S] cluster and 2 Ni atoms bridged via cysteine

sulfurs, cleaves the C-S bond of acetyl-CoA to generate an enzyme-bound acetyl moiety.[81] The A cluster is also the site of C-C bond cleavage.[82] The methyl group is accepted by the γδ complex which catalyzes the transfer of the methyl group to H_4SPT.[83] This is accomplished with a corrinoid-[4Fe-4S] cluster, with the corrinoid known as factor III (Coα-[α-(5-hydroxybenzimidazolyl)]-cobamide).[84] Finally, the CO dehydrogenase activity is facilitated by the $\alpha_2\varepsilon_2$ complex, which contains nine [4Fe-4S] clusters, including one Ni-[4Fe-4S] "C" cluster that binds CO and mediates oxidation to CO_2.[80] The Fe-S clusters facilitate the transfer of electrons to a ferredoxin.[80, 85] Oxidation of the reduced ferredoxin is coupled to H^+ reduction to generate H_2 by the Ech hydrogenase, and the Vht hydrogenase oxidizes H_2 to reduce the membrane-soluble electron carrier methanophenazine. The next steps are similar to the ones described for hydrogenotrophic methanogenesis. The Mtr complex catalyzes the transfer of the methyl group from CH_3-H_4SPT to generate methyl-CoM, and Mcr catalyzed the reduction of the methyl to methane with CoB-SH. The mixed heterodisulfide that is generated is reduced using the membrane-bound HdrDE and methanophenazine.

Methanogens can also reduce the methyl group of methylated compounds to methane by either methyl group disproportionation ("methylotrophic") or in a H_2-dependent pathway ("methyl reduction"). The former is restricted to non-*Methanothrix Methanosarcinales* spp., while the latter has been described in *Methanosphaera*, the recently described *Methanomassiliicoccales*, *Methanonatronarchaeales*, *Ca.* Methanofastidiosa and *Bathyarchaeota* and *Verstraetearcheota* phyla, as well as one species from *Methanosarcinales* orders.[65, 86-89] Methylotrophy is found in sulfate-rich environments, and dominant in hypersaline environments, in which hydrogenotrophic and acetotrophic methanogens are outcompeted for their substrates by sulfate-reducers.[90] In hypersaline environments methylamines, derived from the ubiquitous glycine betaine compatible

solute, are a noncompetitive growth substrate.[90] In both types of methylotrophy, the methyl group of methyl-containing compounds, including methylamines, methylsulfides, methanethiol, methyl alcohol, and tetramethylammonium, is activated to CH_3-S-CoM by specific methyltransferases.[91] This process utilizes two methyltransferases: MT1 and MT2.[91] MT1 consists of a methyltransferase subunit specific for the methylated compound (e.g. MtaB for methanol) that transfers the methyl to a cognate corrinoid protein (e.g. MtaC for methanol) subunit.[91] The methyl is subsequently transferred to MT2, which then transfers the methyl to HS-CoM.[91] Thus, the ability to use specific methylated compounds is restricted based on the methyltransferases ability. For example, *Ca.* Methanofastidiosa lacks methyltransferases for methanol and methylamines, and likely can only utilize methylated thiols as methyl donor.[86] Reductive demethylation of methyl-S-CoM with HS-CoB by Mcr is identical to that already described, and therefore generates the disulfide of CoM-CoB that must be reduced for continued methanogenesis. In methylotrophic methanogenesis, reduced F_{420} and reduced ferredoxin are obtained by oxidizing one methyl-CoM to CO_2 via reversing the central methanogenesis pathway. Reduced F_{420} ($F_{420}H_2$) is generated in the Mer and Mtd-catalyzed oxidation of methyl-H_4SPT and methylene-H_4SPT, respectively, while reduced Fd is obtained in the formylmethanofuran-catalyzed oxidation of formyl-MF to CO_2. Like in other pathways, the transfer of electrons to the heterodisulfide complex in methylotrophic methanogens is dependent on the presence or absence of hydrogenases. In methanogens containing hydrogenases, the reducing equivalents are used to generate H_2 inside the cell by F_{420}-reducing hydrogenase (Frh) and Ech hydrogenase. This hydrogen diffuses to the extracellular side of the plasma membrane to the membrane-bound Vht hydrogenase, which couples H_2 oxidation to methanophenazine reduction. Reduced methanophenazine then is used by the heterodisulfide reductase complex to reduce the CoM-CoB disulfide. In hydrogenase lacking methanogens,

reduced Fd transfers electrons to MP via the Rnf complex in an identical fashion described above, and the F_{420} dehydrogenase (Fpo) transfers electrons to methanophenazine from $F_{420}H_2$. In contrast, in the methyl reduction pathway, electrons that for CH_3-H_4SPT are acquired through the oxidation of methane. This pathway can be employed by hydrogenase-containing *Methanosarcinales*, but, curiously, the more recently methanogenic orders are obligately methyl reducers. These methanogens lack the genetic capacity for oxidative methanogenesis from CH_3-H_4SPT, and therefore require an external electron donor, typically hydrogen.[92] While recently discovered, this form of methanogenesis can be widely distributed. For example, the *Methanomassiliicoccales* order, inhabits the GI tract of animals, rice paddy fields, wetlands, and marine and freshwater sediments.[93]

Anaerobic methanotrophic metabolism. After the discovery of AOM conducted by archaea related to methanogens coupled to sulfate reduction by SRB ("S-AOM"), the biochemistry, ecology, and phylogeny of AOM and ANME began to be investigated. Phylogenetically, ANME is a paraphyletic group composed of three known clades within the Methanomicrobia: ANME-1, ANME-2, and ANME-3.[29, 94] Recently, these clades were assigned taxonomic groups: ANME-1 consists of the *Methanophagales* order, while ANME-2 and ANME-3 are found within the *Methanosarcinales*.[20] ANME-2 consists of the *Methanogasteraceae*, *Methanocomedenaceae*, and *Methanoperedenaceae*.[20] ANME-3 is a genus, *Methanovorans*, within the *Methanosarcinaceae*.[20] An early hypothesis was that AOM is the reversal of methanogenesis with SRB acting as hydrogen scavengers.[30] The difficulty in culturing ANME and the inability to isolate pure cultures has slowed the biochemical characterization of these organisms. However, the hypothesis that AOM is methanogenesis in reverse has been firmly established through metagenomic, metatranscriptomic, and metaproteomic from environmental samples and bioreactor experiments,

as well as *in vitro* experiments.[95] The first published partial genome of an ANME, in 2010, included the complete set of seven central genes for methanogenesis, with the exception of *mer*, and also found that these were expressed.[95] Mer, methylene-H_4MPT reductase, would catalyze the oxidation of CH_3-H_4MPT to CH_2=H_4MPT. ANME-1 express methylene-tetrahydrofolate reductase (MetF), and it has been proposed this could replace the loss of Mer.[96] Subsequent genomic investigations have established that, excluding ANME-1 lacking Mer, ANME encode and express the seven enzymes.[20, 97] However, the mechanics of transferring electrons from one cell-type (ANME) to another (SRB) has been in debate since the discovery of ANME. The initial hypothesis that ANME could produce diffusible electron carriers, such as hydrogen, formate, or acetate, that are subsequently oxidized by sulfate-reducing partner bacteria, did not reconcile with experimental microcosm experiments.[98] Another proposal that ANME-2 couples AOM with sulfate reduction to zero-valent sulfur, that then is disproportioned by SRB that been firmly rejected on multiple bases.[99] In the Euryarchaeota, only the distantly related *Archaeoglobus* have the genetic capacity for dissimilatory sulfate reduction.[100] Some ANME have the genomic potential to assimilate sulfate, thiosulfate, and/or sulfite, but do not have the genetic capacity to conduct dissimilatory sulfate reduction.[101] Instead, electrons from the complete oxidation of methane to CO_2 through a reversal of the central methanogenic pathway are passed directly to partner bacteria through extracellular electron transfer.[97, 102, 103] To facilitate electron transfer, ANME-1, ANME-2, and their respective deltaproteobacterial partners express large extracellular multiheme cytochromes and pili that, in at least the case of ANME-1 partner bacteria, resemble conductive nanowires.[103-105] Further, while S-AOM is the best-studied form of AOM, it has been shown that members of the *Methanoperedenaceae* can couple methane oxidation with the reduction of nitrate, as well as the metals Fe(III) and Mn(IV), and different species have specific

metal preferences.[106-108] In the case of nitrate reduction, *Ca.* Methanoperedens nitroreducens acquired a membrane-bound nitrate reductase through a lateral gene transfer event from bacteria.[108] The reduction of metals takes place, as in *Geobacter* and *Shewenella*, extracellularly, and, like S-AOM, is facilitated by an electron transport chain and extracellular multiheme cytochromes *c*.[104] For example, in Mn(IV) reduction coupled to AOM, as performed by *Ca.* Methanoperedens manganicus and *Ca.* M. manganiredcens, electrons from the regeneration of CoM-S-S-CoB are passed to menaquinone *via* the HdrDE complex, and from CH_3-H_4MPT and CH_2-H_4MPT oxidation *via* the Fpo complex with electrons donated from $F_{420}H_2$.[106] Electrons from reduced menaquinone are passed to extracellular multiheme *c*-type cytochromes for the reduction of Mn(IV) to Mn(II).[106]

1.2 Overview of Mcr and cofactor F_{430}

Methyl-coenzyme M reductase and cofactor F_{430}. The work described in Chapter 2 of this thesis is focused on methyl-coenzyme M reductase (Mcr), the enzyme that catalyzes the final step of methanogenesis in all methanogenic pathways and the initial step in AOM (Figure 1.1). Structurally, the enzyme is a dimer of heterotrimers with an $\alpha_2\beta_2\gamma_2$ configuration containing two active sites, each with one molecule of F_{430} (Figure 1.2).[109] Cofactor F_{430} was first discovered in 1978 and named for its absorption maximum.[110] It was

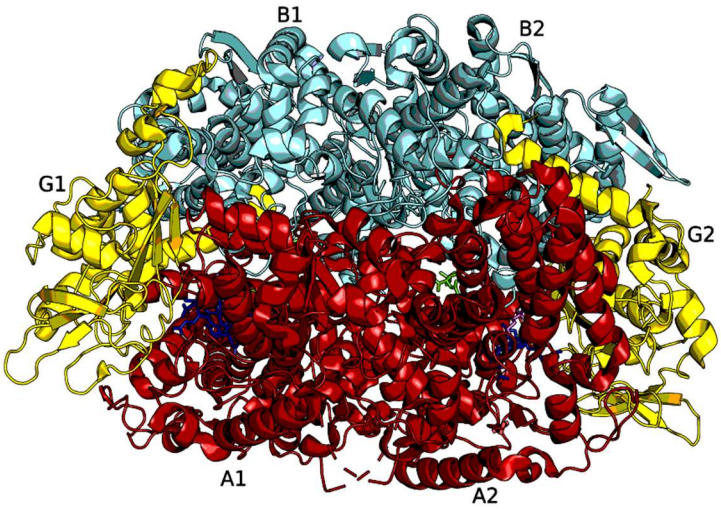

Figure 1.2. The overall structure of Mcr. The α subunits (A1 and A2) are shown in red, the β subunits (B1 and B2) in cyan, and the γ subunits (G1 and G2) in yellow. Cofactor F_{430} can be seen in blue. See Figure 1.4 for a more complete view of the active site.

quickly shown that nickel is required for methanogenic growth and is essential for the biosynthesis of F_{430}.[111, 112] Soon after this, F_{430} was shown to be the prosthetic group of Mcr.[16] The structure and previous experiments demonstrated that F_{430} is a macrocyclic tetrapyrrole, and like other tetrapyrroles, its biosynthesis proceeds from the common intermediates 5-aminolaevulinic acid (5-ALA) and uroporphyrinogen III, the latter being the last common precursor to all tetrapyrroles.[113] Evidence also suggested that dihydrosirochlorin (precorrin 2) is an intermediate in F_{430} biosynthesis, and it was shown that 15,17^3-seco-F_{430}-17^3-acid is the immediate precursor to F_{430}.[114] The structure and stereochemistry was elucidated completely by 1991.[115] It was demonstrated that F_{430} is the most reduced tetrapyrrole, and contains two rings not found in other tetrapyrroles: the γ-lactam E ring, and the carbocyclic F ring. Despite this, the puzzle of F_{430} biosynthesis from precorrin 2 was only unraveled and the enzymes catalyzing its steps elucidated in 2016 (Figure 1.3).[116] The biosynthesis of F_{430} branches from siroheme biosynthesis not from precorrin 2, but from sirohydrochlorin, the precursor to which is precorrin 2. Analogous to siroheme biosynthesis, sirohydrochlorin is the substrate for a chelatase, but in this case a nickel chelatase (CfbA). Next, a glutamine aminotransferase (CfbB) homologous to that found in cobalamin biosynthesis, catalyzes the amidation of the *a*- and *c*- propionic acid side chains. CfbCD then catalyzes

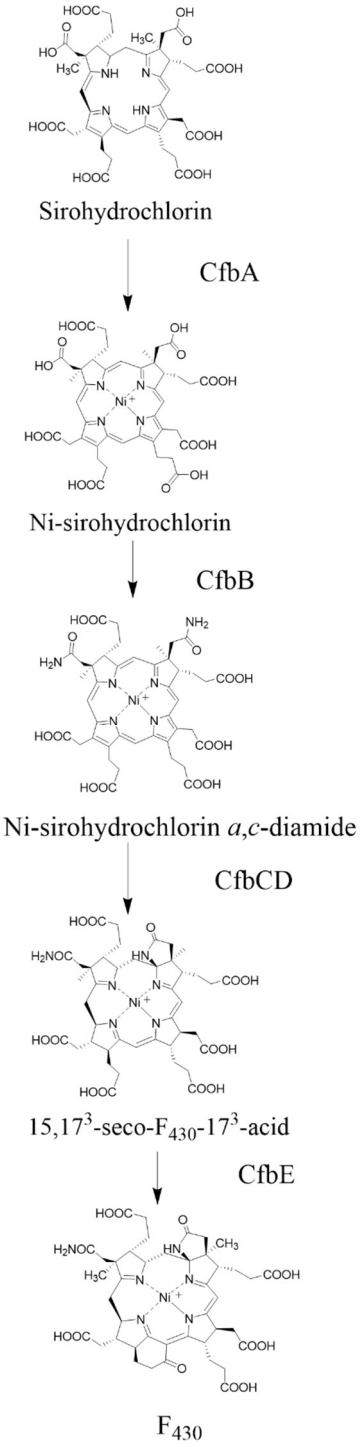

Figure 1.3. F_{430} biosynthesis from sirohydrochlorin.[114]

both the 6 electron reduction of the porphyrin ring system of Ni-sirohydrochlorin *a*,*c*-diamide as well as the cyclization of the *c*-propionic acid chain to give the γ-lactam ring. The final reaction, catalyzed by CfbE, is the cyclization of the *g*-propionate side chain to give the carbocyclic F ring.[116] Both methanogens and ANME contain CfbA-E, however, only in some of these organisms are they expressed as an operon.[116]

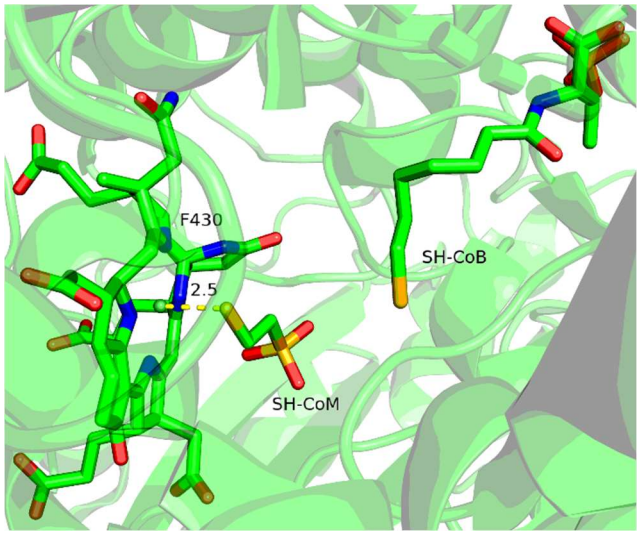

Figure 1.4. The active site of Mcr. Here, carbon atoms are shown in green, oxygen in red, nitrogen in blue, and sulfur in yellow. The thiol sulfur of SH-CoM is positioned directly above the Ni of F_{430}, and SH-CoB sits nearby.

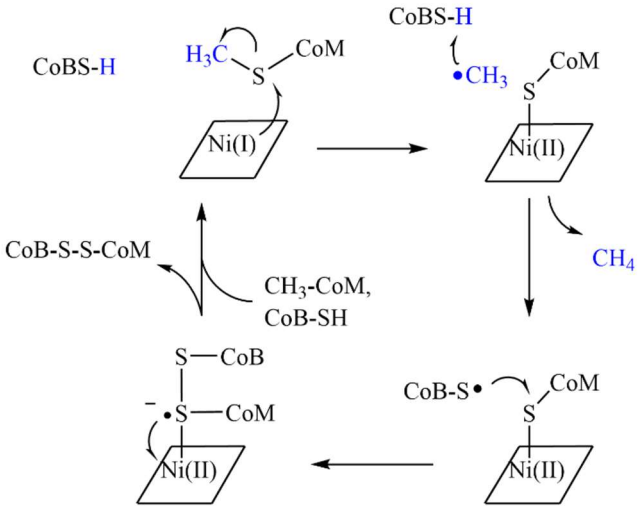

Figure 1.5. The most likely mechanism of Mcr-catalyzed reductive demethylation of CH_3-S-CoM with HS-CoB. Only the Ni atom of cofactor F_{430} is shown.

Cofactor F_{430} has only one known function in nature, the prosthetic group of Mcr.[117] It binds tightly, although not covalently to Mcr.[117] The two active sites of each fully assembled Mcr are found deeply buried in 50 Å channels and the two F_{430} molecules in the active sites are 51 Å apart. Methyl-S-CoM can diffuse into the active site via the 50 Å channel where it finds F_{430} and positions its thioether sulfur directly above the nickel atom of F_{430}.[117] Functionally, F_{430} is the catalytic component of the enzyme. It was understood early on that the nickel atom of cofactor F_{430} must be in the Ni(I) state for enzyme activity, but several mechanisms have been proposed for the reaction.[118] The difficulty in proving conclusively the

mechanism have been due to inability of isolating intermediates. A recent study combined experimental and computational evidence to show that, most likely, the mechanism of Mcr involves the Ni(I) atom of cofactor F_{430} attacking the sulfur atom of methyl-CoM, forming two intermediates: a methyl radical and a Ni(II)-thiolate (Figure 1.5).[71] The methyl radical then abstracts the hydrogen atom of CoB-SH to generate methane and CoB-S•. The radical attacks the sulfur atom of Ni(II)-S-CoM to form a Ni(II)-S-CoM-S-CoB radical anionic disulfide. This goes on to donate an electron to Ni(II), leaving as CoB-S-S-CoB and reducing the Ni atom back to Ni(I), ready to perform another cycle. It has been shown that the product of an additional gene that is found in the *mcr* operon, *mcrC*, of some methanogens and ANME, is involved in a complex that reduces the Ni of F_{430} to the active Ni(I) redox state.[119] Further, another gene product encoded in the operon, *mcrD*, which is expressed conservatively before *mcrA*, is likely a chaperone that delivers F_{430} to Mcr.[116, 120] However, notably, many ANME lack McrC and/or McrD, and these organisms must either have a different system for reducing and/or delivering F_{430} to Mcr, or are not essential for these activities.

Despite only one function known for F_{430}, variants of the standard cofactor have been discovered in methanogens, ANME-1, as well as an ethane oxidizing archaeon.[121-123] ANME-1 contain a version of cofactor F_{430} with the addition of a methylthio group at the 17^2 position and is known as methylthio-F_{430} (Figure 1.6). This variant was initially discovered in cofactor extracts from Black Sea microbial mats, where it was known AOM takes place.[122] The exact mass and structure of methylthio-F_{430} was determined through mass spectrometry and NMR spectroscopy. It was later discovered in the first and only crystal structure of an ANME Mcr.[124] Therefore, it is considered to be the dominant F_{430} utilized by ANME-1. However, ANME-1 also has unmodified cofactor F_{430}, and this is likely the precursor to methylthio-F_{430}.[122] One hypothesized function of

the methylthio moiety is that it participates in an electron relay system involved in ensuring the Ni of F_{430} stays in its reduced, active state.[124] This hypothesis arose from the finding that the methylthio modification exists in the context of a "cysteine rich" patch, consisting of five cystine residues unique to ANME-1 Mcr.[124] Methylthio-F_{430} has not been found in ANME-2 cell extracts, and ANME-2 Mcr does not have the cysteine-rich patch of ANME-1 Mcr.[122, 124] Further, ANME-2 Mcr has the more bulky 2-methylglutamine found in methanogen Mcr structures that would clash sterically with the methylthio group of the modified F_{430}.[124] ANME-1 Mcr replaces this with the far smaller valine.[124]

Since the discovery of methylthio-F_{430}, there has been a discovery of multiple F_{430} variants that are found in methanogens, but not ANME.[121] The most abundant of these was found to be mercaptopropionate-F_{430} (Figure 1.6).[121] The structure has not yet been validated by NMR, but based on its exact mass of 1009.278 Da (104 Da more massive than F_{430}) and its UV-Vis absorbance spectrum, the proposed structure has a cyclic mercaptopropionate, with the thioether in the same position of that of methylthio-F_{430}. This variant was discovered in cell extracts from *M. maripaludis*, as well as the related *Methanocaldococcus jannaschii*.[121] A purified fraction of Mcr was found to only contain unmodified F_{430}, and so it is possible that it does not associate at all with Mcr. Another abundant variant, found in *M. maripaludis*, *Methanococcus vannielli*, as well as ANME-2 cell extracts, contains a vinyl group substituting a propionic acid sidechain.[121] Most recently, another F_{430} variant containing two methyl substitutions, one in the same position as the methylthio group in methylthio-F_{430} has been found in the crystal structure of an MCR from an archaeon that performs ethane oxidation (Figure 1.6).[123] Anaerobic ethanotrophs oxidize ethane completely to CO_2, likely in an analogous pathway to reverse methanogenesis, including the use

of Mcr.[123] However, these organisms are specialized for ethane oxidation, the second most abundant hydrocarbon in the ocean, and are not able to activate other alkanes.[123]

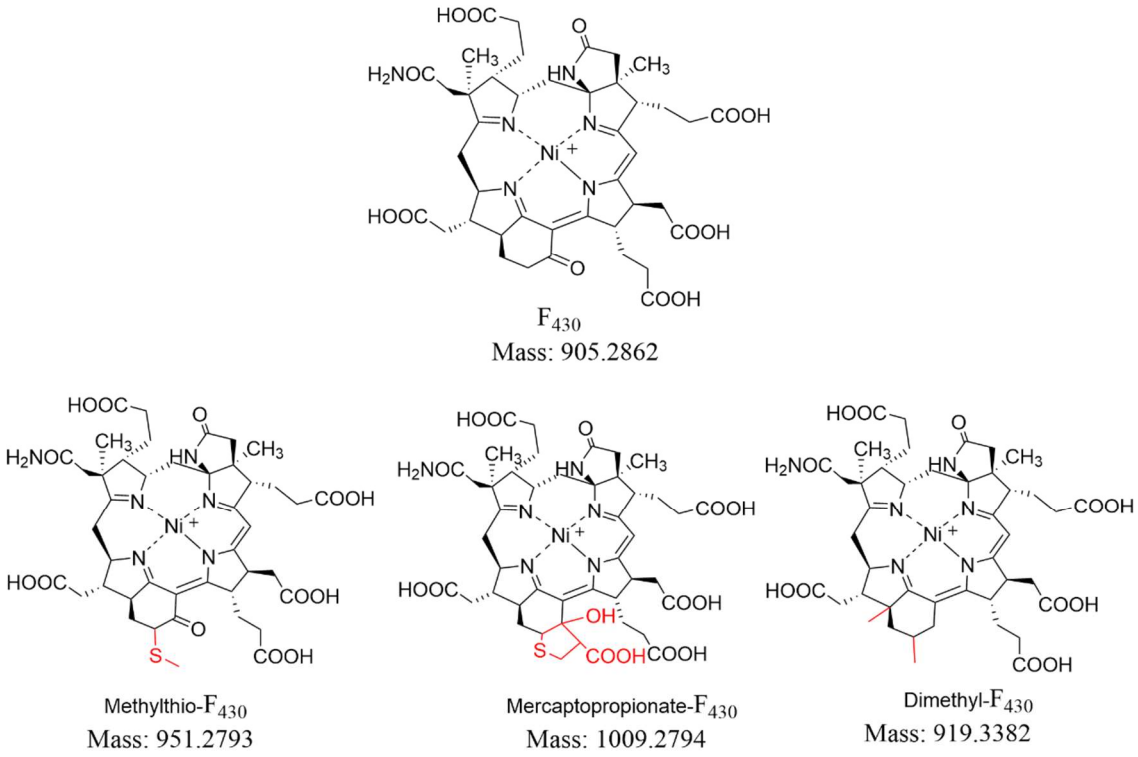

Figure 1.6. The structure of cofactor F_{430} and known variants. Modifications are shown in red.

The discovery of cofactor F_{430} variants raises many exciting questions that should be answered. Since F_{430} variants have been found in methanogens, and whether it binds to any enzyme, including Mcr, is not known, does cofactor F_{430} potentially play other roles in methanogenic cells besides as the prosthetic group of Mcr? If it does not bind to Mcr, what proteins does it bind to? Or, alternatively, it may not bind to any protein. And, if it does bind to Mcr, why are methanogens producing this variant, how does it affect the ability of Mcr to catalyze methane production? Further, while F_{430} biosynthesis has been revealed, it is not known how any of these variants are synthesized. Since F_{430} and its variants are limited to methanogens, ANME, and related archaea, there may be a novel protein involved in sulfur insertion in methylthio- and

mercaptopropioanate-F_{430} synthesis. Alternatively, as enzymes that catalyze sulfur insertion, methylation, as well as both (methylthiolation) are known, it may be that homologous proteins found in methanogens and ANME are used for this process. The focus of the work reported in this thesis is to begin to answer these questions.

Model methanogens: Two distantly related model methanogens, *Methanococcus maripaludis* and *Methanosarcina acetivorans* were used in this work. *M. maripaludis* JJ, isolated from salt marsh sediment near the coast of South Carolina, is a hydrogenotrophic mesophile belonging to the *Methanococcales*.[125] It is a common inhabitant of salt marshes, and various strains have been isolated from these environments, including the S2 strain used for this work.[126] *M. maripaludis* can grow on formate in addition to H_2/CO_2 and has growth optima at temperatures between 35-39 °C and pH 6.8-7.2.[125] *M. acetivorans* C2A, as a *Methanosarcinales,* is distantly related to *M. maripaludis*, but has similar temperature, pH, and salt optima for growth, and was isolated in a marine environment off the coast of California.[127] *M. acetivorans* lacks a functional hydrogenase system and cannot utilize either H_2/CO_2 or formate as growth substrates, but can consume acetate and methylated compounds for methanogenesis. Further, it can grow non-methanogenetically on CO.[128] As model methanogens, these organisms exhibit fast growth on defined medium and are genetically tractable.[129, 130]

1.3 Overview of methylthiotransferases

A brief overview of radical SAM enzymes. Our original proposed candidate for methylthio-F_{430} (Figure 1.6) biosynthesis from F_{430} was a methylthiotransferase (MTTase). MTTases are a subset of the radical SAM (RS) enzyme superfamily. RS enzymes catalyze some of the most challenging reactions known to biochemistry through the conversion of inert substrates to highly reactive radical intermediates. The RS superfamily, first recognized in 2001, has blossomed into

the largest known enzyme superfamily.[131] Radical SAM-catalyzed reactions are diverse and include cofactor synthesis, tRNA modifications, antibiotic synthesis, and DNA repair.[132] To achieve this feat, RS enzymes share some common, but not universal, features. These include a three-cysteine motif, CxxxCxxC, in which the cysteines bind to three iron atoms of a [4Fe-4S] cluster.[132] The fourth iron forms coordinates the α-carboxylate and α-amino groups of a *S*-adenosyl-L-methionine (SAM). When reduced to the 1+ redox state, the Fe-S cluster reductively cleaves SAM to generate a 5'-deoxyadenosyl radical that then abstracts a specific hydrogen from its substrate to generate a radical intermediate that is ripe for further chemistry (Figure 1.7).

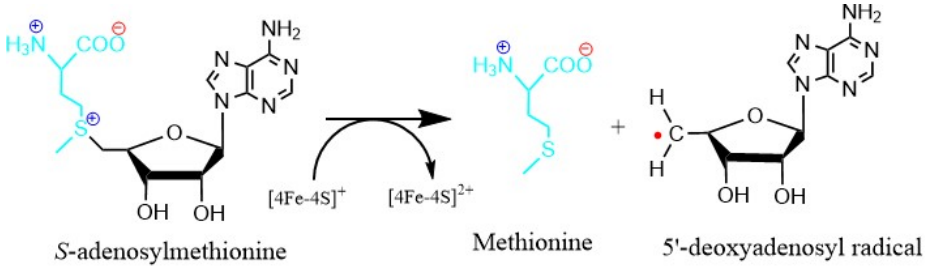

Figure 1.7. The reductive cleavage of SAM with $[4Fe\text{-}4S]^{+1}$ generates a 5'deoxyadenosyl radical and methionine.

Biotin synthase (BioB) and lipoyl synthase (LipA). Before the discovery of radical SAM MTTases, two radical SAM sulfur-insertion enzymes were characterized. BioB and LipA are such enzymes that catalyze sulfur insertion as the last step in the biosynthesis of, respectively, biotin (vitamin B7) and lipoic acid. Biotin contains a bicyclic ring composed of a ureido and a thiophan ring attached to a valerate side chain.[133] It is the covalently-attached prosthetic group of enzymes involved in carboxylation, decarboxylation, and transcarboxylation reactions.[133] Like all RS enzymes, it contains a $[4Fe\text{-}4S]^{2+/1+}$ cluster that is involved in generating a substrate radical.[133] However, the enzyme contains an additional [2Fe-2S] iron-sulfur cluster, and it has been confirmed that this is the source of sulfur for the reaction.[133] The mechanism involves the abstraction of a hydrogen atom from C9 of dethiobiotin, which then attacks the μ-sulfido of the $[2Fe\text{-}2S]^{2+}$ cluster.[133] This is accompanied by the one-electron oxidation of the sulfide with an

inner sphere electron transfer to its adjacent iron, reducing the cluster to $[2Fe\text{-}2S]^{+}$. A similar reaction then ensues with a second SAM entering the active site, resulting in the generation of a second substrate radical, this time at the C6 position. The substrate radical attacks the sulfide, resulting in the dissociation and loss of a sulfide from the cluster to form an unstable [2Fe-S] cluster. BioB exists as a homodimer, and each monomer can only conduct one turnover event.[133] In the Archaea, as of 2018, only the *Methanococcales* and *Thaumarchaeota* were noted to have biotin synthesis clusters, and one such cluster from a Thaumarchaeon has been characterized.[134]

Lipoic acid is a covalently bound cofactor consisting of an *n*-octanoyl with thiols attached to the C6 and C8 carbons. In Bacteria its biosynthesis consists of only two steps.[135] First, an octanoyltransferase, LipB, attaches an octanoyl from fatty acid synthesis onto a specific lysyl residue of a lipoyl carrier protein. Second, LipA inserts sulfurs at C6 and C8 of the protein-bound octanoyllysine. LipA, like BioB, contains two iron-sulfur clusters, with the auxiliary cluster, in this case a [4Fe-4S] cluster, used as the sulfur source. This auxiliary cluster is found near the N-terminus and is ligated by a CX_4CX_5C motif.[136] The mechanism of LipA-catalyzed sulfur insertion, like BioB, requires two equivalents of SAM. The first SAM is reductively cleaved by the RS cluster and used to abstract a hydrogen from C6, which attacks a sulfur of the auxiliary cluster, resulting in the reduction and dissociation of an iron of the cluster.[136] A second SAM is used to abstract a hydrogen from C8, which attacks a second cluster, resulting in an octanoyl intermediate covalently bound via two μ-sulfidos to the auxiliary cluster. The reduction of this intermediate results in lipoic acid dissociating from the iron-sulfur cluster, which itself dissociates from the cluster.

An overview of tRNA modifications. Two of the three known MTTase enzymes are involved in tRNA modification. Transfer RNAs mediate translation of mRNAs into proteins by

delivering amino acids to the ribosome. This is achieved by specific anticodon:codon base pairing. While 61 sense codons exist, cells have far less than 61 tRNAs for decoding.[137] Deciphering all 61 codons by a limited set of tRNAs is accomplished by wobble base pairing, in which the base in the first position of the anticodon is able to pair with more than one nucleoside in an mRNA[137]. To do this, bases in this position are highly post-transcriptionally modified, and this position is the site of the highest number of modifications. In general, post-transcriptional modifications are abundant in tRNAs and play additional roles besides expanding the ability of a tRNA to decode codons. They stabilize the intricate tRNA structure, enable correct charging by aminoacyl-tRNA synthetases, enhance the binding of charged tRNAs to ribosomes, and maintain a correct reading frame.[138] The distribution of tRNA modifications, of which at least 93 exist, can be highly variable.[138] Some tRNA modifications are, for example, found at the same position in all tRNAs throughout all domains of life, while others are found in only one or a few tRNAs in one domain of life[139]. Given the great modification density and variability between tRNAs, the investigation of the role and distribution of specific modifications can be challenging.

The anticodon loop, positions 32-38, includes the anticodon (positions 34-36) and is the most highly modified region of tRNAs.[139] Besides the wobble position (position 34), position 37, directly 3' to the anticodon, is the most modified site. Positions at these two positions are important in maintaining accurate and efficient decoding. In this work, modifications found at position 37 are the most relevant. Position 37 is almost invariably a purine, and modifications include N^6-isopentenyladenosine (i^6A), N^6-threonylcarbamoyladenosine (t^6A), and N^6-hydroxynorvalylcarbamoyladenosine (hn^6A).[140, 141] All three of these modifications can be further methylthiolated at the 2' carbon position (Figure 1.8). The t^6A and ms^2t^6A bases are conserved

among all three domains of life, but i^6A and ms^2i^6A have not been reported in archaeal tRNA, and hn^6A and ms^2hn^6A have not been reported in eukaryotes.[139, 142]

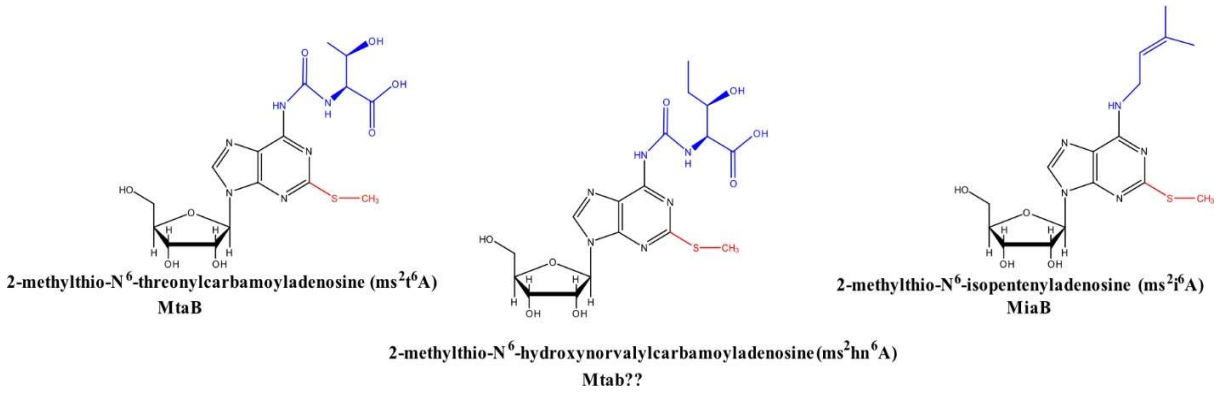

Figure 1.8. Structures of 2-methylthiolated tRNA nucleosides: ms^2t^6A, ms^2hn^6A, and ms^2t^6A.

The tRNA modifications found in methanogens have been studied most extensively in *Methanococcus maripaludis* and *Methanocaldococcus jannaschii*, but complete profiles have been reported in additional methanogens.[137, 143] These include *Methanopyrus kandleri*, the *Methanococcales* members *Methanococcus vaniellii*, *Methanothermococcus thermolithotrophicus*, *Methanotorris igneus*, and one *Methanosarcinales, Methanococcoides burtonii.*[137, 144-146] Methylthiolated nucleosides described include ms^2t^6A and ms^2hn^6A, and their respective un-methylthiolated bases. However, hn^6A and ms^2hn^6A has only been described in *M. burtonii* and *M. jannaschii*, and *M. burtonii* lacks ms^2t^6A, but has the highly conserved t^6A base.[145] *M. kandleri*, in contrast, was reported to have both hn^6A and t^6A, but not any methylthiolated base, although methyl-hn^6A was reported.[146] In addition to the methylthiolated tRNA modifications, other thiolated tRNA modifications exist. These were first reported by Lipsett in 1965, and are a small but important subset of modified nucleosides.[147] In methanogens, these include: 4-thiouridine (s^4U), 2-thiocytidine (s^2C), 5-methylaminomethyl-2-thiouridine (mnm^5s^2U), and 5-cyanomethyl-2-thiouridine (cnm^5s^2U).[137, 144-146] These are well-conserved, but *M. burtonii* lacks

both s^2C and mnm^5s^2U, *M. kandleri* lacks mnm^5s^2U, and cnm^5s^2U has only been reported in *M. jannaschii*.

Biochemical characterization of the methylthiotransferases (MTTases). Three MTTases are known. Like all RS enzymes, they contain a central SAM domain that binds a [4Fe-4S] cluster, and they also contain an N-terminal UPF0004 domain and a C-terminal TRAM domain.[148] The N-terminal domain contains a $Cx_{34-36}Cx_{28-37}C$ motif that binds a second [4Fe-4S] cluster. Two of the known MTTases are involved in analogous reactions with tRNA bases: MiaB catalyzes the methylthiolation of isopentenyladenosine and MtaB catalyzes the methylthiolation of threonylcarbamoyladenosine.[132] Both of these products are found in position 37 of select tRNAs. RimO, in contrast, catalyzes the methylthiolation of aspartate 89 of ribosomal protein S12.[132] RimO, MiaB, and MtaB bacterial homologs have been characterized *in vitro* and the first two crystallized.[149-151] While MTTase *in vitro* studies have focused on bacterial homologs, expression of a eukaryotic MtaB homolog in *E. coli* was shown to result in the production of ms^2t^6A, a base not usually produced by *E. coli*, although this organism produces t^6A.[151] Further, the enzyme catalyzing the methylthiolation of hn^6A has not been described, and it is assumed that MtaB can methylthiolate both t^6A and hn^6A. A phylogenetic analysis showed that MtaB can be separated into two families, one comprising bacterial MtaB, and the other containing eukaryotic and archaeal MtaB.[152] Archaea lack ribosomal protein S12 subunit altogether, and no archaeon has been described that produces ms^2i^6A or i^6A.

The crystal structure of a MiaB has been obtained with a substrate analog and SAM, as well as SAH and 5'deoxyadeonsine byproducts.[148] This has led to the proposal of a mechanism for MTTase reactions. Further, MtaB and MiaB have previously been shown to show substrate selectivity, and the structure of MiaB given insight into how the enzyme selects for its substrate,

i^6A37.[148] tRNAs containing ms^2i^6A37 have an invariant adenosine in position 36, and the structure of MiaB in complex with a tRNA substrate analog shows that the C^6 and C^2 of A36 form hydrophobic interactions with, respectively, Phe348 and Phe350 of the enzyme.[148] Other bases, for example the U37 found in tRNAs containing ms^2t^6A, have hydrophilic groups at the C^2 position. MiaB, however, cannot methylthiolate any adenosine in this position, and the structure of MiaB shows that the enzyme selects for isopentenylated i^6A through the formation of a hydrophobic pocket specific for the isopentenyl moiety. The proposed mechanism involves a SAM first binding to the RS $[4Fe\text{-}4S]^{2+}$ cluster then donating its electrophilic sulfonium $-CH_3$ to the μ_2-sulfido ion of the auxiliary [3Fe-4S] cluster, releasing SAH in the process. The methylated sulfur then attacks C^2 of i^6A to form a tetrahedral intermediate. A second SAM binds to the RS $[4Fe\text{-}4S]^{2+}$ cluster and the reduction of the cluster to $[4Fe\text{-}4S]^{1+}$ results in the reductive cleavage of SAM to methionine and a 5'-deoxyadenosyl radical that abstracts the C^2 hydrogen of i^6A. The substrate radical is transferred to the auxiliary cluster, resulting in the dissociation of the methylthio and reduction of the cluster to $[3Fe\text{-}3S]^{1+}$.

Overview of thesis research. The goals of the research described in this proposal were to investigate the prevalence and distribution of F_{430} variants in methanogens as well as to gain insights into the specific growth conditions that result in enhanced production of F_{430} variants (Chapter II). Additionally, we sought to identify the sulfur insertion enzyme catalyzing the formation of methylthio-F_{430} and the likely related enzyme involved in mercaptopropionate-F_{430} biosynthesis (Chapter III). Although the MTTase we identified did not seem to use F_{430} as a substrate, we describe the first *in vitro* characterization of an archaeal MtaB involved in tRNA modification.

References

1. Ueno, Y.; Yamada, K.; Yoshida, N.; Maruyama, S.; Isozaki, Y., Evidence from fluid inclusions for microbial methanogenesis in the early Archaean era. *Nature* **2006,** *440* (7083), 516-519.

2. Lyu, Z.; Shao, N.; Akinyemi, T.; Whitman, W. B., Methanogenesis. *Curr Biol* **2018,** *28* (13), R727-R732.

3. Berghuis, B. A.; Yu, F. B.; Schulz, F.; Blainey, P. C.; Woyke, T.; Quake, S. R., Hydrogenotrophic methanogenesis in archaeal phylum Verstraetearchaeota reveals the shared ancestry of all methanogens. *Proc Natl Acad Sci U S A* **2019,** *116* (11), 5037-5044.

4. Liu, Y. F.; Chen, J.; Zaramela, L. S.; Wang, L. Y.; Mbadinga, S. M.; Hou, Z. W.; Wu, X. L.; Gu, J. D.; Zengler, K.; Mu, B. Z., Genomic and Transcriptomic Evidence Supports Methane Metabolism in Archaeoglobi. *mSystems* **2020,** *5* (2).

5. Béchamp, A., Lettre à M. Dumas. *Annales de chimie et de physique* **1868,** *4* (13), 103-111.

6. Barker, H. A., Studies upon the methane fermentation. IV. The isolation and culture of *Methanobacterium omelianskii*. *Antonie van Leeuwenhoek* **1940,** *6*, 201-220.

7. Bryant, M. P.; Wolin, E. A.; Wolin, M. J.; Wolfe, R. S., *Methanobacillus omelianskii*, a symbiotic association of two species of bacteria. *Arch Mikrobiol* **1967,** *59* (1), 20-31.

8. Schnellen, C. G. T. P. Onderzoekingen over de methaangistung. TU Delft, 1947.

9. Hungate, R. E., The anaerobic mesophilic cellulolytic bacteria. *Bacteriol Rev* **1950,** *14* (1), 1-49.

10. Hungate, R. E., Chapter IV A Roll Tube Method for Cultivation of Strict Anaerobes. *Methods in Microbiology* **1969,** *3*, 117-132.

11. Balch, W. E.; Wolfe, R. S., New approach to the cultivation of methanogenic bacteria: 2-mercaptoethanesulfonic acid (HS-CoM)-dependent growth of Methanobacterium ruminantium in a pressureized atmosphere. *Appl Environ Microbiol* **1976,** *32* (6), 781-791.

12. Bryant, M. P.; Mcbride, B. C.; Wolfe, R. S., Hydrogen-Oxidizing Methane Bacteria .I. Cultivation and Methanogenesis. *Journal of Bacteriology* **1968,** *95* (3), 1118-1123.

13. Leigh, J. A.; Wolfe, R. S., Carbon dioxide reduction factor and methanopterin, two coenzymes required for CO2 reduction to methane by extracts of Methanobacterium. *J Biol Chem* **1983,** *258* (12), 7536-7540.

14. Leigh, J. A.; Rinehart, K. L.; Wolfe, R. S., Structure of Methanofuran, the Carbon-Dioxide Reduction Factor of *Methanobacterium thermoautotrophicum*. *Journal of the American Chemical Society* **1984,** *106* (12), 3636-3640.

15. Leigh, J. A.; Rinehart, K. L., Jr.; Wolfe, R. S., Methanofuran (carbon dioxide reduction factor), a formyl carrier in methane production from carbon dioxide in Methanobacterium. *Biochemistry* **1985,** *24* (4), 995-999.

16. Ellefson, W. L.; Whitman, W. B.; Wolfe, R. S., Nickel-containing factor F430: chromophore of the methylreductase of Methanobacterium. *Proc. Natl. Acad. Sci. U. S. A.* **1982,** *79* (12), 3707-3710.

17. Thauer, R. K., Biochemistry of methanogenesis: a tribute to Marjory Stephenson. 1998 Marjory Stephenson Prize Lecture. *Microbiology (Reading)* **1998,** *144 (Pt 9)*, 2377-2406.

18. Woese, C. R.; Fox, G. E., Phylogenetic structure of the prokaryotic domain: the primary kingdoms. *Proc Natl Acad Sci U S A* **1977,** *74* (11), 5088-90.

19. Woese, C. R.; Kandler, O.; Wheelis, M. L., Towards a natural system of organisms: proposal for the domains Archaea, Bacteria, and Eucarya. *Proc. Natl. Acad. Sci. U. S. A.* **1990,** *87* (12), 4576-9.

20. Chadwick, G. L.; Skennerton, C. T.; Laso-Perez, R.; Leu, A. O.; Speth, D. R.; Yu, H.; Morgan-Lang, C.; Hatzenpichler, R.; Goudeau, D.; Malmstrom, R.; Brazelton, W. J.; Woyke, T.; Hallam, S. J.; Tyson, G. W.; Wegener, G.; Boetius, A.; Orphan, V. J., Comparative genomics reveals electron transfer and syntrophic mechanisms differentiating methanotrophic and methanogenic archaea. *PLoS Biol* **2022,** *20* (1), e3001508.

21. Ehhalt, D. H., The atmospheric cycle of methane. *Tellus* **1974,** *26* (1-2), 58-70.

22. Martens, C. S.; Berner, R. A., Methane Production in Interstitial Waters of Sulfate-Depleted Marine Sediments. *Science* **1974,** *185* (4157), 1167-1169.

23. Cappenberg, T. E., Interrelations between sulfate-reducing and methane-producing bacteria in bottom deposits of a fresh-water lake. I. Field observations. *Antonie Van Leeuwenhoek* **1974,** *40* (2), 285-295.

24. Barnes, R. O.; Goldberg, E. D., Methane Production and Consumption in Anoxic Marine-Sediments. *Geology* **1976,** *4* (5), 297-300.

25. Davis, J. B.; Yarbroug.Hf, Anaerobic Oxidation of Hydrocarbons by *Desulfovibrio desulfuricans*. *Tex Rep Biol Med* **1965,** *23* (3), 137-144.

26. Hoehler, T. M.; Alperin, M. J.; Albert, D. B.; Martens, C. S., Field and Laboratory Studies of Methane Oxidation in an Anoxic Marine Sediment - Evidence for a Methanogen-Sulfate Reducer Consortium. *Global Biogeochem Cy* **1994,** *8* (4), 451-463.

27. Iversen, N.; Jorgensen, B. B., Anaerobic Methane Oxidation Rates at the Sulfate Methane Transition in Marine-Sediments from Kattegat and Skagerrak (Denmark). *Limnol Oceanogr* **1985,** *30* (5), 944-955.

28. Reeburgh, W. S., Anaerobic Methane Oxidation - Rate Depth Distributions in Skan Bay Sediments. *Earth Planet Sc Lett* **1980,** *47* (3), 345-352.

29. Hinrichs, K. U.; Hayes, J. M.; Sylva, S. P.; Brewer, P. G.; DeLong, E. F., Methane-consuming archaebacteria in marine sediments. *Nature* **1999,** *398* (6730), 802-805.

30. Boetius, A.; Ravenschlag, K.; Schubert, C. J.; Rickert, D.; Widdel, F.; Gieseke, A.; Amann, R.; Jorgensen, B. B.; Witte, U.; Pfannkuche, O., A marine microbial consortium apparently mediating anaerobic oxidation of methane. *Nature* **2000,** *407* (6804), 623-6.

31. Orphan, V. J.; Hinrichs, K. U.; Ussler, W., 3rd; Paull, C. K.; Taylor, L. T.; Sylva, S. P.; Hayes, J. M.; Delong, E. F., Comparative analysis of methane-oxidizing archaea and sulfate-reducing bacteria in anoxic marine sediments. *Appl Environ Microbiol* **2001,** *67* (4), 1922-34.

32. Hallam, S. J.; Girguis, P. R.; Preston, C. M.; Richardson, P. M.; DeLong, E. F., Identification of methyl coenzyme M reductase A (mcrA) genes associated with methane-oxidizing archaea. *Appl Environ Microbiol* **2003,** *69* (9), 5483-5491.

33. Hallam, S. J.; Putnam, N.; Preston, C. M.; Detter, J. C.; Rokhsar, D.; Richardson, P. M.; DeLong, E. F., Reverse methanogenesis: testing the hypothesis with environmental genomics. *Science* **2004,** *305* (5689), 1457-1462.

34. Wegener, G.; Krukenberg, V.; Ruff, S. E.; Kellermann, M. Y.; Knittel, K., Metabolic Capabilities of Microorganisms Involved in and Associated with the Anaerobic Oxidation of Methane. *Front Microbiol* **2016,** *7*.

35. Wang, Y.; Wegener, G.; Ruff, S. E.; Wang, F., Methyl/alkyl-coenzyme M reductase-based anaerobic alkane oxidation in archaea. *Environ Microbiol* **2021,** *23* (2), 530-541.

36. Thauer, R. K.; Kaster, A. K.; Seedorf, H.; Buckel, W.; Hedderich, R., Methanogenic archaea: ecologically relevant differences in energy conservation. *Nat Rev Microbiol* **2008,** *6* (8), 579-591.

37. Angel, R.; Matthies, D.; Conrad, R., Activation of methanogenesis in arid biological soil crusts despite the presence of oxygen. *PLoS One* **2011,** *6* (5), e20453.

38. Knittel, K.; Boetius, A., Anaerobic oxidation of methane: progress with an unknown process. *Annu Rev Microbiol* **2009,** *63*, 311-334.

39. Segarra, K. E. A.; Schubotz, F.; Samarkin, V.; Yoshinaga, M. Y.; Hinrichs, K. U.; Joye, S. B., High rates of anaerobic methane oxidation in freshwater wetlands reduce potential atmospheric methane emissions. *Nature Communications* **2015,** *6*.

40. Kharitonov, S.; Semenov, M.; Sabrekov, A.; Kotsyurbenko, O.; Zhelezova, A.; Schegolkova, N., Microbial Communities in Methane Cycle: Modern Molecular Methods Gain Insights into Their Global Ecology. *Environments* **2021,** *8* (2).

41. Price, P. B., Microbial life in glacial ice and implications for a cold origin of life. *Fems Microbiol Ecol* **2007,** *59* (2), 217-231.

42. Stevenson, D. S.; Zhao, A.; Naik, V.; O'Connor, F. M.; Tilmes, S.; Zeng, G.; Murray, L. T.; Collins, W. J.; Griffiths, P. T.; Shim, S. B.; Horowitz, L. W.; Sentman, L. T.; Emmons, L., Trends in global tropospheric hydroxyl radical and methane lifetime since 1850 from AerChemMIP. *Atmos Chem Phys* **2020,** *20* (21), 12905-12920.

43. Masson-Delmotte, V., P. Zhai, A. Pirani, S.L.; Connors, C. P., S. Berger, N. Caud, Y. Chen, L. Goldfarb, M.I. Gomis, M. Huang, K. Leitzell, E. Lonnoy, J.B.R.; Matthews, T. K. M., T.

Waterfield, O. Yelekçi, R. Yu, B. Zhou *Climate Change 2021: The Physical Science Basis. Contribution of Working Group I to the Sixth Assessment Report of the Intergovernmental Panel on Climate Change*; IPCC: 2021.

44. Prather, M. J.; Holmes, C. D.; Hsu, J., Reactive greenhouse gas scenarios: Systematic exploration of uncertainties and the role of atmospheric chemistry. *Geophys Res Lett* **2012,** *39*.

45. Stocker, T. F., D. Qin, G.-K. Plattner, M. Tignor, S.K. Allen, J. Boschung, A. Nauels, Y. Xia, V. Bex, P.M. Midgley *IPCC, 2013: Climate Change 2013: The Physical Science Basis. Contribution of Working Group I to the Fifth Assessment Report of the Intergovernmental Panel on Climate Change*; IPCC: 2013.

46. Koffi, E. N.; Bergamaschi, P.; Alkama, R.; Cescatti, A., An observation-constrained assessment of the climate sensitivity and future trajectories of wetland methane emissions. *Sci Adv* **2020,** *6* (15), eaay4444.

47. Xue, K.; Yuan, M. M.; Shi, Z. J.; Qin, Y. J.; Deng, Y.; Cheng, L.; Wu, L. Y.; He, Z. L.; Van Nostrand, J. D.; Bracho, R.; Natali, S.; Schuur, E. A. G.; Luo, C. W.; Konstantinidis, K. T.; Wang, Q.; Cole, J. R.; Tiedje, J. M.; Luo, Y. Q.; Zhou, J. Z., Tundra soil carbon is vulnerable to rapid microbial decomposition under climate warming. *Nat Clim Change* **2016,** *6* (6), 595-+.

48. Admistration, U. S. E. I. Electricity explained *Electricity in the United States*.

49. Administration, U. S. E. I. U.S. energy facts explained.

50. Joskow, P. L., Natural Gas: From Shortages to Abundance in the United States. *Am Econ Rev* **2013,** *103* (3), 338-343.

51. Wang, Z. M.; Krupnick, A., A Retrospective Review of Shale Gas Development in the United States: What Led to the Boom? *Econ Energy Env Pol* **2015,** *4* (1), 5-17.

52. Administration, U. S. E. I. How much shale gas is produced in the United States?

53. Wood, D. A.; Nwaoha, C.; Towler, B. F., Gas-to-liquids (GTL): A review of an industry offering several routes for monetizing natural gas. *J Nat Gas Sci Eng* **2012,** *9*, 196-208.

54. Chong, Z. R.; Yang, S. H. B.; Babu, P.; Linga, P.; Li, X. S., Review of natural gas hydrates as an energy resource: Prospects and challenges. *Appl Energ* **2016,** *162*, 1633-1652.

55. Leung, G. C. K., Natural Gas as a Clean Fuel. In *Handbook of Clean Energy Systems*, pp 1-15.

56. Alvarez, R. A.; Zavala-Araiza, D.; Lyon, D. R.; Allen, D. T.; Barkley, Z. R.; Brandt, A. R.; Davis, K. J.; Herndon, S. C.; Jacob, D. J.; Karion, A.; Kort, E. A.; Lamb, B. K.; Lauvaux, T.; Maasakkers, J. D.; Marchese, A. J.; Omara, M.; Pacala, S. W.; Peischl, J.; Robinson, A. L.; Shepson, P. B.; Sweeney, C.; Townsend-Small, A.; Wofsy, S. C.; Hamburg, S. P., Assessment of methane emissions from the U.S. oil and gas supply chain. *Science* **2018,** *361* (6398), 186-188.

57. Mueller, T. J.; Grisewood, M. J.; Nazem-Bokaee, H.; Gopalakrishnan, S.; Ferry, J. G.; Wood, T. K.; Maranas, C. D., Methane oxidation by anaerobic archaea for conversion to liquid fuels. *J Ind Microbiol Biot* **2015,** *42* (3), 391-401.

58. Administration, U. S. E. I. Number of Producing Gas Wells.

59. Moran, J. J.; House, C. H.; Freeman, K. H.; Ferry, J. G., Trace methane oxidation studied in several Euryarchaeota under diverse conditions. *Archaea* **2005,** *1* (5), 303-9.

60. Soo, V. W.; McAnulty, M. J.; Tripathi, A.; Zhu, F.; Zhang, L.; Hatzakis, E.; Smith, P. B.; Agrawal, S.; Nazem-Bokaee, H.; Gopalakrishnan, S.; Salis, H. M.; Ferry, J. G.; Maranas, C. D.; Patterson, A. D.; Wood, T. K., Reversing methanogenesis to capture methane for liquid biofuel precursors. *Microb Cell Fact* **2016,** *15*, 11.

61. McAnulty, M. J.; Poosarla, V. G.; Kim, K. Y.; Jasso-Chavez, R.; Logan, B. E.; Wood, T. K., Electricity from methane by reversing methanogenesis. *Nature Communications* **2017,** *8*.

62. Zhang, L.; Kuroki, A.; Tong, Y. W., A Mini-Review on In situ Biogas Upgrading Technologies via Enhanced Hydrogenotrophic Methanogenesis to Improve the Quality of Biogas From Anaerobic Digesters. *Front Energy Res* **2020,** *8*.

63. Rouviere, P. E.; Wolfe, R. S., Novel biochemistry of methanogenesis. *J Biol Chem* **1988,** *263* (17), 7913-7916.

64. Bapteste, E.; Brochier, C.; Boucher, Y., Higher-level classification of the Archaea: evolution of methanogenesis and methanogens. *Archaea* **2005,** *1* (5), 353-63.

65. Sorokin, D. Y.; Merkel, A. Y.; Abbas, B.; Makarova, K. S.; Rijpstra, W. I. C.; Koenen, M.; Damste, J. S. S.; Galinski, E. A.; Koonin, E. V.; van Loosdrecht, M. C. M., *Methanonatronarchaeum thermophilum* gen. nov., sp nov and *'Candidatus* Methanohalarchaeum thermophilum', extremely halo(natrono)philic methyl-reducing methanogens from hypersaline lakes comprising a new euryarchaeal class Methanonatronarchaeia classis nov. *Int J Syst Evol Micr* **2018,** *68* (7), 2199-2208.

66. DiMarco, A. A.; Bobik, T. A.; Wolfe, R. S., Unusual coenzymes of methanogenesis. *Annu Rev Biochem* **1990,** *59*, 355-94.

67. Costa, K. C.; Lie, T. J.; Jacobs, M. A.; Leigh, J. A., H_2-independent growth of the hydrogenotrophic methanogen *Methanococcus maripaludis*. *Mbio* **2013,** *4* (2), e00062-13

68. Liu, Y.; Whitman, W. B., Metabolic, phylogenetic, and ecological diversity of the methanogenic archaea. *Ann N Y Acad Sci* **2008,** *1125*, 171-189.

69. Gottschalk, G.; Thauer, R. K., The Na(+)-translocating methyltransferase complex from methanogenic archaea. *Biochim Biophys Acta* **2001,** *1505* (1), 28-36.

70. Muller, V.; Blaut, M.; Heise, R.; Winner, C.; Gottschalk, G., Sodium Bioenergetics in Methanogens and Acetogens. *Fems Microbiology Letters* **1990,** *87* (3-4), 373-376.

71. Wongnate, T.; Sliwa, D.; Ginovska, B.; Smith, D.; Wolf, M. W.; Lehnert, N.; Raugei, S.; Ragsdale, S. W., The radical mechanism of biological methane synthesis by methyl-coenzyme M reductase. *Science* **2016,** *352* (6288), 953-958.

72. Milton, R. D.; Ruth, J. C.; Deutzmann, J. S.; Spormann, A. M., *Methanococcus maripaludis* employs three functional heterodisulfide reductase complexes for flavin-based electron bifurcation using hydrogen and formate. *Biochemistry* **2018,** *57* (32), 4848-4857.

73. Heiden, S.; Hedderich, R.; Setzke, E.; Thauer, R. K., Purification of a two-subunit cytochrome-b-containing heterodisulfide reductase from methanol-grown *Methanosarcina barkeri*. *Eur J Biochem* **1994,** *221* (2), 855-61.

74. Jetten, M. S. M.; Stams, A. J. M.; Zehnder, A. J. B., Methanogenesis from acetate - a comparison of the acetate metabolism in *Methanothrix soehngenii* and *Methanosarcina* spp. *Fems Microbiology Letters* **1992,** *88* (3-4), 181-197.

75. Smith, K. S.; Ingram-Smith, C., *Methanosaeta*, the forgotten methanogen? *Trends Microbiol* **2007,** *15* (4), 150-5.

76. *The Prokaryotes*. Springer-Verlag: Berlin, 2014.

77. Fournier, G. P.; Gogarten, J. P., Evolution of acetoclastic methanogenesis in *Methanosarcina* via horizontal gene transfer from cellulolytic *Clostridia*. *J Bacteriol* **2008,** *190* (3), 1124-7.

78. Hibino, A.; Petri, R.; Buchs, J.; Ohtake, H., Production of uroporphyrinogen III, which is the common precursor of all tetrapyrrole cofactors, from 5-aminolevulinic acid by *Escherichia coli* expressing thermostable enzymes. *Appl Microbiol Biotechnol* **2013,** *97* (16), 7337-44.

79. Ferry, J. G., How to make a living by exhaling methane. *Annual Review of Microbiology, Vol 64, 2010* **2010,** *64*, 453-473.

80. Gong, W.; Hao, B.; Wei, Z.; Ferguson, D. J., Jr.; Tallant, T.; Krzycki, J. A.; Chan, M. K., Structure of the alpha2epsilon2 Ni-dependent CO dehydrogenase component of the Methanosarcina barkeri acetyl-CoA decarbonylase/synthase complex. *Proc Natl Acad Sci U S A* **2008,** *105* (28), 9558-9563.

81. Gencic, S.; Grahame, D. A., Two separate one-electron steps in the reductive activation of the A cluster in subunit beta of the ACDS complex in *Methanosarcina thermophila*. *Biochemistry* **2008,** *47* (20), 5544-5555.

82. Funk, T.; Gu, W.; Friedrich, S.; Wang, H.; Gencic, S.; Grahame, D. A.; Cramer, S. P., Chemically distinct Ni sites in the A-cluster in subunit beta of the acetyl-CoA decarbonylase/synthase complex from *Methanosarcina thermophila*: Ni L-edge absorption and X-ray magnetic circular dichroism analyses. *J Am Chem Soc* **2004,** *126* (1), 88-95.

83. Grahame, D. A.; DeMoll, E., Partial reactions catalyzed by protein components of the acetyl-CoA decarbonylase synthase enzyme complex from *Methanosarcina barkeri*. *J Biol Chem* **1996,** *271* (14), 8352-8358.

84. Abbanat, D. R.; Ferry, J. G., Resolution of component proteins in an enzyme complex from *Methanosarcina thermophila* catalyzing the synthesis or cleavage of acetyl-CoA. *Proc Natl Acad Sci U S A* **1991,** *88* (8), 3272-3276.

85. Wang, M.; Tomb, J. F.; Ferry, J. G., Electron transport in acetate-grown *Methanosarcina acetivorans*. *BMC Microbiol* **2011,** *11*, 165.

86. Nobu, M. K.; Narihiro, T.; Kuroda, K.; Mei, R.; Liu, W. T., Chasing the elusive Euryarchaeota class WSA2: genomes reveal a uniquely fastidious methylreducing methanogen. *Isme Journal* **2016,** *10* (10), 2478-2487.

87. Evans, P. N.; Parks, D. H.; Chadwick, G. L.; Robbins, S. J.; Orphan, V. J.; Golding, S. D.; Tyson, G. W., Methane metabolism in the archaeal phylum Bathyarchaeota revealed by genome-centric metagenomics. *Science* **2015,** *350* (6259), 434-8.

88. Vanwonterghem, I.; Evans, P. N.; Parks, D. H.; Jensen, P. D.; Woodcroft, B. J.; Hugenholtz, P.; Tyson, G. W., Methylotrophic methanogenesis discovered in the archaeal phylum Verstraetearchaeota. *Nat Microbiol* **2016,** *1*, 16170.

89. Fricke, W. F.; Seedorf, H.; Henne, A.; Kruer, M.; Liesegang, H.; Hedderich, R.; Gottschalk, G.; Thauer, R. K., The genome sequence of Methanosphaera stadtmanae reveals why this human intestinal archaeon is restricted to methanol and H-2 for methane formation and ATP synthesis. *Journal of Bacteriology* **2006,** *188* (2), 642-658.

90. McGenity, T. J.; Sorokin, D. Y., Methanogens and methanogenesis in hypersaline environments. In *Biogenesis of Hydrocarbons*, Stams, A. J. M.; Sousa, D. Z., Eds. Springer International Publishing: Cham, 2019; pp 283-309.

91. Bose, A.; Pritchett, M. A.; Metcalf, W. W., Genetic analysis of the methanol- and methylamine-specific methyltransferase 2 genes of *Methanosarcina acetivorans* C2A. *J Bacteriol* **2008,** *190* (11), 4017-26.

92. Borrel, G.; O'Toole, P. W.; Harris, H. M.; Peyret, P.; Brugere, J. F.; Gribaldo, S., Phylogenomic data support a seventh order of Methylotrophic methanogens and provide insights into the evolution of methanogenesis. *Genome Biol Evol* **2013,** *5* (10), 1769-80.

93. Borrel, G.; Parisot, N.; Harris, H. M.; Peyretaillade, E.; Gaci, N.; Tottey, W.; Bardot, O.; Raymann, K.; Gribaldo, S.; Peyret, P.; O'Toole, P. W.; Brugere, J. F., Comparative genomics highlights the unique biology of *Methanomassiliicoccales*, a *Thermoplasmatales*-related seventh order of methanogenic archaea that encodes pyrrolysine. *BMC Genomics* **2014,** *15*, 679.

94. Knittel, K.; Losekann, T.; Boetius, A.; Kort, R.; Amann, R., Diversity and distribution of methanotrophic archaea at cold seeps. *Appl Environ Microbiol* **2005,** *71* (1), 467-79.

95. Meyerdierks, A.; Kube, M.; Kostadinov, I.; Teeling, H.; Glockner, F. O.; Reinhardt, R.; Amann, R., Metagenome and mRNA expression analyses of anaerobic methanotrophic archaea of the ANME-1 group. *Environmental Microbiology* **2010,** *12* (2), 422-439.

96. Stokke, R.; Roalkvam, I.; Lanzen, A.; Haflidason, H.; Steen, I. H., Integrated metagenomic and metaproteomic analyses of an ANME-1-dominated community in marine cold seep sediments. *Environ Microbiol* **2012,** *14* (5), 1333-46.

97. Wang, F. P.; Zhang, Y.; Chen, Y.; He, Y.; Qi, J.; Hinrichs, K. U.; Zhang, X. X.; Xiao, X.; Boon, N., Methanotrophic archaea possessing diverging methane-oxidizing and electron-transporting pathways. *Isme Journal* **2014,** *8* (5), 1069-1078.

98. Moran, J. J.; Beal, E. J.; Vrentas, J. M.; Orphan, V. J.; Freeman, K. H.; House, C. H., Methyl sulfides as intermediates in the anaerobic oxidation of methane. *Environmental Microbiology* **2008,** *10* (1), 162-173.

99. Milucka, J.; Ferdelman, T. G.; Polerecky, L.; Franzke, D.; Wegener, G.; Schmid, M.; Lieberwirth, I.; Wagner, M.; Widdel, F.; Kuypers, M. M. M., Zero-valent sulphur is a key intermediate in marine methane oxidation. *Nature* **2012,** *491* (7425), 541-545.

100. Klein, M.; Friedrich, M.; Roger, A. J.; Hugenholtz, P.; Fishbain, S.; Abicht, H.; Blackall, L. L.; Stahl, D. A.; Wagner, M., Multiple lateral transfers of dissimilatory sulfite reductase genes between major lineages of sulfate-reducing prokaryotes. *J Bacteriol* **2001,** *183* (20), 6028-6035.

101. Yu, H.; Susanti, D.; McGlynn, S. E.; Skennerton, C. T.; Chourey, K.; Iyer, R.; Scheller, S.; Tavormina, P. L.; Hettich, R. L.; Mukhopadhyay, B.; Orphan, V. J., Comparative genomics and proteomic analysis of assimilatory sulfate reduction pathways in anaerobic methanotrophic archaea. *Front Microbiol* **2018,** *9*, 2917.

102. Stokke, R.; Roalkvam, I.; Lanzen, A.; Haflidason, H.; Steen, I. H., Integrated metagenomic and metaproteomic analyses of an ANME-1-dominated community in marine cold seep sediments. *Environmental Microbiology* **2012,** *14* (5), 1333-1346.

103. Wegener, G.; Krukenberg, V.; Riedel, D.; Tegetmeyer, H. E.; Boetius, A., Intercellular wiring enables electron transfer between methanotrophic archaea and bacteria. *Nature* **2015,** *526* (7574), 587-90.

104. Skennerton, C. T.; Chourey, K.; Iyer, R.; Hettich, R. L.; Tyson, G. W.; Orphan, V. J., Methane-fueled syntrophy through extracellular electron transfer: uncovering the genomic traits conserved within diverse bacterial partners of anaerobic methanotrophic archaea. *Mbio* **2017,** *8* (4).

105. McGlynn, S. E.; Chadwick, G. L.; Kempes, C. P.; Orphan, V. J., Single cell activity reveals direct electron transfer in methanotrophic consortia. *Nature* **2015,** *526* (7574), 531-5.

106. Leu, A. O.; Cai, C.; McIlroy, S. J.; Southam, G.; Orphan, V. J.; Yuan, Z.; Hu, S.; Tyson, G. W., Anaerobic methane oxidation coupled to manganese reduction by members of the Methanoperedenaceae. *ISME J* **2020,** *14* (4), 1030-1041.

107. Cai, C.; Leu, A. O.; Xie, G. J.; Guo, J.; Feng, Y.; Zhao, J. X.; Tyson, G. W.; Yuan, Z.; Hu, S., A methanotrophic archaeon couples anaerobic oxidation of methane to Fe(III) reduction. *ISME J* **2018,** *12* (8), 1929-1939.

108. Haroon, M. F.; Hu, S.; Shi, Y.; Imelfort, M.; Keller, J.; Hugenholtz, P.; Yuan, Z.; Tyson, G. W., Anaerobic oxidation of methane coupled to nitrate reduction in a novel archaeal lineage. *Nature* **2013,** *500* (7464), 567-70.

109. Ellefson, W. L.; Wolfe, R. S., Role of component C in the methylreductase system of Methanobacterium. *J Biol Chem* **1980,** *255* (18), 8388-9.

110. Gunsalus, R. P.; Wolfe, R. S., Chromophoric Factors F342 and F430 of *Methanobacterium thermoautotrophicum*. *Fems Microbiology Letters* **1978,** *3* (4), 191-193.

111. Schonheit, P.; Moll, J.; Thauer, R. K., Nickel, cobalt, and molybdenum requirement for growth of *Methanobacterium thermoautotrophicum*. *Archives of Microbiology* **1979,** *123* (1), 105-107.

112. Whitman, W. B.; Wolfe, R. S., Presence of nickel in factor F430 from *Methanobacterium bryantii*. *Biochem Biophys Res Commun* **1980,** *92* (4), 1196-1201.

113. Gilles, H.; Thauer, R. K., Uroporphyrinogen III, an intermediate in the biosynthesis of the nickel-containing factor F_{430} in *Methanobacterium thermoautotrophicum*. *Eur J Biochem* **1983,** *135* (1), 109-112.

114. Pfaltz, A.; Kobelt, A.; Huster, R.; Thauer, R. K., Biosynthesis of coenzyme F_{430} in methanogenic bacteria identification of 15,17^3-Seco-F_{430}-17^3-acid as an intermediate. *European Journal of Biochemistry* **1987,** *170* (1-2), 459-467.

115. Farber, G.; Keller, W.; Kratky, C.; Jaun, B.; Pfaltz, A.; Spinner, C.; Kobelt, A.; Eschenmoser, A., Coenzyme F_{430} from methanogenic bacteria - complete assignment of

configuration based on an x-ray analysis of 12,13-Diepi-F_{430} pentamethyl ester and on NMR spectroscopy. *Helv Chim Acta* **1991,** *74* (4), 697-716.

116. Zheng, K.; Ngo, P. D.; Owens, V. L.; Yang, X. P.; Mansoorabadi, S. O., The biosynthetic pathway of coenzyme F_{430} in methanogenic and methanotrophic archaea. *Science* **2016,** *354* (6310), 339-342.

117. Harmer, J.; Finazzo, C.; Piskorski, R.; Ebner, S.; Duin, E. C.; Goenrich, M.; Thauer, R. K.; Reiher, M.; Schweiger, A.; Hinderberger, D.; Jaun, B., A nickel hydride complex in the active site of methyl-coenzyme m reductase: implications for the catalytic cycle. *J Am Chem Soc* **2008,** *130* (33), 10907-10920.

118. Ermler, U.; Grabarse, W.; Shima, S.; Goubeaud, M.; Thauer, R. K., Crystal structure of methyl-coenzyme M reductase: the key enzyme of biological methane formation. *Science* **1997,** *278* (5342), 1457-1462.

119. Prakash, D.; Wu, Y.; Suh, S. J.; Duin, E. C., Elucidating the process of activation of methyl-coenzyme M reductase. *J. Bacteriol.* **2014,** *196* (13), 2491-2498.

120. Lyu, Z.; Chou, C. W.; Shi, H.; Wang, L.; Ghebreab, R.; Phillips, D.; Yan, Y.; Duin, E. C.; Whitman, W. B., Assembly of Methyl coenzyme M reductase in the methanogenic archaeon *Methanococcus maripaludis*. *J. Bacteriol.* **2018,** *200* (7).

121. Allen, K. D.; Wegener, G.; White, R. H., Discovery of multiple modified F(430) coenzymes in methanogens and anaerobic methanotrophic archaea suggests possible new roles for F(430) in nature. *Appl Environ Microbiol* **2014,** *80* (20), 6403-6412.

122. Mayr, S.; Latkoczy, C.; Kruger, M.; Gunther, D.; Shima, S.; Thauer, R. K.; Widdel, F.; Jaun, B., Structure of an F_{430} variant from archaea associated with anaerobic oxidation of methane. *J Am Chem Soc* **2008,** *130* (32), 10758-10767.

123. Hahn, C. J.; Lemaire, O. N.; Kahnt, J.; Engilberge, S.; Wegener, G.; Wagner, T., Crystal structure of a key enzyme for anaerobic ethane activation. *Science* **2021,** *373* (6550), 118-121.

124. Shima, S.; Krueger, M.; Weinert, T.; Demmer, U.; Kahnt, J.; Thauer, R. K.; Ermler, U., Structure of a methyl-coenzyme M reductase from Black Sea mats that oxidize methane anaerobically. *Nature* **2011,** *481* (7379), 98-101.

125. Jones, W. J.; Paynter, M. J. B.; Gupta, R., Characterization of *Methanococcus maripaludis* sp. nov, a new methanogen isolated from salt-marsh sediment. *Archives of Microbiology* **1983,** *135* (2), 91-97.

126. Whitman, W. B.; Shieh, J.; Sohn, S.; Caras, D. S.; Premachandran, U., Isolation and Characterization of 22 Mesophilic *Methanococci*. *Syst Appl Microbiol* **1986,** *7* (2-3), 235-240.

127. Sowers, K. R.; Baron, S. F.; Ferry, J. G., *Methanosarcina acetivorans* sp. nov., an acetotrophic methane-producing bacterium isolated from marine sediments. *Appl Environ Microbiol* **1984,** *47* (5), 971-978.

128. Rother, M.; Metcalf, W. W., Anaerobic growth of *Methanosarcina acetivorans* C2A on carbon monoxide: An unusual way of life for a methanogenic archaeon. *P Natl Acad Sci USA* **2004,** *101* (48), 16929-16934.

129. Buan, N.; Kulkarni, G.; Metcalf, W., Genetic methods for *Methanosarcina* species. *Methods Enzymol* **2011,** *494*, 23-42.

130. Sarmiento, F.; Leigh, J. A.; Whitman, W. B., Genetic systems for hydrogenotrophic methanogens. *Methods Enzymol* **2011,** *494*, 43-73.

131. Sofia, H. J.; Chen, G.; Hetzler, B. G.; Reyes-Spindola, J. F.; Miller, N. E., Radical SAM, a novel protein superfamily linking unresolved steps in familiar biosynthetic pathways with radical

mechanisms: functional characterization using new analysis and information visualization methods. *Nucleic Acids Res* **2001,** *29* (5), 1097-1106.

132. Hutcheson, R. U.; Broderick, J. B., Radical SAM enzymes in methylation and methylthiolation. *Metallomics* **2012,** *4* (11), 1149-1154.

133. Ugulava, N. B.; Sacanell, C. J.; Jarrett, J. T., Spectroscopic changes during a single turnover of biotin synthase: destruction of a [2Fe-2S] cluster accompanies sulfur insertion. *Biochemistry* **2001,** *40* (28), 8352-8358.

134. Chow, J.; Danso, D.; Ferrer, M.; Streit, W. R., The Thaumarchaeon *N. gargensis* carries functional bioABD genes and has a promiscuous E. coli DeltabioH-complementing esterase EstN1. *Sci Rep* **2018,** *8* (1), 13823.

135. Cronan, J. E., Advances in synthesis of biotin and assembly of lipoic acid. *Curr Opin Chem Biol* **2018,** *47*, 60-66.

136. McLaughlin, M. I.; Lanz, N. D.; Goldman, P. J.; Lee, K. H.; Booker, S. J.; Drennan, C. L., Crystallographic snapshots of sulfur insertion by lipoyl synthase. *Proc Natl Acad Sci U S A* **2016,** *113* (34), 9446-9450.

137. Yu, N.; Jora, M.; Solivio, B.; Thakur, P.; Acevedo-Rocha, C. G.; Randau, L.; de Crecy-Lagard, V.; Addepalli, B.; Limbach, P. A., tRNA Modification Profiles and Codon-Decoding Strategies in *Methanocaldococcus jannaschii*. *J Bacteriol* **2019,** *201* (9).

138. Lyons, S. M.; Fay, M. M.; Ivanov, P., The role of RNA modifications in the regulation of tRNA cleavage. *FEBS Lett* **2018,** *592* (17), 2828-2844.

139. Jackman, J. E.; Alfonzo, J. D., Transfer RNA modifications: nature's combinatorial chemistry playground. *Wiley Interdiscip Rev RNA* **2013,** *4* (1), 35-48.

140. Anton, B. P.; Russell, S. P.; Vertrees, J.; Kasif, S.; Raleigh, E. A.; Limbach, P. A.; Roberts, R. J., Functional characterization of the YmcB and YqeV tRNA methylthiotransferases of Bacillus subtilis. *Nucleic Acids Res* **2010,** *38* (18), 6195-6205.

141. Reddy, D. M.; Crain, P. F.; Edmonds, C. G.; Gupta, R.; Hashizume, T.; Stetter, K. O.; Widdel, F.; McCloskey, J. A., Structure determination of two new amino acid-containing derivatives of adenosine from tRNA of thermophilic bacteria and archaea. *Nucleic Acids Res* **1992,** *20* (21), 5607-5615.

142. Schweizer, U.; Bohleber, S.; Fradejas-Villar, N., The modified base isopentenyladenosine and its derivatives in tRNA. *RNA Biol* **2017,** *14* (9), 1197-1208.

143. Wolff, P.; Villette, C.; Zumsteg, J.; Heintz, D.; Antoine, L.; Chane-Woon-Ming, B.; Droogmans, L.; Grosjean, H.; Westhof, E., Comparative patterns of modified nucleotides in individual tRNA species from a mesophilic and two thermophilic archaea. *RNA* **2020,** *26* (12), 1957-1975.

144. McCloskey, J. A.; Graham, D. E.; Zhou, S.; Crain, P. F.; Ibba, M.; Konisky, J.; Soll, D.; Olsen, G. J., Post-transcriptional modification in archaeal tRNAs: identities and phylogenetic relations of nucleotides from mesophilic and hyperthermophilic *Methanococcales*. *Nucleic Acids Res* **2001,** *29* (22), 4699-4706.

145. Noon, K. R.; Guymon, R.; Crain, P. F.; McCloskey, J. A.; Thomm, M.; Lim, J.; Cavicchioli, R., Influence of temperature on tRNA modification in archaea: *Methanococcoides burtonii* (optimum growth temperature [Topt], 23 degrees C) and *Stetteria hydrogenophila* (Topt, 95 degrees C). *J Bacteriol* **2003,** *185* (18), 5483-5490.

146. Sauerwald, A.; Sitaramaiah, D.; McCloskey, J. A.; Soll, D.; Crain, P. F., N6-Acetyladenosine: a new modified nucleoside from *Methanopyrus kandleri* tRNA. *FEBS Lett* **2005,** *579* (13), 2807-2810.

147. Lipsett, M. N., The isolation of 4-thiouridylic acid from the soluble ribonucleic acid of Escherichia coli. *J Biol Chem* **1965,** *240* (10), 3975-3978.

148. Esakova, O. A.; Grove, T. L.; Yennawar, N. H.; Arcinas, A. J.; Wang, B.; Krebs, C.; Almo, S. C.; Booker, S. J., Structural basis for tRNA methylthiolation by the radical SAM enzyme MiaB. *Nature* **2021,** *597* (7877), 566-570.

149. Arragain, S.; Garcia-Serres, R.; Blondin, G.; Douki, T.; Clemancey, M.; Latour, J. M.; Forouhar, F.; Neely, H.; Montelione, G. T.; Hunt, J. F.; Mulliez, E.; Fontecave, M.; Atta, M., Post-translational modification of ribosomal proteins: structural and functional characterization of RimO from *Thermotoga maritima*, a radical S-adenosylmethionine methylthiotransferase. *J Biol Chem* **2010,** *285* (8), 5792-5801.

150. Forouhar, F.; Arragain, S.; Atta, M.; Gambarelli, S.; Mouesca, J. M.; Hussain, M.; Xiao, R.; Kieffer-Jaquinod, S.; Seetharaman, J.; Acton, T. B.; Montelione, G. T.; Mulliez, E.; Hunt, J. F.; Fontecave, M., Two Fe-S clusters catalyze sulfur insertion by radical-SAM methylthiotransferases. *Nat Chem Biol* **2013,** *9* (5), 333-338.

151. Arragain, S.; Handelman, S. K.; Forouhar, F.; Wei, F. Y.; Tomizawa, K.; Hunt, J. F.; Douki, T.; Fontecave, M.; Mulliez, E.; Atta, M., Identification of eukaryotic and prokaryotic methylthiotransferase for biosynthesis of 2-methylthio-N6-threonylcarbamoyladenosine in tRNA. *J Biol Chem* **2010,** *285* (37), 28425-28433.

152. Atta, M.; Arragain, S.; Fontecave, M.; Mulliez, E.; Hunt, J. F.; Luff, J. D.; Forouhar, F., The methylthiolation reaction mediated by the Radical-SAM enzymes. *Biochim Biophys Acta* **2012,** *1824* (11), 1223-1230.

Chapter II: Investigation of modified F_{430} cofactors in methanogens

2.1 Abstract

Methanogenesis is the biological production of methane and is utilized by methanogenic archaea (methanogens) to generate energy. Cofactor F_{430}, a unique nickel-containing porphyrin, serves as the prosthetic group and catalytic component of methyl-coenzyme M reductase (Mcr), the enzyme that catalyzes the final methane-forming reaction in methanogenesis. Recently, F_{430} variants have been discovered in several methanogenic species, including *Methanococcus maripaludis* and *Methanocaldococcus jannaschii*. Here, we further explored the presence of F_{430} variants in these methanogens as well as in *Methanosarcina acetivorans* and the rumen methanogens *Methanobrevibacter smithii*, *Methanobrevibacter rumantium*, and *Methanobacterium bryantii*. In these analyses, we have identified a new variant, termed mercaptopropamide-F_{430}, that was not previously reported and is present in both *M. maripaludis* and *M. acetivorans*. This variant has an exact mass of 1008.3478 Da, a similar absorption spectrum as unmodified F_{430}, and was identified in a fraction of purified Mcr from *M. acetivorans*, suggesting that it functions with Mcr. Based on the exact mass, the identity of the modification is likely a mercaptopropamide moiety. Since it has a similar absorption spectrum to unmodified F_{430}, the modification preserves the adjacent ketone and thus is not cyclized. This is distinct from the previously identified mercaptopropionate-F_{430}. Our experiments have shown that in some conditions, mercaptopropamide-F_{430} comprises 30-50% of the total F_{430} pool. *M. jannaschii* was found to produce both mercaptopropamide-F_{430} as well as the previously described mercaptopropionate-F_{430}. Efforts to determine physiological conditions in which these methanogens consistently produce mercaptopropamide-F_{430} have led to inconsistent results so far, however, there is an apparent correlation in *M. maripaludis* between its production and stationary

phase of growth. In *M. acetivorans*, growth on acetate as the methanogenic substrate has yielded the most consistency in terms of high levels of mercaptopropamide-F_{430} production.

2.2 Introduction

Methanogenesis is the biological production of methane conducted by a group of obligate anaerobic microorganisms known as methanogens.[1] This metabolism has been around for at least 3.5 billion years, and today it produces an estimated total of 1 billion teragrams of methane annually.[2, 3] Methanogens are found in virtually all anaerobic environments in which organic matter is decayed, including the gut of mammals, rice fields, wetlands, ocean sediments, hydrothermal vents, and glacial ice.[1] Importantly, methane is a potent greenhouse gas as well as a globally vital fuel.[4, 5] Remarkably in nature, methanogenesis can also be reversed by the anaerobic methanotrophs (ANME), and this process, the anaerobic oxidation of methane (AOM), consumes about 300 Tg of methane annually.[6] Methanogenesis and AOM are characterized by unique traits that are interesting from both basic and applied scientific points of views. For example, the efficient reversal of methanogenesis to generate liquid fuels from natural gas would revolutionize the way we interact with this fuel.[7]

The major methanogenic pathways are the hydrogenotrophic, acetotrophic, and methylotrophic pathways.[3] Hydrogenotrophic methanogenesis is found in six of the eight methanogenic orders, with five existing as obligate hydrogenotrophs.[8] In this pathway, carbon dioxide is reduced to methane in a set of seven enzyme-catalyzed reactions with reducing equivalents typically generated from hydrogen or formate oxidation.[9] Acetotrophic methanogenesis is barred to only two methanogenic genera within the *Methanosarcinales*, including *Methanosarcina*, but produces two-thirds of methanogenic methane.[10] Here, the methyl group of acetate is reduced to methane, and the carbonyl oxidized to carbon dioxide. In

methylotrophic methanogenesis, found only in the *Methanosarcinales*, three methyl groups from methylated compounds, including methanol and methylamines, are reduced to methane and one oxidized to carbon dioxide.[11] AOM is found in the ANME-1, -2, and -3 clades and has robustly been shown to be essentially the reverse of the hydrogenotrophic methanogenesis, with methane oxidized to carbon dioxide using the same enzymes.[12, 13] Depending on the specific ANME organism(s) involved, the electrons produced in this process are either directly transferred to sulfate-reducing bacteria, the metals Fe(III) or Mn(IV), or used in nitrate reduction.[14-17] The ability to transfer electrons directly to partner bacteria and metals relies on the expression of large multiheme c-type cytochromes as well as pili acting as conductive nanowires.[18, 19]

Methyl-coenzyme M reductase (Mcr) is the central enzyme of methanogenic and AOM pathways (Figure 1.1).[20] Further, divergent Mcr enzymes have been implicated in the oxidation of other short-chain alkanes such as ethane, propane, and butane.[21] In methanogens and AOM, the enzyme catalyzes the rate-limiting step in methane production and oxidation, respectively. Structurally, Mcr is a dimer of a heterotrimer with a $\alpha_2ß_2\gamma_2$ configuration (Figure 1.2).[22] Each fully assembled enzyme contains two active sites, both containing the unique hydrocorphin cofactor F_{430} (Figure 2.1), deeply buried within the enzyme at the bottom of a 50 Å channel (Figures 1.2 and 1.4).[22] This cofactor is the catalytic component of the enzyme, and its only known physiological role is in the Mcr-catalyzed reaction (Figure 1.5).[22] Both the biosynthesis and the mechanism of Mcr-catalyzed reductive demethylation of CH_3-CoM with cofactor F_{430} have been characterized only recently (Figures 1.3 and 1.5).[23, 24]

Despite advances in Mcr-related research, much more is yet to be discovered. Two variants of cofactor F_{430}, one containing a methylthio moiety ("methylthio-F_{430}"), and one containing two methyl group substitutions ("dimethyl-F_{430}") have been discovered in crystal structures of Mcr

enzymes (Figure 1.6).[25, 26] Methylthio-F_{430} was discovered in ANME-1 Mcr, and likely is not found in other ANME clades, and is not found in any methanogens.[26] Recently, more divergent Mcr enzymes have been described.[27] It is likely, then, that more F_{430} variants will be discovered within these Mcrs. Variants of cofactor F_{430} have been discovered in several methanogens.[28] The most abundant of these was found to likely contain a cyclized mercaptopropionate group with a thioether in the same position as methylthio-F_{430} (Figure 2.1).[28] Other than their existence, cofactor F_{430} variants remain completely unstudied, and the function(s) they play in nature are not known. Methylthio-F_{430}, as it is only found in ANME-1, and is the main F_{430} used by this organism, may be involved in specializing Mcr for methane oxidation.

This chapter describes preliminary work undertaken to characterize the physiological roles of the recently identified F_{430} variants found in methanogens. For this, the model organisms *Methanococcus maripaludis* and *Methanosarcina acetivorans* are studied. These two organisms have well defined culturing conditions, established genetic systems, and relatively fast growth rates.[29, 30] Further, they belong to highly divergent methanogenic lineages. *M. maripaludis* is an obligate hydrogenotroph, whereas *M. acetivorans* can grow on methylated compounds and acetate, but not hydrogen. Further, cells from *Methanocaldococcus jannaschii*, a close relative of *M. maripaludis*, as well as the ruminant methanogens *Methanobrevibacter smithii*, *Methanobrevibacter rumantium*, and *Methanobacterium bryantii* were studied here in limited experiments. The original major goal of this project, to describe conditions in which *M. maripaludis* and *M. acetivorans* reliably produce F_{430} variants, produced inconsistent results. However, an apparently novel variant, mercaptopropamide-F_{430} is described that is produced in

high levels in these cells. Further, it was found in purified Mcr from *M. acetivorans*, suggesting it plays a role in Mcr catalysis.

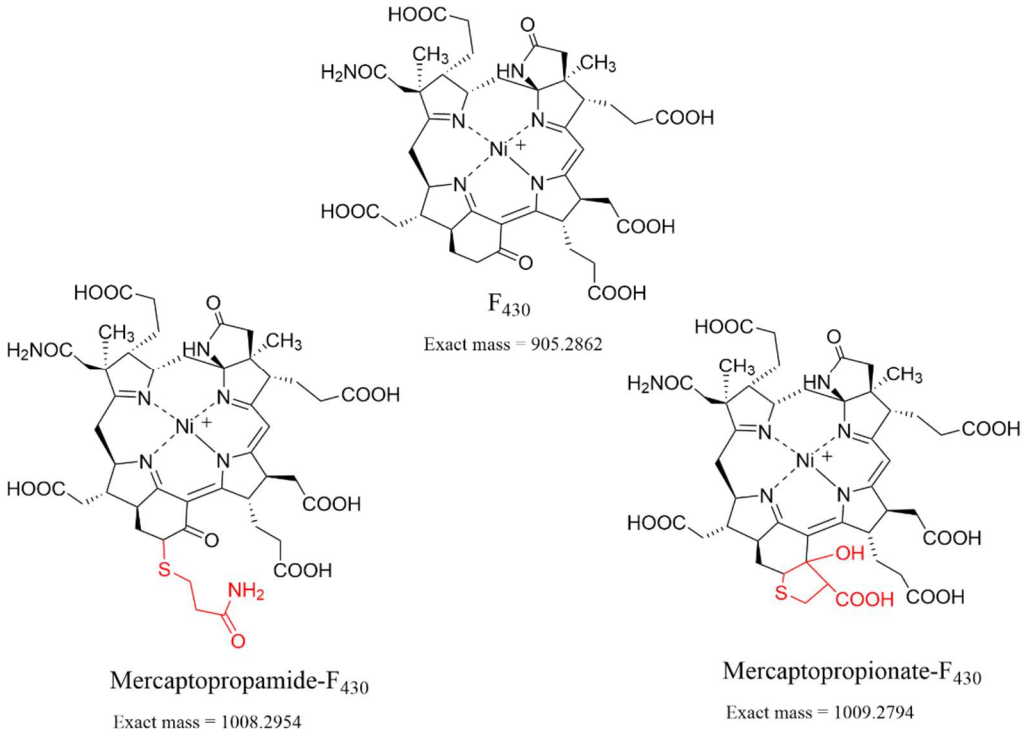

Figure 2.1. Structures of F_{430} and the two variants relevant to this chapter: mercaptopropamide-F_{430} and mercaptopropionate-F_{430}.

2.3 Methods

Cells and growth media. *Methanococcus maripaludis* S2 (DSM 14266) wild-type cells were obtained as a frozen glycerol stock from the Leigh lab (University of Washington). *M. maripaludis* was grown on either McCas, formate, or basal medium as previously described.[29] Cells were grown in either 25 mL Balch tubes (Chemglass) with 5 mL media, 155 mL serum bottles (Chemglass) with 50 mL of media, or 1 L bottles (Chemglass) with 300 mL growth media. When grown on McCas medium, cells were supplied with 80% H_2/20% CO_2 gas at a final pressure of 40 psi unless otherwise noted. Cells grown on formate and basal medium were supplied with 80% N_2/20% CO2 gas at a final pressure of 15 psi. Immediately before inoculating media, *M. maripaludis* media were reduced with 2.5% sodium sulfide to 0.05%. Inoculant was 5% of media

volume. On all media, cells were grown with light shaking at 37°C. Cells were grown to various growth stages, and were grown from anywhere between six to 72 hours.

A glycerol stock of *Methanosarcina acetivorans* C2A (DSM 2834) was obtained from the Ferry lab. Media was made as previously described with some slight deviations.[31] Sodium carbonate, solid Na_2HPO_4, cysteine, and sodium sulfide were omitted at first. After boiling the media for 10-15 min and letting it cool while bubbling with a stream of 80% N_2/20% CO_2, the media were brought into the box. Sodium bicarbonate (3.8g/L), NH_4Cl (1.0 g/L) and 1 M KH_2PO_4 (5 mL/L) were added. Water was added to the correct volume before adding in DTT (0.22 g/L). The media were supplemented with either 50 mM trimethylamine, 125 mM methanol, or 200 mM acetate either in the box while making the media or immediately before inoculating the media. Volumes of media were 10 mL in 25 mL Balch tubes, 75 mL in 155 mL bottles, and 550 mL in 1 L bottles. Immediately before inoculating media, *M. acetivorans* media were reduced to 0.025% sodium sulfide. Cells were inoculated at 10% volume of medium typically from cells freshly grown to exponential or stationary phase. Cells were grown typically from between 24 to 72 hours, or up to one month when grown on acetate. Freshly harvested *Methanolcaldococcus jannaschii* (DSM 2661) cells were obtained from the Mukhopadhyay lab (Virginia Tech). The cells were grown in medium previously described in serum bottles with shaking at 80°C.[32] Frozen cell pellts of *Methanobrevibacter smithii*, *Methanobrevibacter rumantium*, and *Methanobacterium bryantii* cells were also obtained from the Mukhopadhyay lab.

Cofactor F_{430} extraction. Cofactor F_{430} was extracted as previously described with some deviation.[33] *M. maripaludis* and *M. acetivorans* cells were harvested by centrifugation at 6,000 rpm for 15 min in 500 mL centrifuge bottles using a Fiberlite F12-6X500 LEX rotor (ThermoFisher). At first, cells were typically stored frozen, either dried or resuspended in a small

amount of water. However, most of the data described here were obtained with cells that were freshly harvested. In short, cell pellets were resuspended in 4 to 6 mL water, then sonicated for two cycles each for 2 min on ice. Pure formic acid was added to 1% by volume, bringing the pH of the solution down to ~2.5 and samples were then vortexed briefly. Acidified lysates were centrifuged for 5-10 min at 4,400 rpm in a Centrifuge 5702 (Eppendorf). To supernatants, 2.5 volumes of 50 mM Tris, pH = 7.5 ± .25 was added. Samples were subsequently further neutralized to a pH of around 7.0 with 6 M NaOH. Typically this required 3.75 volumes of formic acid initially added. The neutralized lysates were spun down once more, then applied to a 2 x 8 cm column containing Q Sepharose Fast Flow resin (GE Healthcare). The resin was washed with 10 mL 50 mM Tris buffer, pH = 7.5 ± .25, then F_{430} was eluted in 10 mL of 20 mM formic acid. The collected fractions were then concentrated down to 500 µL or less using a Vacufuge (Eppendorf) at 30°C, then applied to an Amicon Ultra filter (Millipore) with a cut off of 3 kDa to remove any remaining proteins. Filters were washed twice with 200 µL of water and the filtrate dried down to 100 µL or less.

Alternative F_{430} extraction procedures were explored in an attempt to determine the effect of different procedures on the distribution of cofactor F_{430} variants. These included using acetonitrile instead of formic acid to denature proteins. Here, acetonitrile was added to 50% total sample volume. After quickly vortexing the sample, the precipitated proteins were removed by a 5-10 min centrifugation at 4,400 rpm. Acetonitrile was removed by drying under vacuum at 30°C to at least the pre-acetonitrile volume (about 20 min). Samples were processed either as described above, or with a step gradient of 1 M ammonium bicarbonate or 1 M ammonium acetate. The pH of the former is basic (~7.9) when freshly made but increases to more than 10.0 over time, so ammonium acetate was tested as an alternative, as it is pH neutral. A typical step gradient is 10%,

20%, 30%, 50%, and 100% of respective salt, with deionized water used as diluent. Other extraction procedures consisted of using HEPES pH = 7.5 buffer in place of Tris.

The extraction procedures as described above, from start to finish, take over a day to complete, and sometimes multiple days. Therefore, the effect of letting samples incubate for periods of time at distinct steps on the distribution of F_{430} was tested. Specifically, samples were left to incubate as total lysate (cells resuspended in water and sonicated), in 1% formic acid, neutralized cell lysate, and as eluant from anion exchange.

Cofactor analysis by LC-MS and HPLC. To detect cofactor F_{430} and the presence or absence of variants, concentrated protein-free samples were routinely analyzed by LC-MS. We employed a Waters Acquity UPLC with a TQD mass spectrometer equipped with an Acquity Premier HSS T3 (2.1 x 100 mm, 1.8 µm pore size) column. Solvent A was 0.1% (v/v) formic acid in water and solvent B was 100% methanol. The flow rate was 0.35 mL/min and the LC program consisted of 2 min at 95% A followed by a 10 min linear gradient to 50% B, then a 3 min gradient to 95% B. The injection volume was typically 2 µL. The source temperature was 150°C, the desolvation temperature was 500°C, the desolvation gas flow was 800 L/hr, and the cone gas flow was 50 L/hr. The mass spectrometer was operated in positive mode and scanned for *m/z* values ranging from 400 to 1200. To detect cofactor F_{430}, which was always present and visible in the total ion chromatogram as one of the most intense peaks, total ion chromatograms were extracted with an *m/z* of 905 Da and a window of 1 Da. Mercaptopromamide-F_{430} and mercaptopropionate-F_{430} were detected by extracting for an *m/z* of 504.5 and 505 or 1009, respectively, all with a window of 1 Da. Typically, mercaptopropamide-F_{430} was most abundant as the doubly charged species, whereas we found mercaptopropionate-F_{430} to be abundant in both doubly and single charges species.

To determine UV-Vis spectra associated with cofactor F_{430} and variants, a Shimadzu HPLC equipped with a photodiode array detector and a Kinetex Polar C18 column (Phenomenex, 2.6 μm, 150 x 4.6 mm) was used. The column oven had a temperature of 30°C. Solvent A was 0.1% (v/v) formic acid in water and solvent B was 100% methanol. The flow rate was 0.7 mL min^{-1} and the method consisted of 95% A for 3 min followed by a 20 min linear gradient to 70% B, then a 1 min linear to 100% B followed by 100% B for 3 min. The PDA scanned for wavelengths between 190 and 800 nm with a frequency of 1.56 Hz. Cofactor F_{430} is known to have an absorbance maximum at 430 nm, and the absorbance spectrum for variants were validated by elution time, which corresponds to elution time in LC-MS analysis. In these analyses, 10 μL of concentrated cell extract was used.

To obtain the exact mass of mercaptopropamide-F_{430}, samples confirmed to contain this variant were sent to a high-resolution mass spectrophotometer operated by the Virginia Tech Mass Spectrometry Incubator. The system consisted of a Waters SYNAPT G2-S high-definition mass spectrometer interfaced to a Waters Acquity UPLC I-class system with an Acquity UPLC BEH C18 column (2.1 x 75 mm, 1.7 μm pore size; Waters). Solvent A was 0.1% formic acid in deionized water and solvent B was acetonitrile. The flow rate was 0.2 mL/min and 10 μL of sample was injected. The gradient began at 95% A with a 6 min linear gradient to 15% B, a 15 min gradient to 35% B, and a 2 min gradient to 65% B. The mass spectral data were collected in high-resolution MSe continuum mode (nonselective MS/MS acquisition mode).

Mcr purification. An Mcr purification was carried out using methods described previously.[34] All steps were carried out in a strictly anoxic glovebox under an atmosphere of roughly 77% N_2, 20% CO_2, and 3% H_2 unless mentioned otherwise. Buffers were made outside the glovebox then brought inside the glovebox in glass bottles at least two days before use. Each

buffer was stirred overnight with its cap off. *M. acetivorans* cells were grown in a mix of thirty-three 155 mL and two 1 L bottles. Thirty of the 75 mL bottles were grown on 40, 100, or 200 mM acetate and half of these were inoculated by cells habituated to methanol. Six (one from each acetate concentration-starter culture combination) of these bottles were harvested after nine days of growth, and the rest were grown for six weeks. Three of the 75 mL bottles and the 1 L bottles were grown for four and a half weeks, and both were grown on 200 mM acetate from acetate-habituated cells. One 75 mL bottle grown for six weeks from each acetate and starter culture condition (six bottles total) was harvested separately and taken through an F_{430} extraction following the above protocol. The rest of the cells, 3.05 L of culture, were harvested together by spinning for 15 min at 6,000 rpm anaerobically. The cell pellet was weighed anaerobically and found to have a mass of 4.42 g, then brought into the glovebox. The cells were resuspended in 11.5 mL 50 mM Tris, pH = 7.6 supplemented with 10 mM coenzyme M (Buffer A). Then, the cells were sonicated for a total of seven two min cycles and spun down at 15,000 rpm in a Sorvall SS-34 rotor for 45 min. To the 10 mL of recovered supernatant, 275 µL were set aside, and to the rest, 23.3 mL saturated (4.1 M) ammonium sulfate was added to give a 70% saturated solution. This was stirred for 30 min then spun down, again at 15,000 rpm. Mcr is soluble in 70% saturated ammonium sulfate, and the soluble fraction, which was a yellow-green color, was poured into a beaker. The pellet was set aside for the time being. To precipitate out all remaining proteins, including Mcr, 7.06g of $(NH_4)_2SO_4$ was slowly added while stirring to give a solution of 100% saturation. However, even after 45 min of stirring, there was noticeable $(NH_4)_2SO_4$ that had not yet dissolved. While trying to avoid carrying over any solid $(NH_4)_2SO_4$, the solution was poured into a centrifuge bottle and spun down, again at 15,000 rpm. After spinning, a noticeable amount of $(NH_4)_2SO_4$ had crashed out of the solution, potentially as $(NH_4)_2SO_4$ saturation was calculated

for 25°C and the rotor was cooled to 4°C. The pellet, however, was noticeable yellow, and was the expected size. The pellet, along with some residual $(NH_4)_2SO_4$, was dissolved in 2.5 mL Buffer A. The solution, which was very yellow in color, was applied to a PD-10 desalt column (GE Healthcare) equilibrated in Buffer A. The excess $(NH_4)_2SO_4$ was removed by eluting protein in 3.5 mL Buffer A. However, a yellow band was noticeably still in the resin, which was collected in the next 5 mL and set aside. To the 3.5 mL, Buffer A was added to 10 mL. A 1 mL aliquot of this was set aside ("pre-AEX sample" below). Then, the solution was applied to a 2 x 8 cm column with about 2 mL Q Sepharose Fast Flow resin equilibrated with Buffer A. The resin was washed with 15 mL Buffer A, then proteins were eluted in a step gradient with Buffer A and Buffer B (50 mM Tris, 1 M NaCl, 10 mM CoM, pH = 7.6). The step gradient consisted of 5 mL fractions of 10%, then 20%, 30%, 40%, 50%, and finally 100% Buffer B, with A as diluent. During this time, the pellet from the 70% $(NH_4)_2SO_4$ precipitation step was dissolved into 2.5 mL Buffer A that had been diluted five-fold. It was then desalted into five-fold diluted Buffer A and set aside. Based off of the yellow color of the 30% B fraction and previous papers, the majority of Mcr was predicted to be localized in the 30% fraction. Immediately, this fraction was concentrated using an Amicon Ultra filter with a cutoff of 100 kDa to 2 mL. Buffer A was added to 2.5 mL, and this was desalted with the same PD-10 desalt column described above equilibrated with five-fold diluted Buffer A. The same buffer was used as the elution buffer. At this step, the sample was brought out of the box and subjected to aerobic conditions. F_{430} was purified as described above. The sample drying and analysis steps were completed the next day, starting roughly three hours after collecting the 20 mM HCOOH eluant, and was completed in the evening. 15 µL samples taken throughout the purification process were analyzed by SDS-PAGE. The 40% and 50% B fractions contained some Mcr, but more so in the former, and the 30% B fraction had about five times as much as the 40%

B fraction. Excess salt and Tris were removed by concentrating these 5 mL fractions down to 1.5 mL with an Amicon Ultra filter with a cut off of 10 kDa, adding two-fold diluted Buffer A to about 12 mL, and concentrating back down to 1.5 mL. This process was repeated once. Alongside these samples, the total lysate sample, desalted 70% $(NH_4)_2SO_4$ pellet, and the "pre-AEX" sample were taken out of the glovebox into aerobic conditions. The 40% and 50%, and lysate samples were diluted to a total volume of 4 mL, the pre-AEX sample to 5 mL, both with water. F_{430} was processed as described above.

Investigation of original methanol and heat extraction on the distribution of F_{430} variants. The initial paper describing F_{430} variants in various methanogens, including mercaptopropionate-F_{430} but not mercaptopropamide-F_{430}, used a different purification scheme than the one described here.[28] Since we began to see mercaptopropamide-F_{430} as the main variant, we tested the effect that the initial protocol has on extracts containing mercaptopropamide-F_{430}, as well as samples containing no F_{430} variant as both a control and a test to see if this would result in the abiotic production of a previously described F_{430} variant. Extracts were first produced and analyzed as described above. Samples were about 100 µL, and to these 1.2 volumes of 100% methanol was added then samples were incubated in water heated to 100°C for fifteen min. Samples were dried on the Vacufuge to less than the original volume, and water was added to roughly the original volume. Samples were injected into the LC-MS system as described above.

2.4 Results and discussion

Growth experiments with M. maripaludis. F_{430} variants have been discovered in both ANME organisms as well as methanogens. In methanogens, the F_{430} variants are generally produced as a minor component compared to the canonical unmodified F_{430}. Thus, methanogens may be producing F_{430} variants in response to specific growth conditions and understanding when

specific variants are produced could provide clues about their functions. To gain insight into potential conditions in which *M. maripaludis* either does or does not produce F_{430} variants, this methanogen was grown in different conditions and the presence of F_{430} variants was analyzed by LC-MS. We found that the molecular ion of the major modified F_{430} produced in these cultures was M^+=1008 and the high-resolution mass of the compound was later shown to be 1008.3478 Da. This is one mass unit less than the previously identified mercaptopriopionate-F_{430} (Figure 2.1) and thus we proposed that this new F_{430} variant contained an amide in place of a carboxylic acid. There are several locations where this conversion could occur to the F_{430} structure, but we currently propose that the modification is a mercaptopropamide moiety (Figure 2.1). The characterization of this new modification will be discussed more below.

Early experiments indicated that incubating *M. maripaludis* at room temperature without shaking after growing to stationary phase is associated with the production of cofactor F_{430} variants. However, experiments set up to either repeat this result, or to test a related condition that could be involved in stimulating F_{430} variant production in this context, failed to give consistent results. Cells were typically frozen for later use, and it was later shown that this could somehow result in the loss of mercaptopropamide-F_{430} (discussed in the *M. acetivorans* section below). Processing samples immediately, or maybe some other cause, resulted in observing mercaptopropamide-F_{430} much more frequently.

After mercaptopropamide-F_{430} began to be found in cell extracts more frequently, experiments were carried out to determine the reproducibility of these experiments. The initial observation that late-stage growth is involved in increased production of F_{430} variants was used as a starting point. As opposed to taking an earlier strategy of testing as many different conditions as possible in each experiment, multiple culture bottles were grown in the same condition per

experiment, and these bottles were individually harvested and processed as opposed to combining media from multiple bottles into one cell pellet.

It was found that results were reproducible between replicates within the same growth experiment, but not so much across different experiments. All the described experiments were carried out with McCas medium, as this was shown early on to result in the most modified F_{430} production. The first experiment consisted of growing five bottles of McCas together and growing three for two days on the shaker followed by one day of sitting on the bench, and growing the other two for the full three days. Here, no culture produced mercaptopropamide-F_{430}. The next experiment consisted of growing six bottles on the shaker for two days, and then all six were removed from the shaker. Three were left on the bench for three days and three for five days before harvesting. All six bottles had a pool of F_{430} consisting of about 40% mercaptopropamide-F_{430} (range: 36.3-50.5%, mean: 42.9%). Like in the previous experiment, in the subsequent experiment six bottles were grown for two days and removed from the shaker together. Two of these bottles were harvested without any time of the bench, another two were harvested after two days of siting on the bench, and the last two after three days on the bench. Thus, this partially replicated the preceding experiment. However, none of these six samples contained mercaptopropamide-F_{430}, with the exception of the cells that were immediately harvested after 2 days of growth, which had relatively low amounts of 1.6% and 6.8%.

After showing that experiments are internally consistent with one another (i.e. replicates of different cultures in a given experiment show similar results), we next attempted to alter growth conditions to potentially identify conditions that result in increased mercaptopropamide-F_{430} production. Some conditions tested were: 1 M NaCl (regular McCas is made with 376 mM), regular salt concentration but made with less dithiothreitol (1.4 mM instead of 3.2 mM), and cells

grown without the addition of sodium sulfide before inoculation. The latter two conditions were meant to induce low levels of oxidative stress. The distribution of F_{430} was as follows: cells grown on regular media that received sodium sulfide had 54.9% mercaptopropamide-F_{430} and the cells grown on regular media that did not receive sodium sulfide had 49.9% mercaptopropionate-F_{430}. Cells grown on 1 M NaCl and without the addition of sodium sulfide had 65.4% and 64.3% mercaptopropionate-F_{430}, and cells grown on the normal salt concentration and also did not receive sodium sulfide had 56.8% and 62.7% mercaptopropionate-F_{430}. Therefore, the replicates had very good internal consistency with one another, and the added stress (osmotic or oxidative) resulted in a modest increase in mercaptopropamide-F_{430}, while sulfide limitation apparently by itself has little-to-no effect. This also validates the hypothesis that there is a correlation between late-stage growth and/or letting cells that have reached stationary phase sit on the bench for some time and mercaptopropamide-F_{430} production, as these cells were grown to stationary phase and left to sit on the bench for a day.

However, while these experiments showed that there is internal consistency within experiments, a limitation of these experiments is that other growth stages were not experimented with. Therefore, we cannot conclude that mercaptopropamide-F_{430} is induced specifically by conditions in late-stage growth, especially as cells grown to stationary phase were shown to not consistently produce mercaptopropamide-F_{430}.

Growth experiments with M. acetivorans. Early on, experiments in *M. acetivorans* failed to obtain significant amounts of any modified F_{430}, including experiments where the organism is grown on either acetate, methanol, or trimethylamine. More recently, probably partly due to the optimization of our purification protocol, we have been able to obtain consistent results with this organism also producing mercaptopropamide-F_{430}. The most consistent results we observed were

with acetate-grown cells, and therefore many of our experiments have focused on this substrate. Acetotrophic methanogenesis, notably, is the least thermodynamically favorable form of methanogenesis, thus the production of mercaptopropamide-F_{430} may be associated with a low energy state in the cell. Different conditions with acetate-grown cells that are described below included different acetate concentrations (40, 100, 200 mM), starting from either methanol- or acetate-habituated starter cultures, and harvesting the cultures at different ODs.

When growing *M. acetivorans* on acetate from methanol-habituated cells, there is a lag phase of about one month. In an early experiment, cells were harvested after about one month of growth (two 500 mL media bottles, combined to one cell pellet, bottles had OD_{600}s of 0.51 and 0.25). A small portion of the cells were immediately used for an F_{430} prep while the rest were stored frozen. Surprisingly, while the cells immediately processed had a significant amount of mercaptopropamide-F_{430} (17.5% relative to total amount of F_{430}), the cells that were first frozen then processed for F_{430} content 1.5 weeks later did not have any modified F_{430} at all. We thought that it must be important, for some reason, to prepare cells immediately. This is significant since a large number of previous F_{430} extractions done up until this point utilized cells that were frozen for later use. In subsequent experiments, freshly harvested cells were immediately put into the F_{430} extraction procedure.

Based off of the *M. maripaludis* experiments, we were especially interested in if the production of F_{430} variants was growth-phase dependent. Thus, a set of four bottles started at the same time were harvested at different OD_{600}s. One bottle was harvested at an OD of 0.29 and was found to have 24.8% mercaptopropamide-F_{430}. Another bottle was harvested at an OD of 0.54 and was found to have 56.4%. The third bottle was harvested at an OD of 0.70 and found to have 14.9%. The last bottle was allowed to sit in the incubator for another week, and had an OD of 0.76

when harvested, and found to have no mercaptopropamide-F_{430}. Therefore, at least for this experiment, there was a general trend associated with greater amounts of the modified F_{430} in early-to-mid log phase and a decrease in later stages of growth. Another experiment was conducted to try to repeat this finding. Similar to above, four bottles were started, but this time one was inoculated with acetate-habituated cells, while the three other bottles were inoculated with methanol-habituated cells. After six days of growth, the bottle started from acetate-habituated cells reached an OD of 0.58 and was harvested. The cells were found not to contain any modified F_{430}. About a month after starting the cells, one of the three remaining bottles was harvested at an OD of 0.18. The cells were found to have 48.4% mercaptopropamide-F_{430}. The remaining two bottles were used for an Mcr prep along with other cells (below).

To test if the switch from methanol to acetate might trigger the production of modified F_{430} variants, as well as the effect of varying acetate concentration, cells were grown in 75 mL media from acetate-or methanol-habituated cells with media supplied with either 40, 100, or 200 mM acetate in five-fold replication (a total of 30 bottles). A set, one bottle of each acetate concentration, of cells from the acetate-to-acetate experiment (3 bottles total) were grown for ten days, at which point they had already reached stationary phase, then harvested. For cells grown on 40 mM acetate stationary phase was found to be reached at an OD of 0.25, on 100 mM this was about 0.50, and on 200 mM this was 0.85. The cells grown on 40 mM were found to have 5.2% mercaptopropamide-F_{430}, 100 mM had 9.67%, and 200 mM had 3.7%. The remaining cultures were life in the incubator for an additional four weeks, when they were used in an Mcr purification (below). Notably, these cells that were grown for a longer time period and were started at the same time, had far greater concentrations of mercaptopropamide-F_{430}.

After having some consistency with finding mercaptopropamide-F_{430} in *M. acetivorans* cells grown on acetate, we decided to try to purify Mcr in order to gain evidence for this F_{430} variant associating, or not associating, with the enzyme. Cells were harvested in batch from two different experiments, both described above. A set of 75 mL bottles comprising the three acetate concentrations and inoculation from either methanol- or acetate-habituated cells (6 in total) were set aside at the onset of the Mcr purification were not analyzed until the next day. All six of the resulting F_{430} samples were found to contain mercaptopropamide-F_{430}. Precisely, the samples had a range from 43.7% to 56% mercaptopropamide-F_{430} relative to the total pool of F_{430}. There was no apparent correlation between acetate concentration and the percent of the modified F_{430}, but samples started from methanol-habituated cells had a slightly increased percentage (52.1% vs 44.8%).

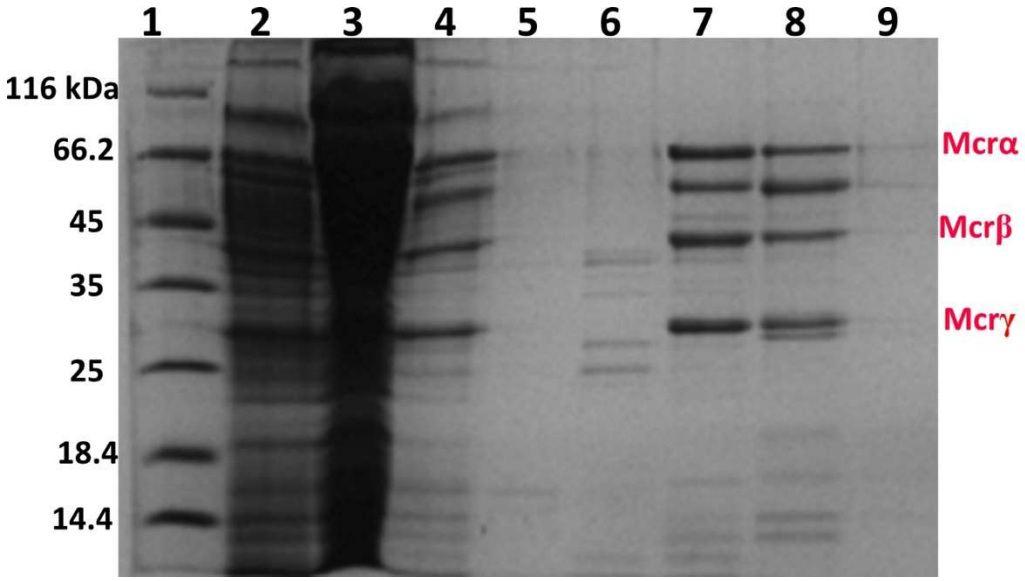

Figure 2.2. Gel image from *M. acetivorans* Mcr purification. From left: lane 1: protein marker, 2: total cell lysate, 3: 70% $(NH_4)_2SO_4$ pellet, lane 4: before anion exchange (sample in 3.5 mL), lane 5: 100 mM NaCl, lane 6: 200 mM NaCl, lane 7: 300 mM NaCl, lane 8: 400 mM NaCl, lane 9: 500 mM NaCl. Mcrα is 62 kDa, Mcrβ is 42.8 kDa, and Mcrγ is 27.6 kDa

Mcr was purified using ammonium sulfate precipitation and anion exchange chromatography under anaerobic conditions. The majority of Mcr eluted in the 300 mM NaCl fraction from the anion exchange column, with lower, but significant amounts in the 400 mM fraction and a very low amount in the 500 mM NaCl fraction (Figure 2.2). It was found that the 300 mM NaCl fraction, which had the most Mcr, had a significant amount of mercaptopropamide-F_{430}, at 59.5% of the total F_{430} pool (Figure 2.3). In contrast, the 400 mM and 500 mM NaCl Mcr fractions were found to contain only unmodified F_{430}. This could be a result of structural influences mercaptopropamide-F_{430} plays on Mcr. Potentially, this could also be a result of relatively how quickly the samples were purified. The F_{430} was purified from the 300 mM NaCl fraction immediately, while other fractions were not processed for about 24 hours. Interestingly, the total lysate sample left aside at the start of the purification was also found to contain only F_{430}. This sample was left at room temperature for well over 24 hours. At the same time, the F_{430} distribution of the pre-anion exchange sample that was set aside was coherent with the idea that there existed two fractions of Mcr, one containing mercaptopropamide-F_{430} and one containing only the

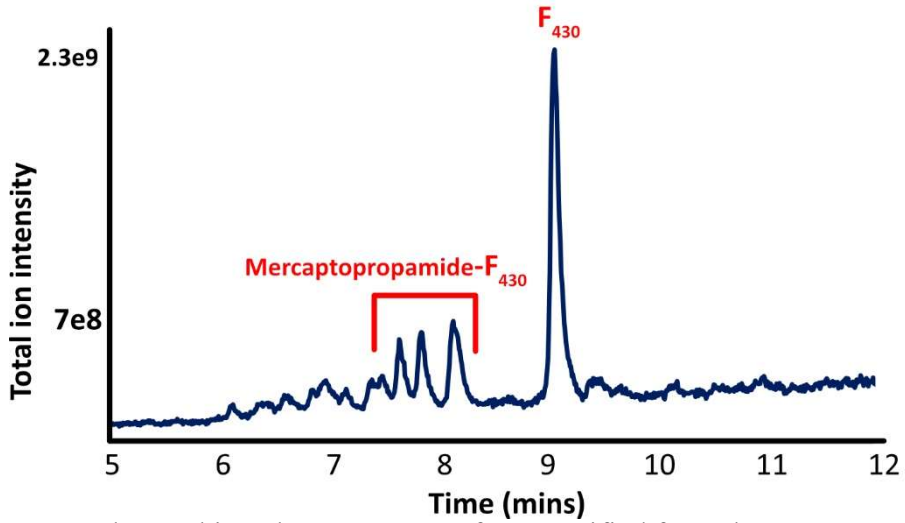

Figure 2.3. The total ion chromatogram of F_{430} purified from the 300 mM NaCl fraction (Figure 2.2, above). Peaks that correspond to mercaptopropamide-F_{430} and the major F_{430} peak are labeled.

unmodified version, and that these two fractions were partially isolated in the subsequent column purification. Specifically, this sample had 41.2% mercaptopropamide-F_{430}.

Analysis of F_{430} distribution in M. jannaschii*,* M. smitii*,* M. ruminantium*, and* M. bryantii.

We were interested in seeing how widespread mercaptopromamide-F_{430} and mercaptopropionate-F_{430} are in methanogens as a whole. Also, phylogenetically distinct methanogens may produce novel variants. *M. jannaschii* is far more closely related to *M. maripaludis* relative to *M. acetivorans*, but is a hyperthermophile that grows optimally at 85°C. Also, *M. jannaschii* was shown previously to produce mercaptopropionate-F_{430}, and we were interested in seeing if we would, in our new F_{430} purification scheme, see mercaptopropamide-F_{430} in place of the original mercaptopropionate variant.[28] Another relevant difference between *M. jannaschii* and the other methanogens we have previously studied is that this organism produces two isozymes of Mcr, and it would be of interest to see if only one of these isozymes (if any) binds an F_{430} variant. The cells we obtained from Dr. Mukhopadhyay's lab were grown to an OD of 0.98, which corresponds to late-exponential to early-stationary phase for this organism. Interestingly, we found that the cell extracts contained both mercaptopropamide-F_{430} and mercaptopropionate-F_{430}, and produced mercaptopropionate-F_{430} in high abundance (Figures 2.4 and 2.5). Specifically, the F_{430} pool consisted of 39.74% mercaptopropionate-F_{430}, 7.15% mercaptopropamide-F_{430}, and 53.13% unmodified F_{430}. The finding of mercaptopropionate-F_{430} in these samples validates this compound as a natural methanogenic product. In recent experiments, we have not seen mercaptopropionate-F_{430} in *M. maripaludis* or *M. acetivorans*, and our current F_{430} purification scheme is far different from the one described in the original paper. Thus, *M. jannaschii* is an attractive route to further characterize this F_{430} variant.

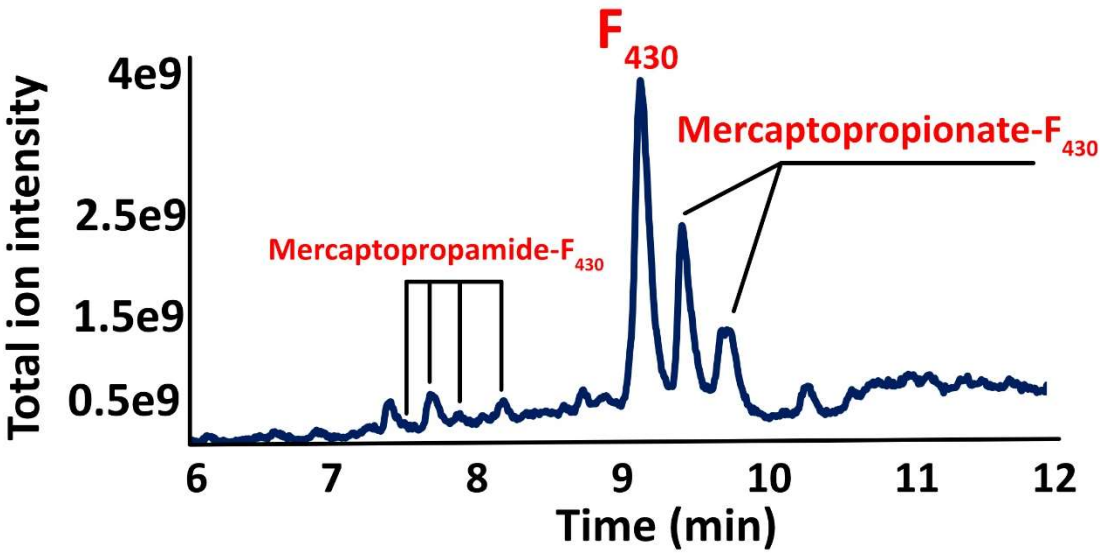

Figure 2.4. Total ion chromatogram from F_{430} purification performed on *M. jannaschii* cells. Peaks found to be associated with cofactor F_{430} and its variants are labelled.

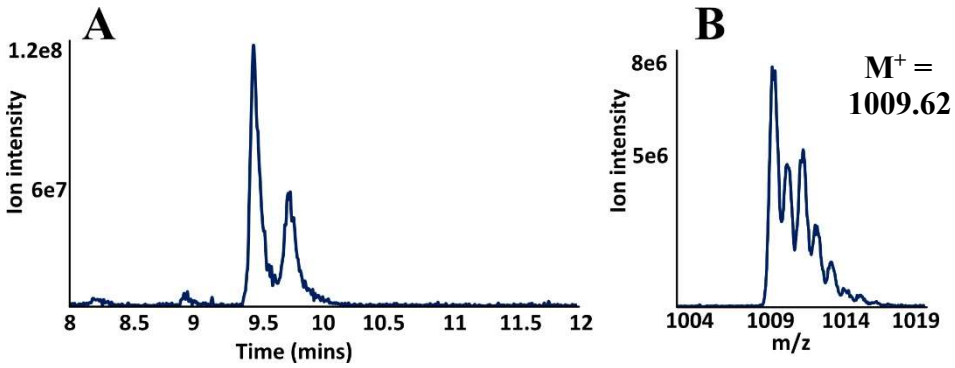

Figure 2.5. A: Extracted ion chromatogram for an *m/z* of 1009 and a window of 1.0. **B**: The mass spectrum associated with mercaptopropionate-F_{430}. Note mercaptopropionote-F_{430} has an exact mass of 1009.2794. Here, in our TQD mass spectrometer it is observed as 1009.62. This mass of this sample will be confirmed by high-resolution mass spec in the future.

Methanobrevibacter smithii, *Methanobrevibacter rumantium*, and *Methanobacterium bryantii* are members of an entirely different order from the other methanogens studied here. Specifically, these are found in the *Methanobacteriales*.[35] All three of these organisms only have the capacity for hydrogenotrophic methanogenesis, and *M. bryantii* also does not have the capacity to utilize formate for methanogenesis.[36] *M. rumantium* and *M. smithii* are common inhabitants of

the complex rumen microbiome, with the latter also being the most abundant archaeon in the human gut.[37, 38] Therefore, these species represented an opportunity to diversify the scope of F_{430} variants to another order and lifestyle of methanogenic archaea. However, no F_{430} variants were found in the cells provided to us. The lack of modified F_{430} compounds in the analyzed samples could potentially have been a result of freezing the cells before F_{430} analysis.

Characterizing the UV-Vis spectrum of F_{430} variants. The original description of mercaptopropionate-F_{430} showed the molecule has a drastic difference in absorption spectrum compared to unmodified F_{430}.[28] This was used as evidence for the proposed structure, as it

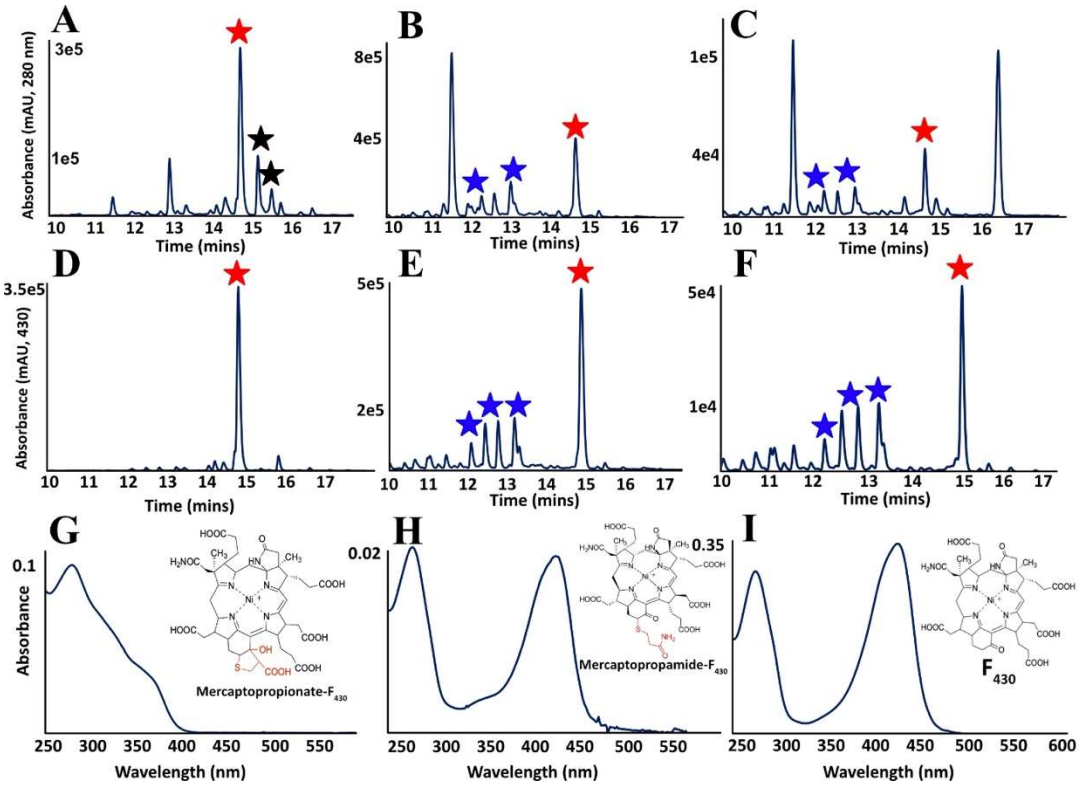

Figure 2.6. Analysis of samples shown to have mercaptopropionate or mercaptopropamide-F_{430} by LC-MS using an HPLC connected to a photodiode array detector. Panels **A-C**: Absorbance chromatograms at 280 nm of samples from *M. jannaschii* (**A**), *M. acetivorans* (**B**), and *M. maripaludis* (**C**) samples. Panels **D-F**: Absorbance chromatograms at 430 nm from *M. jannaschii* (**D**), *M. acetivorans*, and (**E**) *M. maripaludis* samples. Panels **G-I**: UV-spectrum of mercaptopropionate-F_{430} (**G**), mercaptopropamide-F_{430} (**H**) and unmodified F_{430} (**I**). Red stars indicate peaks corresponding to unmodified F_{430}, blue stars to peaks corresponding to mercaptopropamide-F_{430}, and black stars to mercaptopropionate-F_{430}.

indicated the reduction of the 17[3] ketone to an alcohol. To characterize the novel mercaptopropamide-F_{430}, we used high-performance liquid chromatography coupled to a photodiode array detector. The absorbance at 280 nm allowed us to simultaneously detect all cofactor variants, and the absorbance at 430 nm was used to detect F_{430} and any other variant that absorbs at 430 nm. It was found that mercaptopropamide-F_{430} does indeed have a very similar absorption spectrum as unmodified F_{430} (Figure 2.6). In contrast, mercaptopropionate-F_{430} found in the *M. jannaschii* extract allowed us to confirm the previously described absorption spectrum for mercaptopropionate-F_{430} (Figure 2.6).

Effect of methanol and heat on the distribution of F_{430} variants. The cofactor F_{430} purification scheme differs significantly from the protocol used in the paper that originally described methanogenic F_{430} variants.[28] The protocol used here is in essence the same as the one used to isolate methylthio-F_{430}.[33] Since we have only really seen mercaptopropamide-F_{430} as the dominant F_{430} variant, and this variant is not described in the original paper, we were interested in determining the effect of the methanol and heat protocol has on mercaptopropamide-F_{430}. Further, we wanted to see what happens to cofactor F_{430} when treated in this manner.

The methanol and heat protocol was found to result in a decrease in both cofactor F_{430} and mercaptopropamide-F_{430} and an increase in other *m/z* values containing a Ni isotopic pattern that are absent in non-treated samples. Mercaptopropionate-F_{430} was not found in the treated samples. This gives credence to mercaptopropionate-F_{430} not being a byproduct of the methanol and heat purification scheme. Further, none of the degradation products containing a nickel signature were described in the original paper.

The effect of alternative purification schemes on F_{430} distribution. While our protocol is essentially the protocol described elsewhere, it is still true that there are at times extreme

differences in F_{430} distribution in cells grown in similar conditions (though, rarely when replicates are grown together). We therefore wanted to try different purification schemes using acetonitrile in place of formic acid. Downstream, we also tried swapping formic acid for volatile salts such as ammonium acetate and ammonium bicarbonate in anion exchange. Further, the purification scheme as described in this work takes, at best, 1-3 days between lysing the cells and LC-MS analysis. Samples, by necessity, are left overnight at discrete steps. Therefore, we also tried to measure the effect of this on F_{430} distribution. However, to date, nothing of value has come from these experiments. In the times we tried alternative methods or incubating the samples at prolonged times in discrete purification steps, no sample, including, importantly in samples prepared side-by-side using our established purification scheme, has shown to have an F_{430} variant.

2.5 Concluding remarks

In this chapter we describe mercaptopropamide-F_{430}, a novel F_{430} variant that is highly produced in some conditions in three methanogens: *M. maripaludis*, *M. acetivorans*, and *M. jannaschii*. This variant has a similar absorption spectrum as unmodified F_{430}, has an exact mass of 1008.3478 Da, and associates with Mcr purified from *M. acetivorans*. Based on its absorption spectrum and exact mass, we propose a structure (Figure 2.1). We further describe certain conditions in *M. maripaludis* and *M. acetivorans* in which there is a correlation with mercaptopropamide synthesis. Also, we demonstrate *M. jannaschii* produces this novel variant as well as the previously described mercaptopropionate-F_{430}. The purification scheme we developed here differs significantly from that used to first characterize mercaptopropionate-F_{430}, and validates this molecule as a natural product that is likely physiologically relevant. Future investigations will more rigorously show these variants are not abiotically produced, identify more

specific conditions in which the variants are produced, and determine their physiological relevance.

References

1. Lyu, Z.; Shao, N.; Akinyemi, T.; Whitman, W. B., Methanogenesis. *Curr. Biol.* **2018,** *28* (13), R727-R732.

2. Ueno, Y.; Yamada, K.; Yoshida, N.; Maruyama, S.; Isozaki, Y., Evidence from fluid inclusions for microbial methanogenesis in the early Archaean era. *Nature* **2006,** *440* (7083), 516-519.

3. Thauer, R. K.; Kaster, A. K.; Seedorf, H.; Buckel, W.; Hedderich, R., Methanogenic archaea: ecologically relevant differences in energy conservation. *Nature reviews. Microbiology* **2008,** *6* (8), 579-591.

4. Admistration, U. S. E. I. Electricity explained *Electricity in the United States*.

5. Alvarez, R. A.; Zavala-Araiza, D.; Lyon, D. R.; Allen, D. T.; Barkley, Z. R.; Brandt, A. R.; Davis, K. J.; Herndon, S. C.; Jacob, D. J.; Karion, A.; Kort, E. A.; Lamb, B. K.; Lauvaux, T.; Maasakkers, J. D.; Marchese, A. J.; Omara, M.; Pacala, S. W.; Peischl, J.; Robinson, A. L.; Shepson, P. B.; Sweeney, C.; Townsend-Small, A.; Wofsy, S. C.; Hamburg, S. P., Assessment of methane emissions from the U.S. oil and gas supply chain. *Science* **2018,** *361* (6398), 186-188.

6. Knittel, K.; Boetius, A., Anaerobic oxidation of methane: progress with an unknown process. *Annu Rev Microbiol* **2009,** *63*, 311-334.

7. Soo, V. W.; McAnulty, M. J.; Tripathi, A.; Zhu, F.; Zhang, L.; Hatzakis, E.; Smith, P. B.; Agrawal, S.; Nazem-Bokaee, H.; Gopalakrishnan, S.; Salis, H. M.; Ferry, J. G.; Maranas, C. D.; Patterson, A. D.; Wood, T. K., Reversing methanogenesis to capture methane for liquid biofuel precursors. *Microb. Cell Fact.* **2016,** *15*, 11.

8. Pan, X.; Angelidaki, I.; Alvarado-Morales, M.; Liu, H.; Liu, Y.; Huang, X.; Zhu, G., Methane production from formate, acetate and H2/CO2; focusing on kinetics and microbial characterization. *Bioresour Technol* **2016,** *218*, 796-806.

9. Rouviere, P. E.; Wolfe, R. S., Novel biochemistry of methanogenesis. *J Biol Chem* **1988,** *263* (17), 7913-7916.

10. Jetten, M. S. M.; Stams, A. J. M.; Zehnder, A. J. B., Methanogenesis from Acetate - a Comparison of the Acetate Metabolism in Methanothrix-Soehngenii and Methanosarcina Spp. *FEMS Microbiol. Lett.* **1992,** *88* (3-4), 181-197.

11. Mand, T. D.; Metcalf, W. W., Energy conservation and hydrogenase function in methanogenic archaea, in particular the genus *Methanosarcina*. *Microbiol. Mol. Biol. Rev.* **2019,** *83* (4), e00020-19

12. Stokke, R.; Roalkvam, I.; Lanzen, A.; Haflidason, H.; Steen, I. H., Integrated metagenomic and metaproteomic analyses of an ANME-1-dominated community in marine cold seep sediments. *Environ. Microbiol.* **2012,** *14* (5), 1333-1346.

13. Meyerdierks, A.; Kube, M.; Kostadinov, I.; Teeling, H.; Glockner, F. O.; Reinhardt, R.; Amann, R., Metagenome and mRNA expression analyses of anaerobic methanotrophic archaea of the ANME-1 group. *Environ. Microbiol.* **2010,** *12* (2), 422-439.

14. McGlynn, S. E.; Chadwick, G. L.; Kempes, C. P.; Orphan, V. J., Single cell activity reveals direct electron transfer in methanotrophic consortia. *Nature* **2015,** *526* (7574), 531-5.

15. Leu, A. O.; Cai, C.; McIlroy, S. J.; Southam, G.; Orphan, V. J.; Yuan, Z.; Hu, S.; Tyson, G. W., Anaerobic methane oxidation coupled to manganese reduction by members of the *Methanoperedenaceae*. *ISME J* **2020,** *14* (4), 1030-1041.

16. Cai, C.; Leu, A. O.; Xie, G. J.; Guo, J.; Feng, Y.; Zhao, J. X.; Tyson, G. W.; Yuan, Z.; Hu, S., A methanotrophic archaeon couples anaerobic oxidation of methane to Fe(III) reduction. *The ISME journal* **2018,** *12* (8), 1929-1939.

17. Haroon, M. F.; Hu, S.; Shi, Y.; Imelfort, M.; Keller, J.; Hugenholtz, P.; Yuan, Z.; Tyson, G. W., Anaerobic oxidation of methane coupled to nitrate reduction in a novel archaeal lineage. *Nature* **2013,** *500* (7464), 567-570.

18. Wegener, G.; Krukenberg, V.; Riedel, D.; Tegetmeyer, H. E.; Boetius, A., Intercellular wiring enables electron transfer between methanotrophic archaea and bacteria. *Nature* **2015,** *526* (7574), 587-590.

19. Skennerton, C. T.; Chourey, K.; Iyer, R.; Hettich, R. L.; Tyson, G. W.; Orphan, V. J., Methane-fueled syntrophy through extracellular electron transfer: Uncovering the genomic traits conserved within diverse bacterial partners of anaerobic methanotrophic archaea. *MBio* **2017,** *8* (4), e00530-17

20. Chadwick, G. L.; Skennerton, C. T.; Laso-Perez, R.; Leu, A. O.; Speth, D. R.; Yu, H.; Morgan-Lang, C.; Hatzenpichler, R.; Goudeau, D.; Malmstrom, R.; Brazelton, W. J.; Woyke, T.; Hallam, S. J.; Tyson, G. W.; Wegener, G.; Boetius, A.; Orphan, V. J., Comparative genomics reveals electron transfer and syntrophic mechanisms differentiating methanotrophic and methanogenic archaea. *PLoS Biol* **2022,** *20* (1), e3001508.

21. Wang, Y.; Wegener, G.; Ruff, S. E.; Wang, F., Methyl/alkyl-coenzyme M reductase-based anaerobic alkane oxidation in archaea. *Environ. Microbiol.* **2021,** *23* (2), 530-541.

22. Harmer, J.; Finazzo, C.; Piskorski, R.; Ebner, S.; Duin, E. C.; Goenrich, M.; Thauer, R. K.; Reiher, M.; Schweiger, A.; Hinderberger, D.; Jaun, B., A nickel hydride complex in the

active site of methyl-coenzyme m reductase: implications for the catalytic cycle. *J Am Chem Soc* **2008,** *130* (33), 10907-10920.

23. Zheng, K.; Ngo, P. D.; Owens, V. L.; Yang, X. P.; Mansoorabadi, S. O., The biosynthetic pathway of coenzyme F430 in methanogenic and methanotrophic archaea. *Science* **2016,** *354* (6310), 339-342.

24. Wongnate, T.; Sliwa, D.; Ginovska, B.; Smith, D.; Wolf, M. W.; Lehnert, N.; Raugei, S.; Ragsdale, S. W., The radical mechanism of biological methane synthesis by Methyl-coenzyme M reductase. *Science* **2016,** *352* (6288), 953-958.

25. Hahn, C. J.; Lemaire, O. N.; Kahnt, J.; Engilberge, S.; Wegener, G.; Wagner, T., Crystal structure of a key enzyme for anaerobic ethane activation. *Science* **2021,** *373* (6550), 118-121.

26. Shima, S.; Krueger, M.; Weinert, T.; Demmer, U.; Kahnt, J.; Thauer, R. K.; Ermler, U., Structure of a Methyl-coenzyme M reductase from Black Sea mats that oxidize methane anaerobically. *Nature* **2011,** *481* (7379), 98-101.

27. Evans, P. N.; Boyd, J. A.; Leu, A. O.; Woodcroft, B. J.; Parks, D. H.; Hugenholtz, P.; Tyson, G. W., An evolving view of methane metabolism in the Archaea. *Nat Rev Microbiol* **2019,** *17* (4), 219-232.

28. Allen, K. D.; Wegener, G.; White, R. H., Discovery of multiple modified F(430) coenzymes in methanogens and anaerobic methanotrophic archaea suggests possible new roles for F(430) in nature. *Appl Environ Microbiol* **2014,** *80* (20), 6403-6412.

29. Sarmiento, F.; Leigh, J. A.; Whitman, W. B., Genetic systems for hydrogenotrophic methanogens. *Methods Enzymol.* **2011,** *494*, 43-73.

30. Buan, N.; Kulkarni, G.; Metcalf, W., Genetic methods for methanosarcina species. *Methods Enzymol.* **2011,** *494*, 23-42.

31. Sowers, K. R.; Boone, J. E.; Gunsalus, R. P., Disaggregation of *Methanosarcina* spp. and growth as single cells at elevated osmolarity. *Appl Environ Microbiol* **1993,** *59* (11), 3832-3839.

32. Mukhopadhyay, B.; Johnson, E. F.; Wolfe, R. S., Reactor-scale cultivation of the hyperthermophilic methanarchaeon *Methanococcus jannaschi*i to high cell densities. *Appl Environ Microb* **1999,** *65* (11), 5059-5065.

33. Mayr, S.; Latkoczy, C.; Kruger, M.; Gunther, D.; Shima, S.; Thauer, R. K.; Widdel, F.; Jaun, B., Structure of an F_{430} variant from archaea associated with anaerobic oxidation of methane. *J. Am. Chem. Soc.* **2008,** *130* (32), 10758-10767.

34. Duin, E. C.; Prakash, D.; Brungess, C., Methyl-coenzyme M reductase from *Methanothermobacter marburgensis*. *Methods Enzymol.* **2011,** *494*, 159-87.

35. Bonin, A. S.; Boone, D. R., The Order Methanobacteriales. In *The Prokaryotes: Volume 3: Archaea. Bacteria: Firmicutes, Actinomycetes*, Dworkin, M.; Falkow, S.; Rosenberg, E.; Schleifer, K.-H.; Stackebrandt, E., Eds. Springer New York: New York, NY, 2006; pp 231-243.

36. Guyot, J. P.; Brauman, A., Methane production from formate by syntrophic association of *Methanobacterium bryantii* and *Desulfovibrio vulgaris* Jj. *Appl Environ Microb* **1986,** *52* (6), 1436-1437.

37. Patra, A.; Park, T.; Kim, M.; Yu, Z. T., Rumen methanogens and mitigation of methane emission by anti-methanogenic compounds and substances. *J Anim Sci Biotechno* **2017,** *8*.

38. Samuel, B. S.; Hansen, E. E.; Manchester, J. K.; Coutinho, P. M.; Henrissat, B.; Fulton, R.; Latreille, P.; Kim, K.; Wilson, R. K.; Gordon, J. I., Genomic and metabolic adaptations of *Methanobrevibacter smithii* to the human gut. *P Natl Acad Sci USA* **2007,** *104* (25), 10643-10648.

Chapter III: Initial characterization of an archaeal methylthiotransferase

3.1 Abstract

Methanogenesis is the biological production of methane from simple carbon compounds and is utilized by methanogenic archaea (methanogens) to generate energy. In contrast, the anaerobic oxidation of methane (AOM), carried out by the anaerobic methanotrophs (ANME), oxidizes methane. Methyl-coenzyme M reductase (Mcr) catalyzes the final reaction of methanogenesis in methanogens and the first reaction in AOM. Cofactor F_{430}, a unique nickel-containing tetrapyrrole, serves as the prosthetic group and catalytic component of Mcr. A variant of standard cofactor F_{430} containing a methylthio group substitution at the 17^2 carbon was discovered in the active site of the crystal structure of MCR from an ANME-1 organism. Further, two F_{430} variants hypothesized to contain thioethers have been discovered to be produced by several methanogenic species, including *Methanococcus maripaludis*, *Methanosarcina acetivorans*, and *Methanocaldococcus jannaschii*. These two variants are termed mercaptopropionate-F_{430} and mercaptopropamide-F_{430} based on their exact masses and absorbance spectra (described in Chapter II).

We are interested in discovering and characterizing the enzymes involved in methylthio-F_{430}, mercaptopropamide-F_{430}, and mercaptopropionate-F_{430} biosynthesis. The biosynthetic pathway of these variants may share a common initial sulfur insertion reaction. Initially, it was hypothesized that the insertion of the methylthio moiety in at least methylthio-F_{430} is catalyzed by a methylthiotransferase (MTTase) homolog present in ANME. However, the work described here with a purified ANME-1 MTTase fails to show this activity with cofactor F_{430}. Instead, the purified enzyme catalyzes the methylthiolation of N^6-threonylcarbamoyladenosine (t^6A) in tRNA, and is therefore a true ortholog of the previously characterized bacterial MtaB. We also show that

Methanosarcina acetivorans, which contains one MTTase, contains 2-methylthio-N^6-hydroxynorvalyladenosine (ms^2hn^6A), but 2-methylthio-N^6-threonylcarbamoyladenosine ms^2t^6A, the product of MtaB, was not identified. Likely, archaeal MTTases are able to methylthiolate both hn^6A and t^6A. Future *in vitro* and bioinformatic investigations will need to be conducted to either determine reaction conditions in which the ANME MTTase may catalyze the methylthiolation of F_{430}, or to identify the true enzyme catalyzing this reaction.

3.2 Introduction

The anaerobic oxidation of methane (AOM), as carried out by the anaerobic methanotrophs (ANME), plays a key role in the carbon cycle by oxidizing up to 90% of methane that would be otherwise released in marine sediments.[1] The key enzyme that catalyzes methane activation is methyl-coenzyme M reductase (Mcr).[2] Active Mcr exists as a dimer of heterotrimers in an $\alpha_2\beta_2\gamma_2$ configuration, with two active sites each binding a cofactor F_{430} (Figure 1.2).[3] It was discovered that one clade of ANME, the ANME-1 (*Methanophagales*) uniquely contain a methylthio addition to the 17^2 carbon of F_{430} (Figure 1.6).[4] Methylthio-F_{430} was subsequently found in the active site of a crystal structure of Mcr, and there it is likely the main F_{430} these organisms use.[5] Thus, it may be involved in specializing F_{430} for methane oxidation. However, the enzyme responsible for installing the methylthio moiety remains a mystery, and any influence methylthio-F_{430} has on methane oxidation or methyl-CoM reduction is unknown. Since this will likely be unknown until the efficient production of methylthio-F_{430} either *in vivo* or *in vitro* is realized, it is important to elucidate the enzyme(s) catalyzing its production.

Sulfur comprises 1% of cell biomass and is an essential element for all life.[6] It is found in the amino acids methionine and cysteine, cofactors such as iron-sulfur clusters, coenzyme M, coenzyme B, *S*-adenosylmethionine, biotin, lipoic acid, and thiamine, and various modified tRNA

nucleosides including 2-methylthio derivatives of N^6-threonylcarbomoyladenosine (t^6A), N^6-isopentenylcarbamoyladenosine (i^6A), and N^6-hydroxynorvalylcarbamoyladenosine (hn^6A).[6, 7] In bacteria, all three of these methylthiolated (ms) tRNAs have been reported, although they are not all conserved amongst all bacteria. For instance, while both ms^2t^6A and ms^2i^6A has been reported in *Bacillus subtilis*, *E. coli* has only ms^2i^6A.[7] And, while *B. subtilis* has ms^2t^6A, it is has been mapped unambiguously to only $tRNA^{Lys}_{UUU}$.[8]

The enzymes that catalyze C-S bond formation on an inert carbon substate are a subclass of radical SAM enzymes, which transform inert substrates into highly reactive intermediates through the selective abstraction of a hydrogen atom.[9] These include biotin synthase and lipoyl synthase, as well as a group of enzymes that catalyze both sulfur insertion and methylation. The latter enzymes are known as methylthiotransferases and include MiaB, MtaB, and RimO.[9] MiaB and MtaB insert a methylthio group onto their respective tRNA substrate, while RimO acts upon the bacterial ribosomal protein S12.

A major goal of methanogenic research is to establish a biological system for the efficient conversion of natural gas to liquid fuels. The slow growth rate of ANME (doubling time of 1.1-7.5 months) makes these organisms a poor host for establishing this system.[2] However, methanogens contain all of the enzymes required for methane oxidation, and the *Methanosarcinales* also express cytochromes *c* that have been shown to be a common mediator of AOM.[10, 11] Indeed, the conversion of 9% of methane to acetate has been described in *Methanosarcina acetivorans* through the heterologous expression of ANME-1 Mcr.[12] ANME-1 Mcr is also the most divergent Mcr relative to methanogen Mcrs.[5] As any future system used to efficiently oxidize methane to more desirable products will likely exist as a methanogen expressing ANME Mcr, it will be important to rigorously dissect the influence methylthio-F_{430} has on Mcr

catalysis. The original work, for example, describing the conversion of methane to acetate with ANME-1 Mcr did not attempt to incorporate methylthio-F_{430} into its active site.[12] It could be possible a significant increase in efficiency would be obtained by having the methanogen host produce methylthio-F_{430} as the major F_{430}. Since the most immediate precursor of methylthio-F_{430} is likely either cofactor F_{430} or a thiolated intermediate, a methanogen host would contain all the machinery required to produce methylthio-F_{430}, minus the enzyme(s) catalyzing the final step(s) in its biosynthesis.

3.3 Methods

Bioinformatics to identify archaeal sulfur insertion enzymes. Protein BLAST (blastp) was used to identify genes potentially involved in the catalytic insertion of a (methyl)thio group into F_{430}.[13] Genomes and metagenomes were downloaded using the publicly available GenBank and Integrated Microbial Genomes (IMG) databases. To identify homologs in a certain (meta)genome, blastp was used within the publicly available Blast2GO program. Downloaded sequences or (meta)genomes were used to construct a BLAST database within Blast2GO and/or to search against an existing database with the blastp program. Sulfur insertion enzymes were then queried against these databases. The default parameters of an E-value cutoff of 1.0E-3 and a restriction to 20 hits were used. Any resulting hits were further analyzed on the basis of: E-value, localization of homology, the presence or absence of known motifs associated with an enzyme, and experimentally verified information.

Another approach consisted of comparing predicted radical SAM proteins in methanogens as well as ANME that are known to produce methylthio-F_{430} (ANME-1) and those that likely do not (ANME-2). Radical SAM proteins were identified by searching downloaded (meta)genomes for the radical SAM motif "CxxxCxxC" in SnapGene. Proteins containing this motif within a

particular (meta)genome were exported as a text file then loaded into Blast2GO. BLAST databases were constructed, and the databases compared against each other using the blastp program. Similarly, since many sulfur-insertion enzymes contain iron-sulfur clusters, MetalPredator was used to identify predicted iron-sulfur binding proteins.[14]

A third approach consisted of analyzing the genes around the F_{430} biosynthesis operon (CfbA-E) in *M. acetivorans*. *M. acetivorans* is an organism that has been shown to produce both mercaptopropionate-F_{430} and mercaptopropamide-F_{430}, and contains CfbA-E as an operon.[15] This is in contrast to ANME-1, as well as the other methanogens we have identified to produce cofactor F_{430} variants. Similarly, the publicly available STRING program was used to identify co-occurring genes. Multiple sequence alignments were conducted using the publicly available ClustalO program and visualized using UGENE.

Cloning, transformation, and expression of plasmids in E. coli *lineages.* Plasmids capable of expressing genetic material in either *E. coli*, *B. subtilis*, *M. maripaludis*, or *M. acetivorans* used in this work are: pET15b, pHCMC05, pJAR-derived plasmids, and pJK027A. Cloning was achieved with Gibson assembly using the 2x Gibson Assembly Master Mix (NEB) and the protocol recommended by the supplier.[16] Gibson assembly requires two components in addition to the mix: digested plasmid and an insert, the latter obtained either *via* a polymerase chain reaction (PCR) or as a g-block purchased from Integrated DNA Technologies (IDT). Forward and reverse primers (from IDT) for PCRs contain a 15-25 region overlapping with the plasmid at the cut site on either side, and either first or last 15-25 bp of the gene. PCR is accomplished using the VeriFi Polymerase 2x mix (PCRBIO) and the manufacturer's instructions. The 20 µL Gibson assembly reactions are carried out according to the manufacturer's instructions.

Gibson assembly product was added to thawed competent cells on ice. Zymo Mix and Go! DH5α cells (Zymo Research) were used for initial transformations. After gentle mixing, the cells are incubated on ice for ten min, subjected to a heat shock at 42°C for thirty seconds, then grown in SOC at 37°C for an hour with shaking then are plated with selection.

Plasmids are isolated by first transferring clonal cells to LB liquid broth culture under antibiotic selection and growing with shaking at 37°C for about 16-20 hours. Plasmid DNA is purified using the ZymoPURE Plasmid Miniprep Kit. Plasmids are then verified by Sanger sequencing by the Genomics Sequencing Center at Virginia Tech. Sequence-verified plasmids are re-transformed into DH5α cells as well as other cells as needed.

For protein expression in *E. coli*, sequence-verified pET15b plasmids were transformed into BL21(DE3), BL21(DE3)-RIL, or ArcticExpress(DE3)-RIL cells. "RIL" designates the cells harbor a plasmid expressing *argU*, *ileY*, and *leuW*, which encode for tRNAs which read anti-codons rare in *E. coli*. It confers resistance to chloramphenicol, and so these cells are selected with 50 μg/mL chloramphenicol as well as ampicillin. ArcticExpress(DE3)-RIL cells contain this plasmid (but conferring streptomycin resistance instead) and an additional plasmid that constitutively expresses homologs of the native *GroEL-GroES* chaperonin system of *E. coli* from a psychrophilic organism.[17] For tRNA expression, the pHCMC05 plasmid is used, which is a shuttle vector capable of autonomous replication in *E. coli* and *B. subtilis* conferring ampicillin and chloramphenicol resistance.[18] Cloned genes are expressed with the IPTG-inducible P_{spac} promoter consisting of the SPO-1 phage promoter hybridized with the *lacO* operator.[18] The expression of genetic material encoding for either a protein (pET15b-derived plasmids) or tRNA (pHCMC05-derived plasmids) is induced by the addition of 100-1,000 μM IPTG at an OD of 0.6-0.8. When expressing protein, $FeCl_3$ is added to 500 μM and cysteine to 250 μM at an OD of

around 0.4. Cells were generally grown at 37°C for an additional four hours post-induction, except in the case of ArcticExpress(DE3)-RIL cells, which were grown at 12°C or less for an additional 24 hours. Cells were harvested by centrifugation at 6,000 rpm for 15 min. Cell pellets were either immediately used for protein or RNA purification, or frozen for latter use at -20°C.

Protein purification. All protein purifications followed this general procedure. All of the steps described here took place inside a strictly anoxic glovebox in an atmosphere of 97% N_2 and 3% H_2. Buffers were made outside the glovebox then brought inside the glovebox in glass bottles at least two days before use. Each buffer was stirred overnight with its bottlecap off. Buffer A consisted of 500 mM KCl, 10-40 mM imidazole, and 50 mM HEPES, pH = 8.0. The elution buffer was identical but contained 500 mM imidazole. Aliquots of all buffers used were supplemented with 5 mM DTT before use. Cell pellets were brought into the glovebox and resuspended in lysis buffer volume equal to 2.5 times the pellet mass in grams in mLs. The resuspension was sonicated for 1 min, then phenylmethylsulfonyl fluoride was added to 1 mM. The subsequent sonication cycles were 2 min (alternating 1 sec on and 1 sec off), and the number of cycles was equal to the mass of the pellet rounded up. Homogenized cells were transferred to a sealed anaerobic centrifuge tube and spun down at 15,000 rpm in a Sorvall SS-34 rotor. The supernatant was filtered by passing it through a syringe connected to a 0.45 μm filter. This was applied to a 2 x 8 cm column of Ni Sepharose 6 Fast Flow resin. The column was washed with 10-15 mL lysis buffer, then eluted in a step-wise gradient of increasing eluant buffer concentration. Typically, this was 6 mL fractions of 10% eluant buffer, 30%, then 100%. Fractions were concentrated to < 1.0 mL with an Amicon Ultra filter and 15 μL samples analyzed by SDS-PAGE. Fractions containing protein are adjusted to 2.5 mL. Exchange buffer, consisting of lysis buffer but without imidazole, is used to bring the volume to 2.5 mL if needed. The 2.5 mL is applied to a PD-10 desalt column (GE Healthcare) and

eluted in 3.5 mL exchange buffer. If not needed immediately, the protein is aliquoted into 0.5-1.0 mL anaerobic cryovials containing O-ring seals (Olympus) then flash frozen in liquid N_2. Purifications are routinely analyzed by collecting samples at different steps and subjecting to SDS-PAGE.

Purifying BSM21210 from inclusion bodies. Initial steps were carried out as described above. After centrifuging down the lysate, however, the supernatant was discarded. The pellet was resuspended in Buffer A (8 M urea, 300 mM NaCl, 50 mM HEPES, pH = 8.0). This was spun down at 15k rpm for 30 min and the supernatant was filtered and applied to Ni Sepharose 6 Fast Flow resin that was equilibrated with Buffer A, and protein was eluted from the column as described above. However, the elution buffer was Buffer A with the addition of 500 mM imidazole. Fractions that had BSM21210, as determined by SDS-PAGE were combined and 0.4 µmol methionine/g cell pellet was added. Slowly, 1.5 µmol $FeCl_3$/g of original cell pellet, 1.5 µmol cysteine/g, and 150 µg DTT /g was added to the protein sample. The solution was then diluted to about 0.5 M urea (~15 fold) to allow the protein to refold overnight. The next day, this was centrifuged at 8,000 rpm in 250 mL centrifuge bottles. The supernatant was concentrated with a Amicon Ultra filter with a 30 kDa cutoff to about 2.5 mL and adjusted to 2.5 mL. The next day, this was desalted as described, and samples analyzed for protein content by SDS-PAGE.

Transformation and expression of BSM21210 in M. maripaludis *and* M. acetivorans. Genes desired to be transformed into *M. maripaludis* were first cloned into either the pJAR046 or pJAR50CT using methods described above. The latter has a C-terminal hexahistidine-tag and therefore can be used to also express a gene without a his-tag by inclusion of the native stop codon. In contrast, pJAR046 contains a N-terminal hexahistidine-tag. Plasmids were transformed using the polyethylene glycol method.[19] Solid plates for selection were made with McCas media (see

Chapter II) with a final concentration of 2.5 μg/mL puromycin. One day before plating, plates to be used were incubated in a closed anaerobic environment at 20 psi 80% H_2/20% CO_2 containing a paper towel twisted and fully submerged in a solution of 20% sodium sulfide. After plating, the solid plates were incubated in this environment until colonies emerged, typically four to seven days. Colonies are added to liquid McCas medium containing puromycin. The described plasmids result in the constitutive expression of protein, and for purifications transformants were grown in large batches (~ 1 L McCas). Cells were harvested after 2-3 days of growth and purification steps were as described above.

For heterologous expression in *M. acetivorans*, cloning began with inserting a gene into the pJK027A plasmid. This is retrofitted into the pAMG40 plasmid using BP clonase II (Invitrogen) as described previously.[20] The retrofitted plasmid can be checked by restriction digest. The resulting plasmid can autonomously replicate in *M. acetivorans* and gene expression is inducible by the addition of tetracycline. Plasmids are then transformed into WWM60 cells using the liposome-mediated transformation as described previously.[21] Plating took place as described above, however, *M. acetivorans* medium was used (described in Chapter II). The expression of genes in the resulting transformants is accomplished by adding tetracycline from a sterile stock to cells at mid-exponential phase. Cells are allowed to grow for another day then protein is purified as described.

Cloning, expression, and purification of G60 MTTase. Predicted protein coding sequences of the ANME-1 G60 metagenome (assembly: PQXC00000000.1) was downloaded from NCBI.[22] Identification of a methylthiotransferase homolog in this metagenome was accomplished as described above. A g-block, below, was designed containing the gene (C4B56_05415) and flanking regions to clone the gene into the NdeI site of pET15b.

CTGGTGCCGCGCGGCAGCCATATGAGCGAGATTATCGGGAGTTATGGCTCAGGAGCAGAAACAGGAGCAGGAACAAGAGCAAGA
GTCCACATAGAGACCTTTGGCTGCACTGCAAATGCCGGCGATACGCAGAAACTGCGCGCTATATTGAAGAGGAGTGGATATCAAC
TGGTAACGGACTATAAAAAAGCCGATTGTGTCATCGTGAACACATGCACAGTGACGAAGCGGACGGAACTGAATGTGGTGAAGC
GGCTGGAGGAACTGAAGAAGCAGGGCAAGCATGTAATCGTAGCCGGCTGTATGGCTGCGGCACAGCCCGAACTGGTGAAGAGCG
TTCTGGGGAAGGATACAATTATGATAACGCCTGAAGAGCTATACCCGGTTATGGATTTTGATTTTGACAACAACTCCTCCGTGGTT
GGTATAATCCCGATATCAATGGGCTGTCTCGGAGAATGCACCTATTGCATTGTGAAGAGAGCGAGGGGGAGACTGAAGAGCCTG
AGTCCCGATAGGATATGCAGCGCGTTAAGGTCCGCAGTGGCGGCTGGTGTGAAGGAAATAAGAATAACAGCCCAGGATTGTGCC
GCTTACGGGTTCGACCGCACGGATATGGGTATGGATATGGCTGTGAAACTACCTGAGCTCCTGCGGATGCTGACCGAAGTGGAAG
GCGATTTTAGAATTCGTATAGGCATGATGAACCCCTTCACACTACTCTGCATCATAGATGAGCTCCTTGAGGCTTTTGAATCCGAT
AAGGTGTTCAAGTTCTTCCACATACCGGTTCAGTCGGGCTCTGATAAGGTGCTAAGCGATATGCGCAGGAATTACAAAGTCGCTG
ACTTCGTAGAGATAGTGAGAAGAATAAGGAGGCGATTCCATTACTGCACCATCTGTACAGATTTTATCGTTGGATTTCCAACAGA
GGATGAGGATGATTTCCGGGCGTCACTGCAGCTACTGGAGGAAGTGAAGCCTGAGAAGGTGAACATTACGCGATTCTCACCGCGA
CCGGGGACGGAGGCATCGAAACTCAAGGACATGCTGGCTCGCGATAAGAAGATGAGGTCGCGAACGATGTCGGCGATTTATCAC
AGGATGGCACTTGAAGCCAATAACCAACTGATAGGAGCGGAACTACCGGTTCTGGTTACCGAACGCGGTGATAAAGGCGGTGTG
ATTGCCCGTGACCCATCTTATAAGACGATAATATTGGAGGAGGATTTGCCGCCCGGTTCATTCCATAAGGTGCGTGTGAAGGATG
CGAGGAGCACTTATCTGGTTGCCTCTGTGATTTCATGATGCTCGAGGATCCGGCTGCT

The g-block was cloned into pET15b as described above. An initial induction study was performed to determine a starting point for IPTG concentration for protein expression. Two 5 mL LB cultures were grown at 37°C with shaking, and protein expression was induced at an IPTG concentration of either 100 μM or 1 mM. Cell samples were taken before IPTG addition and 21 hours and expression level was compared between the cells using SDS-PAGE.

For protein purification, cells were grown routinely in 3 L flasks containing 1.5 L LB each at 37°C at 200 rpm in an Innova 43 shaker (New Brunswick Scientific). At an OD_{600} of around 0.4, cysteine was added to 250 μM and $FeCl_3$ to 500 μM, then at an OD of about 0.6-0.8 (roughly 3-4 hours of growth), IPTG was added to 100 μM. Cells were grown for an additional four hours and then harvested at 6,000 rpm for 15 min. The cell pellet was frozen at -20°C or immediately purified.

Thermostability assays with purified G60 MTTase. Since ANME-1 G60 is a thermophile, we were interested in characterizing the thermostability of the MTTase. This allowed us to estimate a temperature at which the protein would be most active and the heat treatment allowed further purification of the desired protein. A 100 μL sample of protein was set aside and left at room temperature, and three additional 100 μL samples were aliquoted into separate microfuge tubes. These were incubated at 37°C, 50°C, and 70°C for one hour under anaerobic conditions. Protein

concentration equaled about 150 μM. Samples of each were taken and analyzed by SDS-PAGE gel.

Iron and sulfide determination. The iron and sulfide content of the as-purified protein was estimated using previously described methods.[23] For iron determination, the following solutions were made. Sodium acetate was dissolved in water to saturation (3.41 M). To this, about 2 mL of glacial acetic acid was added to a pH of less than 6.0. This took about 2 mL of glacial acetic acid. The pH was determined with pH paper. Thioglycolic acid was added to 1 mL per L solution. A phenanthroline/isoamyl alcohol solution was made previously and this was used for all iron determinations completed in this work. It had been made by adding 200 mg bathophenanthroline into 250 mL isoamyl alcohol, then allowed to stir overnight. This solution was added to a concentration of 50 mL per L solution. The phases were allowed to separate, and the isoamyl was extracted with a Pasteur pipette. The extraction was repeated two more times. Trace phenanthroline was removed by adding pure isoamyl alcohol to 100 mL per L solution. The upper isoamyl alcohol layer was removed and this extraction repeated once. The following solutions were made fresh the day of iron determinations. Reagent A consisted of 1.35 g SDS dissolved in 30 mL water and 0.45 mL saturated iron-free acetate; reagent B consisted of 270 mg ascorbic acid and 9 mg sodium metabisulfite dissolved in 5.6 mL water and 0.4 mL saturated iron-free acetate; reagent C consisted of 5,6-di(2-furyl)-1,2,4-triazine-5',5"-disulfonic acid dissolved in 1 mL water. Finally, for the standard curve, a solution of 0.5 nmol $FeCl_3$ was produced.

To generate the standard curve, samples containing 1, 2, 4, 8, 16, 20, and 25 nmol of iron were generated. For assays with protein, solutions containing 0.5, 1, 2, and 3 nmol were generated. To each of these samples, water was added to 300 μL. Then, 300 μL reagent A was added followed

by 300 µL reagent B. The solutions were incubated at 30°C for 15 min. Reagent C was added immediately before taking the absorbance at 593 nm with a 100 Bio UV Vis (Cary).

The following reagents were prepared for the sulfide determination: 1% zinc acetate in water, 12% NaOH in water, 0.1% N,N-dimethyl-p-phenylenediamine monohydrochloride in 5 M HCl (aq), and 23 mM $FeCl_3$ in 1.2 M HCl (aq). Solids were weighed out aerobically then brought into the glovebox and dissolved in anoxic water. The subsequent steps were done in the glovebox. To make the standard curve, sodium sulfide solutions of between 1 to 10 nmol were prepared. Solutions of 0.5-3 nmol protein were also prepared. All samples were diluted to 100 µL with water then 300 µL zinc acetate solution was added and mixed by stirring. Next, 15 µL 12% NaOH was added to denature proteins. The solution was stirred again to homogeneity then incubated at room temperature without stirring for 30 min. Following this, 25 µL $FeCl_3$ was added and the samples stirred. The samples were incubated for an additional 30 min then the absorbance at 670 nm was measured aerobically.

In vitro assays with F_{430}. Reactions with purified cofactor F_{430} were carried out in slightly different conditions and different components in an attempt to show activity. All reactions were carried out in an anoxic glovebox. Reaction components consisted of: protein (50-150 µM), cofactor F_{430}, SAM (1 mM), sodium sulfide (500 µM), and a reducing agent, either dithionite (2 mM), titanium citrate (2 mM), or both NADH (1 mM) and NADPH (1 mM). Cofactor F_{430} was obtained by purifying as described in Chapter II. The concentration of F_{430} was never determined for these assays. Instead, an amount that was in clear excess as determined by LC-MS was used, typically in a volume of ~100 µL or less. In one set of reactions, unfractionated *M. acetivorans* cell extract was also supplied in addition to these components. 300 mL of cells were grown on 50 mM TMA as described in Chapter II, and the cells pellet was resuspended in 1.5 mL. Cells were

sonicated, and 200 µL of this was set aside ("lysate"). The remaining cells were centrifuged, and 200 µL of this was added to reactions containing either one of the three reducing agents described above. 200 µL of the lysate was added to one reaction containing NADPH/NADH. Reaction volumes were 500 µL or less, and were carried out at either 37°C or 50°C overnight (~12 hours), or at 50°C for two hours. Reactions were quenched with either 50% acetonitrile or 1% formic acid then concentrated to < 100 µL by drying at 30°C under a vacuum. Control reactions were carried out as described, but without the addition of either protein or F_{430}. Assays were analyzed for product formation by LC-MS using methods described in Chapter II.

SAM cleavage and S-adenosyl homocysteine (SAH) assays. To detect 5'-deoxyadenosine and SAH, reactions were carried out as described above and analyzed by LC-MS, however with a different LC method. Buffer A was 1% formic acid in deionized water and Buffer B was 100% methanol. The method consisted of 2 min at 98% A, a linear gradient of 10 min to 50% B, then a 2 min gradient to 95% B and five min of 95% B. Radical SAM cleavage was detected by detecting one of its byproducts, 5'-deoxyadenosine, which has an *m/z* of 252 in positive ion mode. SAH production was detected to analyze the ability of the putative MTTase to use SAM as a methyl group donor. Selected ion monitoring methods were employed scanning 252/136 for 5'-deoxyaenosine and 385/136 for SAH. The collision energy was 15 V.

Electron paramagnetic resonance (EPR) spectroscopy. EPR spectroscopy was employed to characterize the redox state of the $[4Fe\text{-}4S]^{3+/2+/1+}$ clusters of as-purified G60 MTTase in three conditions. 4 mm EPR tubes (Norrell) were brought into the glovebox several hours before continuing. Reaction components were first added to microfuge tubes. One reaction received protein only, another received protein and 4 mM dithionite, and the last received protein, 4 mM dithionite, and 1 mM SAM. Buffer (500 mM KCl, 50 mM HEPES, pH = 8.0) was added to 300

μL. Each reaction received protein to a final concentration of about 108.5 μM. The reactions were allowed to incubate for about ten min before snap freezing in cold isopentane (~77 K). The liquid pentane was chilled in liquid N_2 until crystals began to form at the bottom of the bottle. At this point, it was cycled into the box. The EPR tubes containing the reactions were slowly dropped into the liquid pentane and left for about ten seconds. They were then removed from the glove box and stored in liquid N_2. Low temperature X-band EPR spectra were obtained on a Bruker ER073 EMX Spectrophotometer with an EMX High Sensitivity Probehead and a liquid helium variable temperature system (ER4112HV). Spectra were recorded under the following conditions: 9.376 GHz, 10 G modulation amplitude, 3400 G center field, 1000 G sweep width, 1 mW power, 0.3 s time constant, 10K, 5 X 1 min scans.

Cloning $tRNA^{Lys}$ into pHCMC05. *E. coli* DH5α harboring pHCMC05 (strain ECE190) was obtained from the Bacillus Genetic Stock Center. The gene that encodes $tRNA^{Lys}$ was described previously and the sequence was confirmed by searching through the Modomics and NCBI databases.[24] A g-block to clone this gene into pHCMC05 was designed as follows. First, we included 4 bp upstream and 15 bp downstream of the gene found within the *B. subtilis* 168 genome. Then, regions flanking the BamHI restriction enzyme cut site on pHCMC05 were added. The 148 bp g-block, below, was then ordered from IDT.

CAATTAAGCTTAAGGAGGTGAGGATCCTTATGAGCCATTAGCTCAGTTGGTAGAGCATCTGACTTTTAATCAGAGGGTCGAAGGT
TCGAGTCCTTCATGGCTCACCATT TCGTGAAGGCCCGCTCTAGAGTCGACGTCCCCGGGGCAG

The pHCMC05 plasmid was obtained by growing 5 mL of ECE190 in LB broth supplemented with chloramphenicol to 10 μg/mL. The pHCMC05 plasmid was purified using the ZymoPURE Plasmid Miniprep Kit. The purified plasmid was digested with FastDigest BamHI, purified by gel-electrophoresis and the DNA Clean and Concentrator Kit (Zymo Research). The

g-block containing $tRNA^{Lys}$ and the purified digested plasmid were assembled via Gibson assembly as described above. Sequence-verified plasmids, termed pKB550, were obtained also as described above.

Bacillus subtilis *competent cell prep and pKB550 transformation.* A strain of *B. subtilis* 168 in which its native MtaB locus is replaced by the gene conferring kanamycin resistance (*B. subtilis* 168 *ΔyqeV::kan*, or BKK25430) was produced in a genome-scale deletion study.[25] We obtained it from the Bacillus Genetic Stock Center as spore suspensions absorbed on filter disks and recovered cells by placing the disks on solidified LB agar containing 7.5 µg/mL kanamycin. This *B. subtilis* strain was made competent as previously described.[26] A 5 mL overnight culture of BKK25430 was grown in LB at 37°C. The next day, 500 µL of this was used to inoculate 5 mL SPI medium and this was grown at 37°C with shaking. Two hours into the growth, the OD_{600} of the culture was checked, and then checked every 30 min until the cells reached stationary phase, as determined by a lack of growth between two 30 min increments (five hours of growth in total). Then, 500 µL of this culture was used to inoculate 90 mL SPII medium and this was incubated for an additional 90 min at 37°C. Cells were collected by centrifugation and 9 mL of the resulting supernatant was used to resuspend the pellet. Two aliquots of 100 µL of the competent cells were set aside and 1 mL of 87% glycerol was added to the remaining cells. After mixing well, the cells were aliquoted 100 µL at a time into individual microfuge tubes then flash frozen in liquid nitrogen and stored at -80°C.

For the transformations, 1 µg of sequence-verified pKB550 was added to the 100 µL aliquots of competent cells set aside as described. The cells were incubated at 37°C for one hour with shaking without antibiotic selection. The cells were then plated onto LB plates solidified with

1.5% agar and containing 7.5 µg/mL kanamycin and 5 µg/mL chloramphenicol. The next morning, plates were checked for colonies. The resulting strain was named KB550.

Transfer RNA extraction protocol. A protocol was adapted for our use from multiple papers.[27,28] *B. subtilis* strains were typically grown in flasks containing 500 mL LB and appropriate antibiotics for about 18 hours at 37°C with shaking. The overexpression of $tRNA^{Lys}$ in KB550 cells was induced by the addition of 300 or 500 µM IPTG around an OD_{600} of 0.6. For obtaining tRNA from *M. acetivorans,* the organism was grown in 550 mL MA medium (described in Chapter II) with 50 mM trimethylamine at 37°C without shaking to various growth stages. All cells were harvested at 6,000 rpm for 15 min.

All water and buffers used were treated with diethyl pyrocarbonate (DEPC) to 1% with stirring for a minimum overnight, then autoclaved for 30 min to destroy RNase and any contaminating RNA. DEPC readily reacts with amino groups, so buffers utilizing Tris or HEPES were instead directly made with DEPC-treated water in RNase-free glassware or plasticware. Surfaces and other equipment were cleaned with a solution of 10% bleach, 1% NaOH, and 1% Sparkleen then washed extensively with DEPC-treated water.

Cell pellets were first washed with 30 mL 0.9% NaCl and centrifuged at 4,400 rpm if necessary. The wash cells were usually frozen at -20°C then thawed as needed, but occasionally (and always in the case of *M. acetivorans*) they were used fresh. Cells were then resuspended in 18-20 mL 50 mM sodium acetate, 10 mM magnesium acetate, pH = 5. *M. acetivorans* cells, but not *B. subtilis* cells, were sonicated at this stage. This suspension was decanted into an Erlenmeyer flask and an equal amount of phenol saturated with 0.1 M citrate, pH ± 0.2 (Sigma) was added. The emulsion was incubated with shaking (200 rpm) for 15 min at room temperature then spun down at 4.4 rpm in 50 mL Falcon tubes. The upper aqueous phase was transferred to a second tube

and 2-5 mL chloroform added, then spun down again. The upper aqueous phase was transferred to a centrifuge tube and 5 M NaCl was added to 0.2 M, then one volume molecular-grade isopropanol was added. This was either allowed to incubate at 4°C overnight or 30 min at -20°C. To remove residual salt, the pellet was washed with 70% ethanol, and if needed, centrifuged. Next, the pellet was resuspended in 50 mM sodium acetate, 10 mM $MgCl_2$, and 150 mM NaCl, then 12 M LiCl added to a final concentration of 2 M. This was incubated on ice for one hour before spinning down at 11,000 rpm in a Sorvall SS-34 rotor for 15 min. The supernatant was removed to a clean centrifuge bottle and the pellet discarded. To precipitate RNAs, one volume of isopropanol was added then spun down. The pellet was washed twice with 70% ethanol, spun down as necessary, then resuspended in 100-500 µL ultra pure water (Apex). To fully purify tRNAs from this mixture, which contains contaminating rRNA, the solution was subjected to anion exchange chromatography using the NucleoBond RNA/DNA 400 kit (Macherey-Nagel). The kit was used according to the provided instructions. Transfer RNAs are eluted from the column with 650 mM KCl after a wash with 400 mM KCl. The KCl concentration of eluants is adjusted by the addition of two volumes of water, then are precipitated with one volume of isopropanol. The solution is incubated and centrifuged as described above, and pellets are washed twice with 70% ethanol. Finally, tRNAs are resuspended in 100-200 µL pure water, then froze for later use at -80°C.

Analysis of tRNA extracts. RNA concentration was measured using a Nanodrop One C. For purity assessment, nucleic acid species in tRNA extracts were routinely separated *via* agarose gel electrophoresis. Working agarose concentration was either 1.5% or 2.0% (2.0% if only anion-exchange purified tRNAs were being analyzed). Voltage was set to 70 V and ran for 70 min. When possible, three amounts of AEX purified tRNA were ran on the same gel: 1, 3, and 6 µg. If the sample is from one of the earlier steps, typically around 10 µg is loaded.

To analyze modification profiles of extracts, tRNAs were first digested and dephosphorylated to completion. Around 100-200 μg of pure tRNA was transferred to a centrifuge tube in a volume of 44 μL or less then incubated at 100°C for three min. The solution was quickly placed in an ice-water bath to cool. Then water was added to 44 μL, 5 μL ammonium acetate (pH 5.3-5.4) was added, then 10 U of nuclease P1 (1 μL of 1:10 diluted enzyme; NEB). This was incubated at 37°C overnight (at least 12 hours). Then, 5 μL 100 mM ammonium bicarbonate was added. This has a pH of about 8.0 when freshly made and is not adjusted, but rises overtime, so it is typically freshly made. Next, 1 μL of 0.01 U/μL *Crotalus adamanteus* phosphodiesterase I was added (Sigma) and this was incubated at 42°C for two hours. Then, 1 μL of 1 U/μL alkaline phosphatase (calf intestinal; Promega) was added and this was incubated for an additional two hours. Finally, this solution was concentrated to 35 μL in an Eppendorf Vacufuge then injected into an LC/MS system.

We employed a Waters Acquity UPLC with a TQD mass spectrometer equipped with an Acquity Premier HSS T3 (2.1 x 100 mm, 1.8 μm particle size) column. Solvent A was 0.1% (v/v) formic acid in water and solvent B was 100% methanol. The flow rate was 0.35 mL/min and the LC program consisted of 2 min at 98% A followed by a 13 min linear gradient to 75% B, then a 15 min gradient to 100% B and 3 min at 100% B. The injection volume was typically 5 μL. The source temperature was 150°C, the desolvation temperature was 500°C, the desolvation gas flow was 800 L/hr, and the cone gas flow was 50 L/hr. The mass spectrometer was operated in positive mode and scanned for *m/z* values ranging from 100 to 800. The main species of digested tRNA detected by mass spectrophotometry are the molecular ion and the base. These two *m/z* values are well characterized for dozens of nucleosides. These masses in combination with well-characterized elution times are used to identify specific nucleosides.

In vitro assays with tRNA and MTTase. Three 150 µL *in vitro* assays were set up as follows in an anaerobic glove box. All three assays received 120 µg purified tRNA from the BKK25430 $tRNA^{Lys}$-overexpression strain, 500 µM sodium sulfide, and 1 mM SAM. Two reactions received protein to a final concentration of 40 µM. One of these received 2 mM dithionate and the other 2 mM titanium citrate. The third assay received 2 mM dithionite but did not receive any protein. Buffer (500 mM KCl, 50 mM HEPES, pH = 8, made with DEPC-treated water) was added to 150 µL. The reactions were incubated at 50°C for 2.75 hours when they were brought out of the glove box and stopped by the addition of one volume of acetonitrile. They were concentrated by drying at under a vacuum at 45°C to roughly 45 µL. RNAs were extracted with an isopropanol extraction then digested to nucleosides as described above.

3.4 Results and Discussion

Initial identification of BSM21210. The goal of this study was to identify and characterize the putative MTTase involved in 17^2-methylthio-F_{430} biosynthesis (Figure 1.6). Earlier work in our laboratory identified a single potential MTTase, BSM21210, in a Black Sea mat ANME-1 archaeon that was known experimentally to produce methylthio-F_{430}.[29] This first metagenome was published in 2010, and in the years between that and our initial bioinformatics, few ANME-2 genomes were published. Comparative bioinformatics established that ANME-1 contain a MTTase homolog of the known MTTases, and that ANME-2, which does not produce F_{430}-2, does not. Therefore, there was a potential link between the MTTase and F_{430} methylthiolation to produce 17^2-methylthio-F_{430}.

Expression and purification of BSM21210 in E. coli *BL21(DE3) and BL21(DE3)-RIL.* After the identification of BSM21210 as the potential MTTase required for methylthio-F_{430} biosynthesis, we cloned the gene into pET15b and attempted to express and purify the protein from

E. coli. The protein was found to be completely insoluble in BL21(DE3), as well as in BL21(DE3)-RIL, and BL21(DE3) + pDB1818 (strain containing Fe-S cluster chaperones). The addition of iron and cysteine to the growth medium did not change this. We next attempted to modulate either or both expression conditions in *E. coli*(DE3)-RIL cells as well as the purification scheme.

All attempts to express BSM21210 in *E. coli*(DE3)-RIL cells were unsuccessful. This included to grow the cells at a low temperature (30°C, 20°C, and 18°C), a common strategy that slows down the protein expression and folding process, giving the protein more time to fold properly. We further attempted to induce at low concentration of IPTG (down to 25 µM) and induce the cells at a later growth stage (~1.2 OD) as opposed to mid-exponential. Also, it has been noted in the literature that different growth media can impact solubility of proteins. Thus, we tried, Dynamite, a nutrient-rich medium, as well as M9 Minimal medium, a medium less rich than LB, and growing at a slower rpm (~100 vs 200). We focused on these efforts, but we also tried to change some purification parameters, such as 300 mM NaCl instead of 500 mM KCl in our buffers, and using resin containing Co(II) instead of Ni(I). None of these attempts resulted in even a slightly soluble protein.

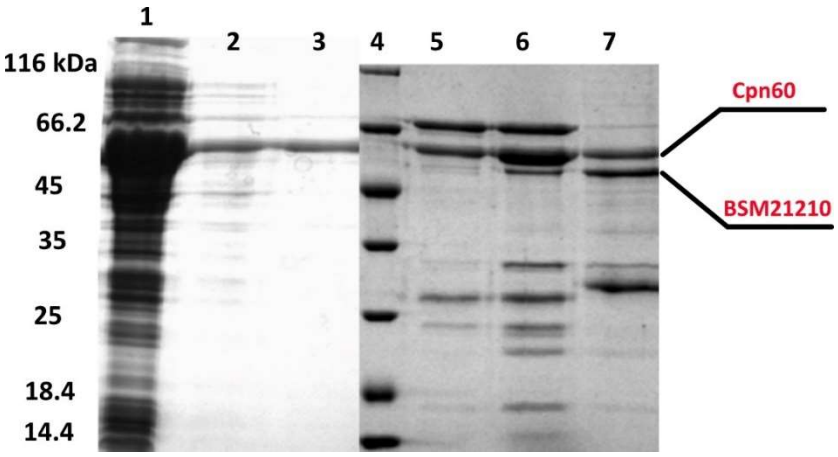

Figure 3.1. First purification of BSM21210 from Arctic Express cells. (Note: figure is combined from two gels). Lanes are marked 1-7. Lane 1: insoluble pellet, 2: lysis buffer wash, 3: wash with 1.5 M Urea, 4: protein ladder, 5: 5% B fraction, 6: 20% fraction, 7: 100% B fractions. Imidazole fractions were first concentrated to 500 µL.

After unsuccessfully expressing BSM21210 in a soluble form in *E. coli*(DE3-RIL), we tried to express the protein in *E. coli*(DE3-RIL) Arctic Express. In the initial

expression and purification, we found that a significant (relatively) amount of protein was found in the imidazole fractions (Figure 3.1). However, these fractions co-eluted with the constitutively-expressed Cpn60 chaperonin. We found that washing the resin with 2 M urea did get rid of a significant amount of this impurity, but we also could not replicate the amount of soluble BSM21210 that we obtained in the initial purification. However, it felt like this was a significant progress relative to past purifications, and we next tried to optimize the expression system. This included expressing in a range of temperatures and IPTG concentrations. However, none of these attempts were successful in either ridding ourselves of the Cpn60 impurity, which always purified in amounts at least equal to BSM21210 (determined by SDS-PAGE), or improving the amount of soluble BSM21210.

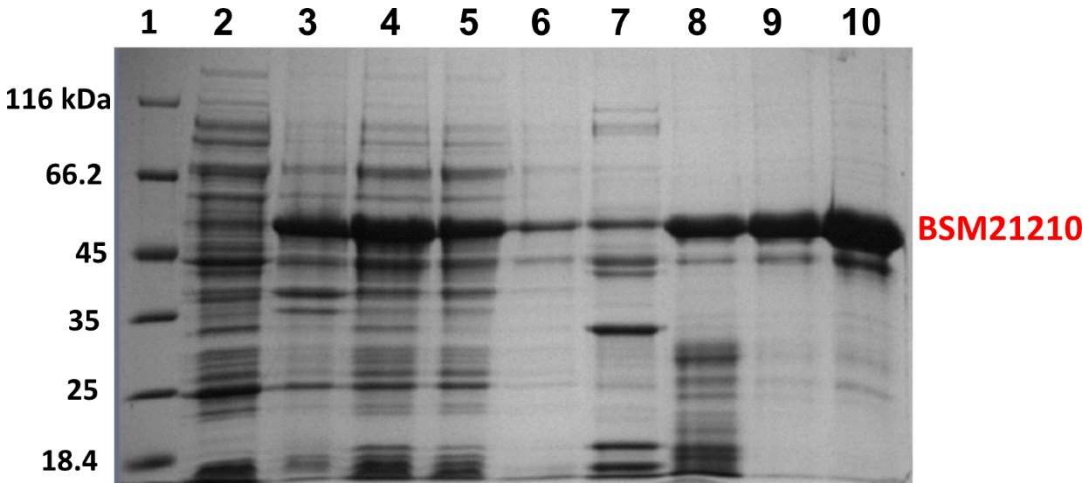

Figure 3.2. Gel image from purification of BSM21210 inclusion bodies. Lane 1: protein ladder, 2: lysis supernatant, 3: urea pellet, 4: urea lysate (this was applied to Ni resin), 5: flow through, 6: lysis buffer wash, 7: 10% imidazole fraction, 8: 30%, 9: 50%, 10: 100%. (imidazole fractions not concentrated from 6 mL)

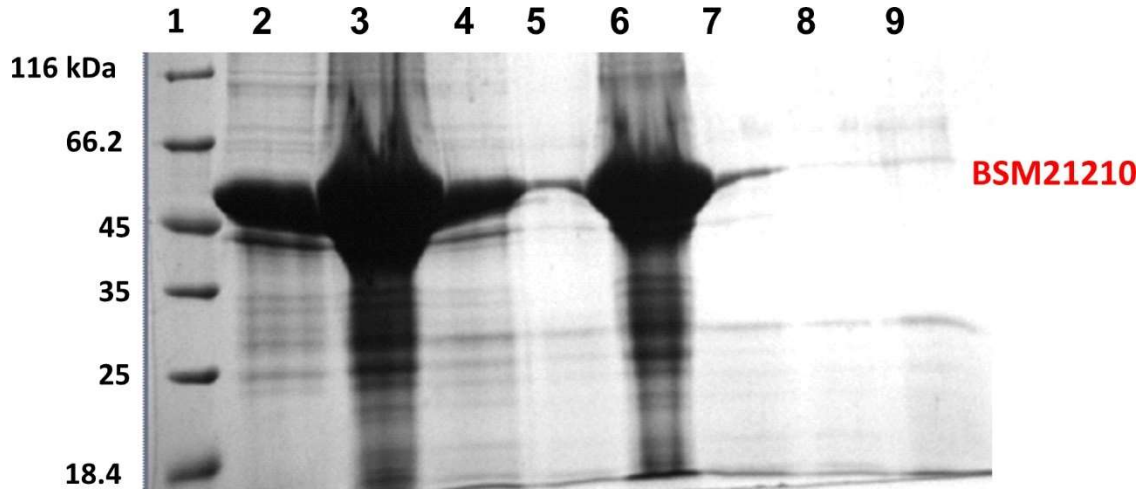

Figure 3.3. Gel image from refolding BSM21210 inclusion bodies. Lane 1: Protein ladder, 2: Sample taken from material precipitated from diluted imidazole fractions, 3 and 6: samples taken from material precipitated out during concentrating, lanes 4 and 5: samples taken from supernatants of concentrated samples, 7: sample taken after before salting concentrated solution, 8: sample taken after desalting, 9: sample taken after desalting and concentrated to ~1 mL.

After the above attempts failed, we next attempted to purify BSM21210 from the insoluble inclusion bodies, and re-fold the protein. This is a major strategy to obtain a soluble protein after other attempts are unsuccessful. However, while this resulted in a large amount of purified BSM21210 in urea, attempts to re-fold the protein in buffer were not successful (Figures 3.2 and 3.3). Precipitate formed after leaving the diluted imidazole fractions in DTT, sulfide, iron, and methionine, and after spinning down there remained some insoluble particulate matter in the supernatant. When concentrating this down ~100-fold, this built up considerably. Desalting got rid of this, but it was determined by SDS-PAGE that this fraction had little-to-no BSM21210 (Figure 3.3).

Transformation, expression, and purification of BSM21210 in M. maripaludis *and* M. acetivorans. These methanogens were also explored as a possible alternative to purifying BSM21210. Strains transformed as described were confirmed to have the correct plasmid by PCR. In both cases, no protein could be found in concentrated imidazole fractions (Figure 3.4). Thus, the protein was either not expressed or it was also insoluble when expressed in *M. maripaludis*. Transformed plasmids were checked to ensure that they had the correct gene sequence as well as the correct transcription and translation sequence features. Different expression conditions were not explored rigorously in either organism.

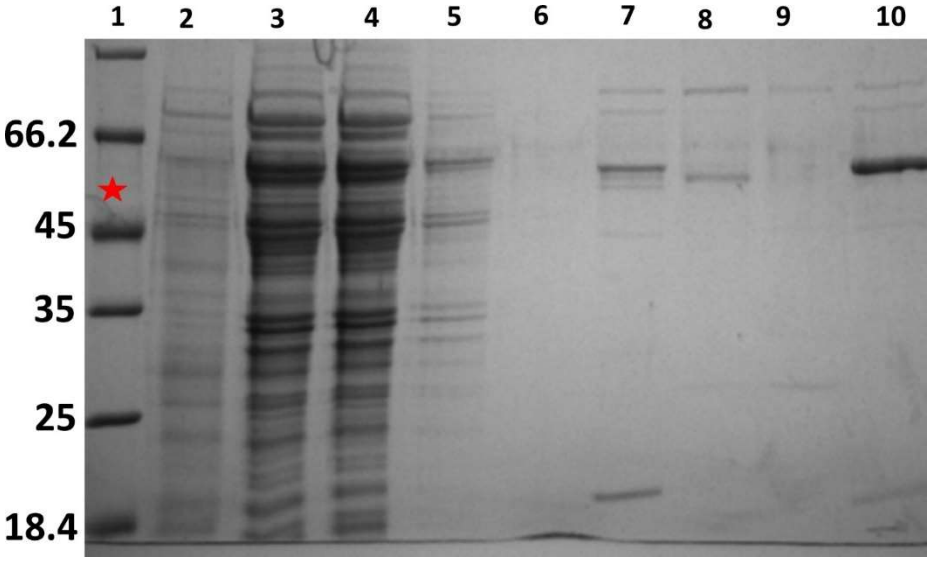

Figure 3.4. Gel image from attempted purification of BSM21210 in *M. maripaludis* S2. Lane 1: protein ladder, 2: insoluble pellet, 3: supernatant, 4: filtered lysate, 5: 5% imidazole fraction, 6: 10%, 7: 20%, 8: 30%, 9: 50%, 10: 100%. The red star denotes the expected mass for recombinant BSM21210 (50.4 kDa).

Initial identification of G60 MTTase. All attempts to obtain BSM21210 were not successful. We next decided to attempt to clone and purify a different MTTase homolog found in another ANME-1 strain. ANME-1 G60 is a thermophilic organism that is found in Guaymas basin sediment.[22] The ANME-1 in this sediment was previously determined to produce methylthio-F_{430}.[4] Bioinformatics identified PXF52554.1 as the only homolog of any radical SAM enzyme that performs sulfur insertion (E-value of 1.5 E-43, Table 1 below).

Protein	Hits	E-value
MiaB (*E. coli* K12)	PXF52554.1	1.55201 E-43
MtaB (*B. subtilis)*	PXF52554.1	6.65392 E-43
RimO (*E. coli* K12)	PXF52554.1	1.88307 E-38
BioB	None	N/A
LipA	None	N/A
LipS1 (TK2109 from T. kodakarensis)	None	N/A

Table 3.1. A bioinformatics analysis of the potential radical SAM sulfur insertion enzymes found in the ANME-1 G60 metagenome. Only one protein had significant homology to any of the enzymes, and this protein only had homology to the known methylthiotransferases.

Expression and purification of G60 MTTase in E. coli DE(3)-RIL. The G60 MTTase (PXF52554.1) was cloned into pET15b for subsequent expression in *E. coli*. It was initially found that G60 MTTase is not expressed in *E. coli*(DE3), but that it is expressed well in *E. coli*(DE3)-RIL. There was no discernable effect between induction at 100 µM and 1 mM IPTG, so we preceded with 100 µM

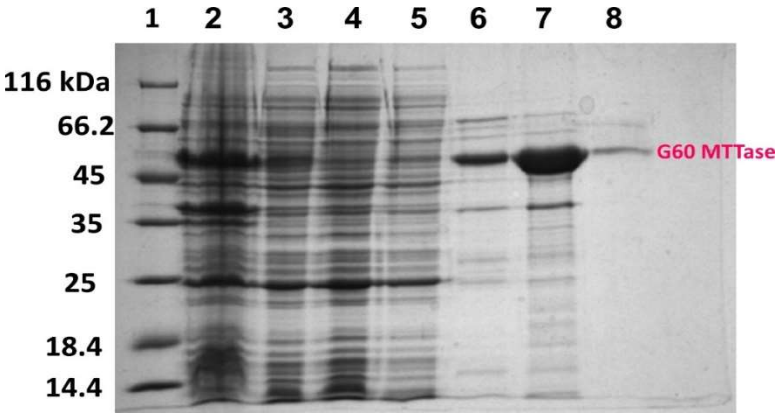

Figure 3.5. Results from an ANME-1 G60 MTTase purification. Lane 1: protein ladder, 2: cell pellet, 3: supernatant, 4: flow through 5: lysis buffer wash, 6: 10% elution buffer fraction, 7: 30% elution buffer fraction, 8: 100% elution buffer fraction. The elution buffer fractions are not concentrated (in 6 mL).

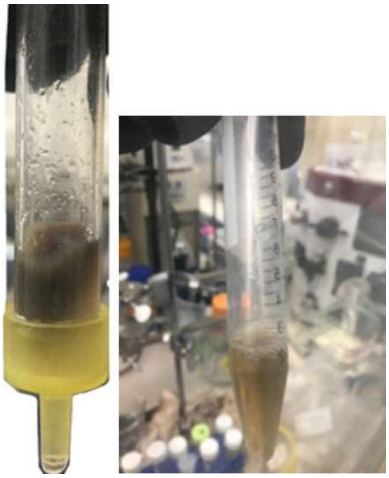

Figure 3.6. Pictures from an ANME-1 purification. Left: Ni-resin after application of protein sample turns brown. Right: concentrated protein in solution is also brown. This is an indication of good iron-sulfur incorporation in the protein as it is expressed in *E. coli*.

for subsequent expressions. An initial expression with 100 μM IPTG, ferric chloride, and cysteine, with growth at 37°C for four hours post-induction, as described in the Methods section resulted in significant protein expression in the soluble fraction (Figure 3.5). Further, the protein purifies with a very prominent brown color, a hallmark of iron-sulfur clusters (Figure 3.6).

Iron and sulfur determination of as-purified G60 MTTase. The $[4Fe\text{-}4S]^{2+}$ clusters present in radical SAM enzymes have a broad absorption spectrum with a shoulder at around 420 nm, and the absorption at this wavelength relative to absorption at 280 nm can be used to roughly estimate iron and sulfur incorporation. Dithionite reduces the iron-sulfur clusters to the 1+ redox state, and this can be further used to show that the [4Fe-4S] cluster is redox active. Therefore, as a starting point in characterizing iron and sulfur content of our as-purified protein, the UV-Vis spectrum was taken. As expected, a broad shoulder between 420-450 nm was detected (Figure 3.7, purple spectrum). This shoulder was abolished by the addition of dithionite (Figure 3.7, yellow spectrum).

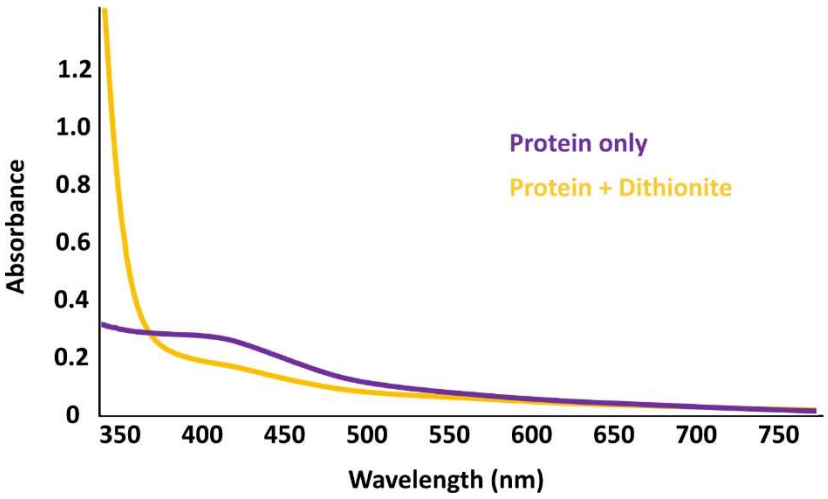

Figure 3.7. UV-Vis spectrum of G60 MTTase as-purified (purple), and the protein treated with dithionite (yellow).

The as-purified protein displayed significant iron-sulfur incorporation based off of the UV-Vis spectrum as well as the dark brown color of the purified protein. Next, we sought to more rigorously calculated iron-sulfur cluster incorporation by measuring the amount of iron and sulfide incorporated into the as-purified protein on a molar basis. We obtained some inconsistent results, and so we cannot report iron and sulfur incorporation values with confidence yet. The iron determination was more consistent and gave us ~6.1 mol iron mol^{-1} protein. The sulfide value is likely similar, but in our sulfide determinations we obtained values greater than 10 mol sulfide mol^{-1} protein. MTTases are known to have two [4Fe-4S] clusters; thus, 8 mol of both iron and sulfide are expected for full incorporation, and the as-purified enzyme does not have complete iron-sulfur cluster incorporation. In the future, it will be important to repeat these iron and sulfide quantitation experiments with reproducible results. This should include establishing a reconstitution procedure for full iron and sulfide incorporation to the expected 8 mol per mol protein. However, for the purpose of initially determining the substrate of this enzyme, we were satisfied with the iron and sulfide incorporation we obtained with the as-purified protein and did not pursue any reconstitution experiments.

Thermostability of G60 MTTase. Before carrying out assays with potential substrates, we checked to see the highest temperature at which the purified protein is stable. The thermostability assay demonstrated that after incubating the protein at 50°C, or any temperature below this, the protein was completely stable in solution (Figure 3.8). However, at 70°C, the protein displayed significant (~50%) precipitation. While this removed most contaminating proteins, and significant G60 MTTase remained, we decided to use a temperature of 50°C for our next assays. In the future, 60°C should be tested.

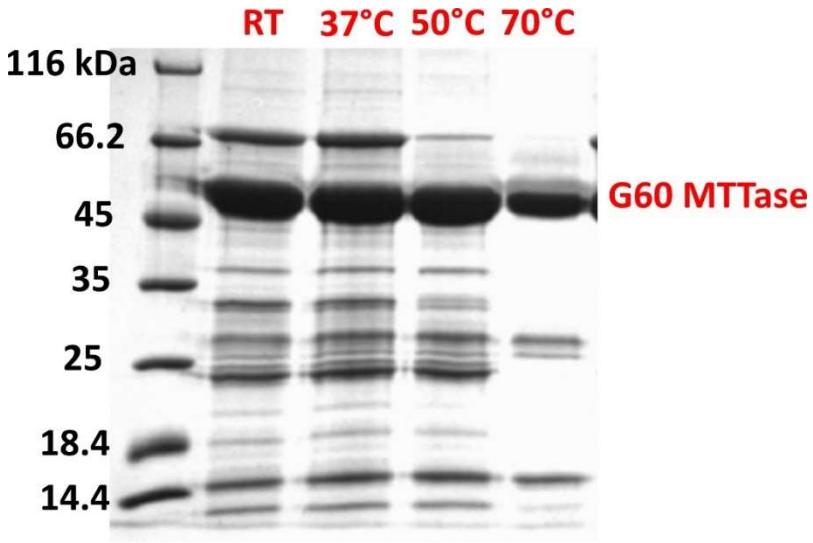

Figure 3.8. Thermostability assay with G60 MTTase. Lane 1: protein ladder, lane 2: sample incubated at root temperature, 3: sample incubated at 37°C, lane 4: sample incubated at 50°C, lane 5: sample incubated at 70°C.

EPR studies with G60 MTTase. EPR is a common technique when studying proteins with metal cofactors, since it gives an insight into the redox state of the metal cofactor in different conditions and stages of reactions. The [4Fe-4S] clusters of radical SAM enzymes typically exist in either the 2+ or 1+ redox states, but can also be oxidized to the 3+ redox state. The cluster can be reduced with a reducing agent to the 1+ redox state, then it is oxidized back to the 2+ state in the reductive cleavage of SAM (Figure 1.7). Since only the 1+ and 3+ redox states are EPR-active, and the 2+ state EPR-silent, it is possible to test *in vitro* if the enzyme can be reduced to the 1+ state with a strong reducing agent and if interactions with SAM can cause the cluster to be re-oxidized.

In our experiment, we analyzed three samples with EPR: protein only, protein with dithionite, and protein, dithionite and SAM. The protein only sample had an EPR signal (g = 2.03) associated with a fully oxidized 3+ cluster, or an incomplete $[3Fe\text{-}4S]^{1+}$ cluster (Figure 3.9, black spectrum). The addition of dithionite changed the signal to one that is characteristic of $[4Fe\text{-}4S]^{1+}$ clusters (Figure 3.9, yellow spectrum). The addition of SAM partially attenuates the 1+ signal (Figure 3.9, purple spectrum), showing that the iron-sulfur cluster reductively cleaves SAM to give an EPR-silent 2+ signal.

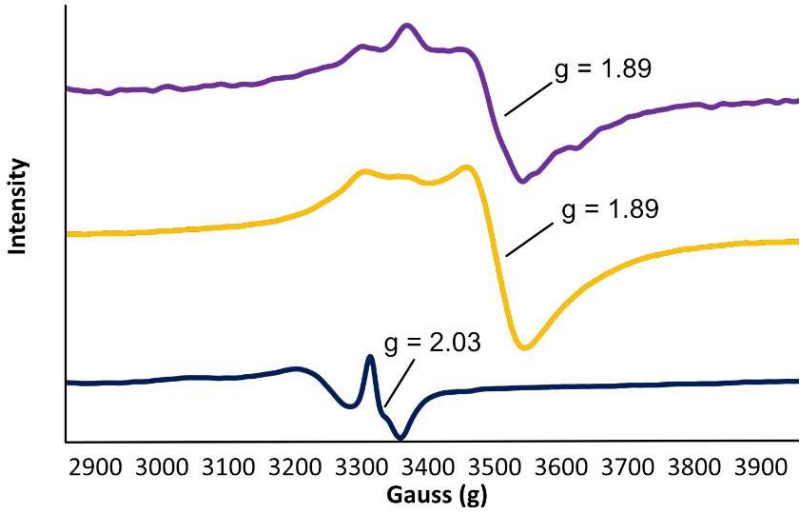

Figure 3.9. EPR data. Black: protein only sample, Gold: protein + dithionite, purple: protein + dithionite + SAM

In vitro assays with F_{430} extracts and G60 MTTase. The various reaction conditions described above that were carried out with cofactor F_{430} did not result in the production of methylthio-F_{430}, or any discernable variant of cofactor F_{430}. The only discernable difference between controls with and without F_{430} was that dithionite reduces F_{430}. While this will be an important consideration in future assays with F_{430}, reactions with other reducing agents that did not produce this effect similarly did not produce any product.

Since the reductive cleavage of SAM is the key step in radical SAM enzyme catalysis and is at least partially decoupled from product formation, we analyzed some of the reactions that did not produce any methylthio-F_{430} for evidence of reductive cleavage of SAM, which produces 5'-deoxyadenosine (Figure 1.7). Also, MTTases use SAM as the methyl donor, a reaction that produces SAH as a byproduct, and so we also analyzed for the production of this byproduct. We found that there was a very large increase in both SAM cleavage (13-fold greater) and SAH production (4.4-fold greater) in assays with protein compared to control assays without protein (Figure 3.10) . This was in spite of any reaction with our candidate substrate, F_{430}. This provided us with evidence that the reaction conditions were most likely not interfering with the ability of the enzyme to perform catalysis, and that cofactor F_{430} may not be a substrate for the enzyme.

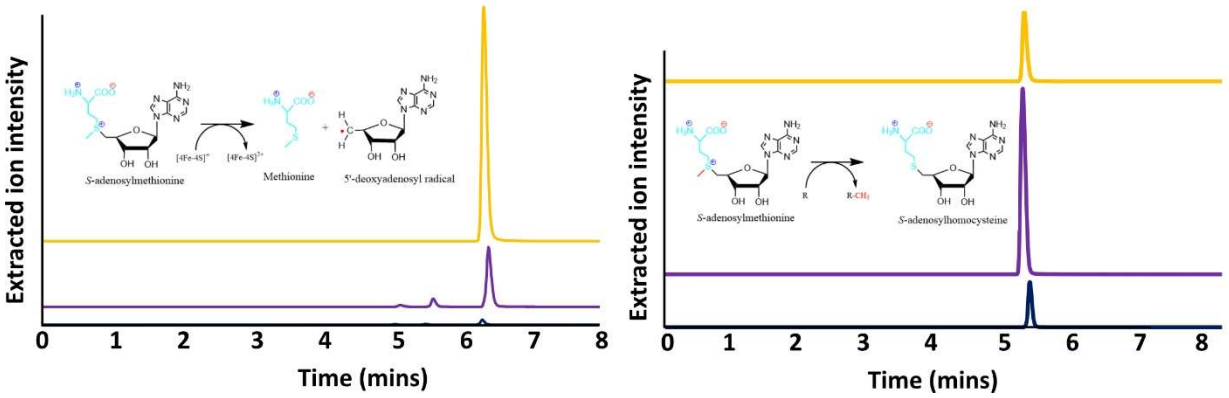

Figure 3.10. A: LC-MS chromatograms of SAM cleavage. In **black**: control assay (no protein), **purple**: 5'-deoxyadenosine standard, **orange**: assay with protein. **B:** LC-MS chromatograms of *S*-adenosylhomocysteine production. Colors are as before.

Cloning, transforming, and expressing pHCMC05-tRNA^{Lys} into BKK25430. Since we found that the G60 MTTase did not appear to catalyze the methylthiolation of F_{430}, we considered that the G60 MTTase was actually MtaB (Table 3.1), which catalyzes the methylthiolation of N^6-threonylcarbamoyladenosine (t^6A). As discussed, methanogens (and likely ANME) contain the methylthiolated derivative of this base, but do not contain the substrate nor product, i^6A and ms^2i^6A, respectively, of the other MTTase (MiaB) that acts upon tRNA. Further, the third known

methylthiotransferase, RimO, acts upon the bacterial-specific ribosomal protein subunit S12 and therefore is not present in archaea. Thus, we next moved on to attempt to determine if the MtaB substrate, t^6A, is the substrate for our protein.

B. subtilis is known to contain ms^2t^6A in its $tRNA^{Lys}$, therefore, we used this organism as a host for producing our substrate of interest, t^6A. *B. subtilis* 168 (wild-type) and *B. subtilis 168 yqeV::kan* (BKK25430) were obtained from the Bacillus Genetic Stock Center, as well as the pHCMC05 plasmid. BKK25430 contains the gene conferring kanamycin resistance substituting *yqeV*, the gene that encodes MtaB. The yqeV gene product from *B. subtilis* has been studied *in vitro*.[30] Thus, BKK25430 cannot produce ms^2t^6A, but does produce t^6A. We cloned the gene encoding $tRNA^{Lys}$ into the pHCMC05 plasmid (Figure 3.11) and transformed the construct into BKK25430 cells. The resulting transformant was named KB550. This strain overexpresses the $tRNA^{Lys}$ and cannot perform the methylthiolation reaction, thus resulting in the overproduction of our substrate of interest.

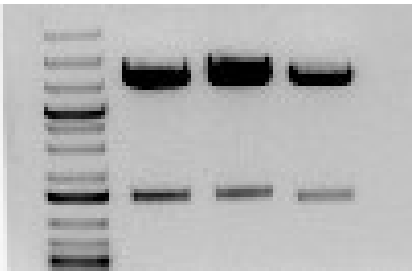

Figure 3.11. Successful cloning of $tRNA^{Lys}$ into pHCMC05 is shown. There is a slight increase in DNA length in cloned constructs (middle two lanes) compared to an empty vector (far right lane).

Transfer RNA extraction from B. subtilis *strains.* We adapted literature procedures for purifying tRNA from various, which resulted in consistently pure tRNA (Figure 3.12) as judged by the absence of any larger bands that would correspond to other nucleic acids on an agarose gel.[28] We next had to optimize both the enzymatic digestion and LC-MS analysis protocols. We had poor results with the LC-MS buffers reported in the literature (A: 250 mM ammonium acetate; B: 40% acetonitrile).[31] When we switched to buffers we have used for other LC-MS methods (0.1% formic acid, 100% methanol), we obtained chromatograms that

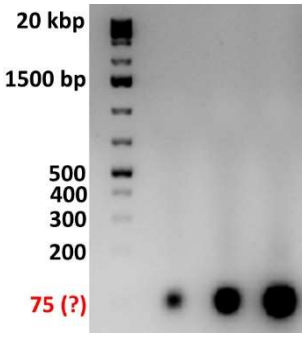

Figure 3.12. Agarose gel image of tRNA purified from B. subtilis. Far left: DNA ladder. From left to right, 1 µg RNA, 3 µg RNA, and 6 µg RNA

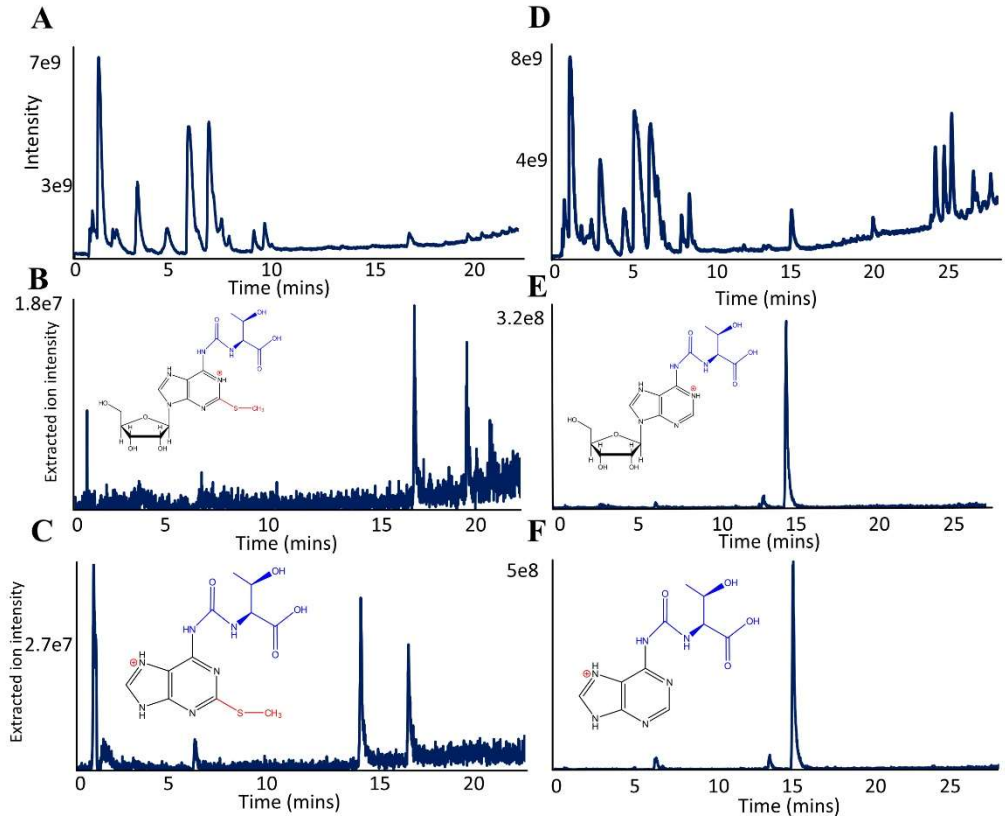

Figure 3.13. LC-MS data for tRNA purified from *B. subtilis* strains. **A**: Total ion chromatogram for *B. subtilis* 168 tRNA. **B**: XIC for ms^2t^6A molecular ion fragment (459 *m/z*), **C**: XIC for ms^2t^6A base fragment (327 *m/z*). **D**: Total ion chromatogram for KB550 tRNA. **E**: XIC for the molecular ion of t^6A (413 *m/z*), and **F**: XIC for base ion of t^6A (281 *m/z*)

we could then analyze. Enzymatic digestion of tRNAs yields the corresponding nucleosides, which are readily ionized. Both the molecular ion and base fragments are observed via LC-MS, with the latter losing its ribose sugar. Thus, by extracting for both the molecular ions and base forms for specific nucleosides and their elution times, we were able to determine the presence and absence of those bases. For instance, ms^2t^6A has a molecular ion of 459 *m/z* and a base of 327 *m/z*. When peaks for these two *m/z* values line up exactly, then that is good evidence that the modified base of interest is present. We were able to show in this manner that wild-type *B. subtilis* 168 produces ms^2t^6A, as expected (Figure 3.13 A-C, peak elutes at 17.5 min), and that purified KB550 tRNA does not since it lacks the gene encoding MtaB (Figure 3.13 D-F, peak for t^6A elutes at 15 min). Taken together, this work provided the methodology and LC-MS standards to measure ms^2t^6A production in an *in vitro* assay with the purified G60 MTTase

In vitro assays with tRNA and G60 MTTase. After failing to show methylthiolation activity with the purified G60 MTTase and cofactor F_{430}, and having success in tRNA purification and analysis, we were finally able to test the other likely substrate of our purified protein: tRNA that has only t^6A, and not ms^2t^6A (reaction scheme shown in Figure 3.14). In our assays with the G60 MTTase, dithionite, SAM, and purified KB550 tRNA, we identified ms^2t^6A (Figure 3.15, purple spectra). A control assay lacking the G60 MTTase did not contain ms^2t^6A, as expected (Figure 3.15, copper spectra). Interestingly, product formation was not observed when titanium (II) citrate was used instead of the dithionite as a

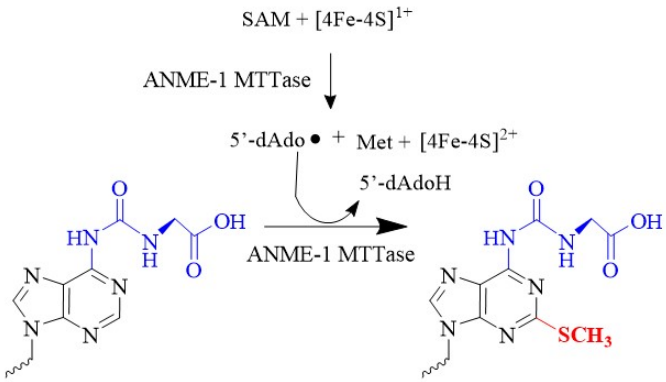

Figure 3.14. Reaction scheme for MTTase-catalyzed methylthiolation of threonylcarbamoyladenosine-36

reducing agent. Both of these are common reducing agents used to generate the $[4Fe\text{-}4S]^{1+}$ cluster in radical SAM enzymes, but apparently only dithionite is effective for this purpose in the case of the G60 MTTase. In summary, these data show that the G60 MTTase methylthiolates t^6A to produce ms^2t^6A, thus defining it as MtaB.

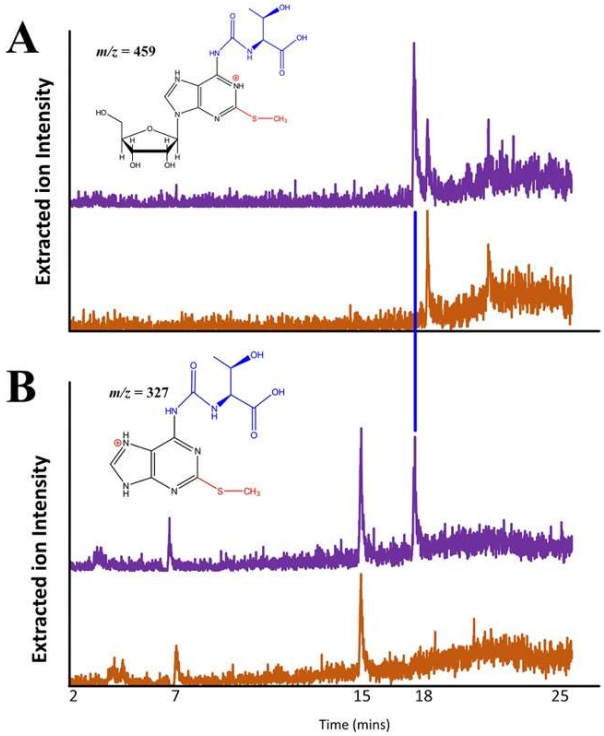

Figure 3.15. Extracted ion chromatograms for the molecular ion (A) and base fragment (B) of ms^2t^6A. In both cases, the control in shown in copper, and the reaction in purple. A blue line is drawn that connects with the peaks associated with ms^2t^6A.

Transfer RNA extraction from M. acetivorans cells. We were interested in analyzing the modified tRNAs produced by *M. acetivorans* primarily to determine what, if any, methylthiolated nucleosides this model methanogen related to ANME-1 produces. Further, the tRNA modification profile produced by *M. acetivorans* has not been described, despite the fact that this methanogen is one of the best-studied methanogens and it having one of the most sophisticated genetic systems of any archaeon. *M. acetivorans* contains the largest genome of any archaeon known, and it could

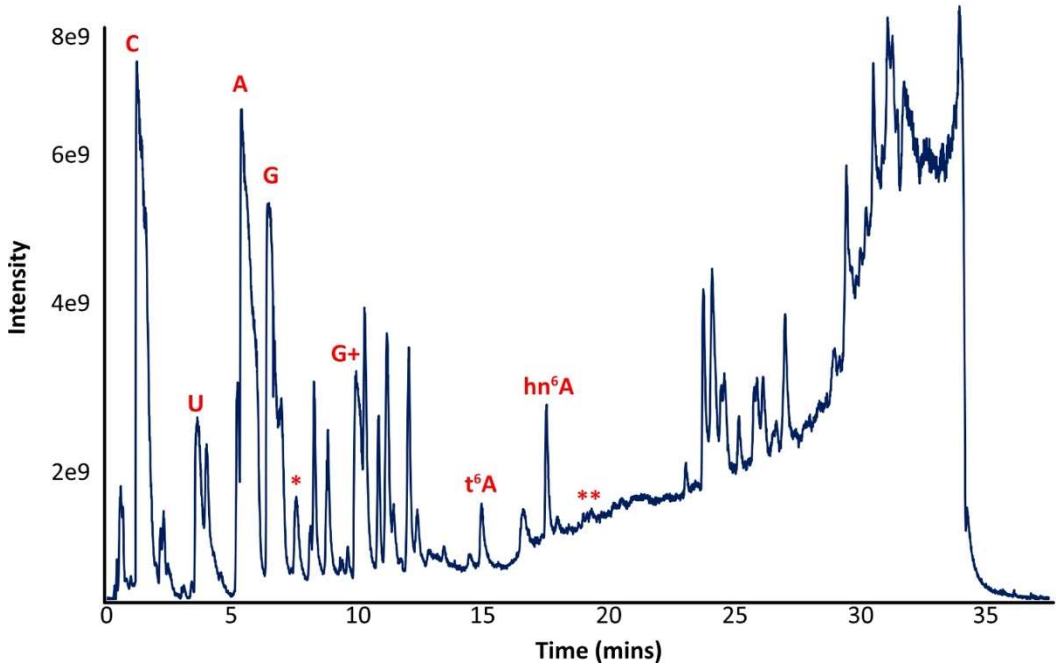

Figure 3.16. Total ion chromatogram obtained from purified tRNA from *M. acetivorans*. Some peaks are labeled in red directly above the peak. The standard bases (C, U, A, G) are labeled, as well as s^4U (*), archaeosine (G^+), t^6A, hn^6A, and ms^2hn^6A (**).

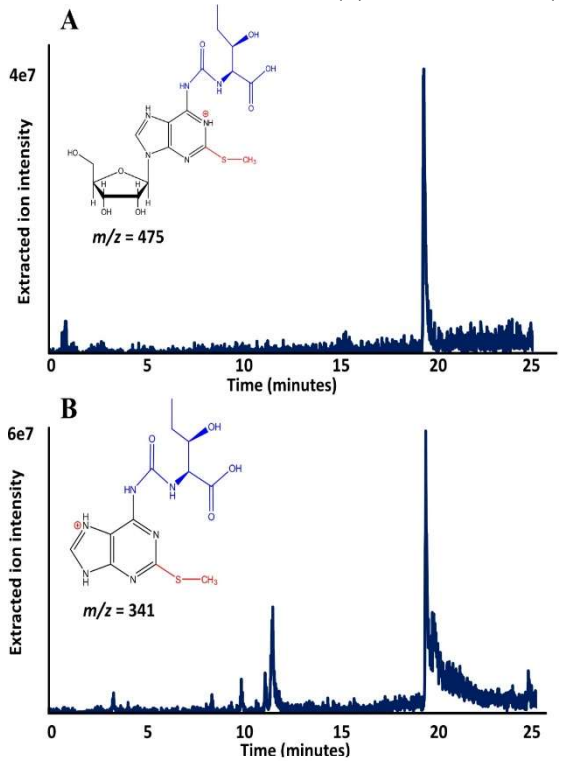

Figure 3.17. Extracted ion chromatograms for the molecular ion of ms^2hn^6A (**A**; *m/z* = 475) and its base (**B**; *m/z* = 341) from *M. acetivorans* tRNA

also have interesting and unknown tRNA modifications. In the literature, two methylthiolated nucleosides from methanogens are described: ms^2t^6A and ms^2hn^6A (Figure 1.8). Some, like *Methanocaldococcus jannaschii* have been described to have both, while others, like *Methanococcoides burtonii*, only one, in this case ms^2hn^6A.[28, 32] In the tRNA purified from *M. acetivorans*, we found evidence for the production of 4-thiouridine (s^4U) and ms^2hn^6A (Figures 3.16 and 3.17). The production of ms^2hn^6A and the lack of ms^2t^6A, as well as the presence of a genetic

system, makes *M. acetivorans* a good candidate to create an MTTase knockout to demonstrate the function of MTTases in methanogens. This knockout could additionally provide non-methylthiolated hn^6A for use in *in vitro* assays to determine whether the G60 MTTase can methylthiolate hn^6A as well as t^6A.

3.5 Concluding remarks

Here we describe the first characterization of an archaeal methylthiotransferase. The protein was readily expressed and purified from *E. coli*, and the protein as-purified contains significant iron-sulfur incorporation, as shown by its color, UV-Vis spectrum changes when treated with a reducing agent, EPR, SAM cleavage and SAH production. We proposed the enzyme may be involved in the biosynthesis of methylthio-F_{430} but this is most likely not the case, as shown by its lack of methylthiolation activity when incubated with F_{430} in various conditions. Instead, the protein was shown to be active in the methylthiolation of threonylcarbamoyladenosine, and therefore the protein is an MtaB ortholog. *M. acetivorans* was shown to likely not produce the MtaB reaction product, but likely contains 2-methylthio-hydroxynorvalylcarbamoyladenosine (ms^2hn^6A). Future work will elucidate the protein(s) involved in the methylthiolation of F_{430}, as well as determine if this MtaB homolog can react with hn^6A.

References

1. Knittel, K.; Boetius, A., Anaerobic oxidation of methane: progress with an unknown process. *Annu Rev Microbiol* **2009,** *63*, 311-334.

2. Timmers, P. H.; Welte, C. U.; Koehorst, J. J.; Plugge, C. M.; Jetten, M. S.; Stams, A. J., Reverse methanogenesis and respiration in methanotrophic archaea. *Archaea* **2017,** *2017*, 1654237.

3. Ellefson, W. L.; Wolfe, R. S., Role of component C in the methylreductase system of Methanobacterium. *J Biol Chem* **1980,** *255* (18), 8388-8389.

4. Mayr, S.; Latkoczy, C.; Kruger, M.; Gunther, D.; Shima, S.; Thauer, R. K.; Widdel, F.; Jaun, B., Structure of an F430 variant from archaea associated with anaerobic oxidation of methane. *J Am Chem Soc* **2008,** *130* (32), 10758-10767.

5. Shima, S.; Krueger, M.; Weinert, T.; Demmer, U.; Kahnt, J.; Thauer, R. K.; Ermler, U., Structure of a methyl-coenzyme M reductase from Black Sea mats that oxidize methane anaerobically. *Nature* **2011,** *481* (7379), 98-101.

6. Liu, Y. C.; Beer, L. L.; Whitman, W. B., Sulfur metabolism in archaea reveals novel processes. *Environmental Microbiology* **2012,** *14* (10), 2632-2644.

7. Cavuzic, M.; Liu, Y., Biosynthesis of Sulfur-Containing tRNA Modifications: A Comparison of Bacterial, Archaeal, and Eukaryotic Pathways. *Biomolecules* **2017,** *7* (1).

8. Vold, B. S.; Keith, D. E., Jr.; Buck, M.; McCloskey, J. A.; Pang, H., Lysine tRNAs from *Bacillus subtilis* 168: structural analysis. *Nucleic Acids Res* **1982,** *10* (10), 3125-3132.

9. Atta, M.; Arragain, S.; Fontecave, M.; Mulliez, E.; Hunt, J. F.; Luff, J. D.; Forouhar, F., The methylthiolation reaction mediated by the Radical-SAM enzymes. *Biochim Biophys Acta* **2012,** *1824* (11), 1223-1230.

10. Holmes, D. E.; Ueki, T.; Tang, H. Y.; Zhou, J.; Smith, J. A.; Chaput, G.; Lovley, D. R., A membrane-bound cytochrome enables *Methanosarcina acetivorans* to conserve energy from extracellular electron transfer. *Mbio* **2019,** *10* (4), e00789-19.

11. McGlynn, S. E.; Chadwick, G. L.; Kempes, C. P.; Orphan, V. J., Single cell activity reveals direct electron transfer in methanotrophic consortia. *Nature* **2015,** *526* (7574), 531-535.

12. Soo, V. W.; McAnulty, M. J.; Tripathi, A.; Zhu, F.; Zhang, L.; Hatzakis, E.; Smith, P. B.; Agrawal, S.; Nazem-Bokaee, H.; Gopalakrishnan, S.; Salis, H. M.; Ferry, J. G.; Maranas, C. D.; Patterson, A. D.; Wood, T. K., Reversing methanogenesis to capture methane for liquid biofuel precursors. *Microb Cell Fact* **2016,** *15*, 11.

13. Altschul, S. F.; Gish, W.; Miller, W.; Myers, E. W.; Lipman, D. J., Basic local alignment search tool. *J Mol Biol* **1990,** *215* (3), 403-410.

14. Valasatava, Y.; Rosato, A.; Banci, L.; Andreini, C., MetalPredator: a web server to predict iron-sulfur cluster binding proteomes. *Bioinformatics* **2016,** *32* (18), 2850-3852.

15. Zheng, K.; Ngo, P. D.; Owens, V. L.; Yang, X. P.; Mansoorabadi, S. O., The biosynthetic pathway of coenzyme F_{430} in methanogenic and methanotrophic archaea. *Science* **2016,** *354* (6310), 339-342.

16. Gibson, D. G.; Young, L.; Chuang, R. Y.; Venter, J. C.; Hutchison, C. A., 3rd; Smith, H. O., Enzymatic assembly of DNA molecules up to several hundred kilobases. *Nat Methods* **2009,** *6* (5), 343-345.

17. Ferrer, M.; Chernikova, T. N.; Yakimov, M. M.; Golyshin, P. N.; Timmis, K. N., Chaperonins govern growth of *Escherichia coli* at low temperatures. *Nat Biotechnol* **2003,** *21* (11), 1266-1267.

18. Nguyen, H. D.; Nguyen, Q. A.; Ferreira, R. C.; Ferreira, L. C.; Tran, L. T.; Schumann, W., Construction of plasmid-based expression vectors for *Bacillus subtilis* exhibiting full structural stability. *Plasmid* **2005,** *54* (3), 241-8.

19. Tumbula, D. L.; Makula, R. A.; Whitman, W. B., Transformation of *Methanococcus-maripaludis* and identification of a Psti-like restriction system. *Fems Microbiol Lett* **1994,** *121* (3), 309-314.

20. Guss, A. M.; Rother, M.; Zhang, J. K.; Kulkarni, G.; Metcalf, W. W., New methods for tightly regulated gene expression and highly efficient chromosomal integration of cloned genes for *Methanosarcina* species. *Archaea* **2008,** *2* (3), 193-203.

21. Metcalf, W. W.; Zhang, J. K.; Apolinario, E.; Sowers, K. R.; Wolfe, R. S., A genetic system for Archaea of the genus *Methanosarcina*: liposome-mediated transformation and construction of shuttle vectors. *Proc Natl Acad Sci U S A* **1997,** *94* (6), 2626-31.

22. Krukenberg, V.; Riedel, D.; Gruber-Vodicka, H. R.; Buttigieg, P. L.; Tegetmeyer, H. E.; Boetius, A.; Wegener, G., Gene expression and ultrastructure of meso- and thermophilic methanotrophic consortia. *Environ Microbiol* **2018,** *20* (5), 1651-1666.

23. Beinert, H., Micro methods for the quantitative determination of iron and copper in biological material. *Methods Enzymol* **1978,** *54*, 435-45.

24. Boccaletto, P.; Stefaniak, F.; Ray, A.; Cappannini, A.; Mukherjee, S.; Purta, E.; Kurkowska, M.; Shirvanizadeh, N.; Destefanis, E.; Groza, P.; Avsar, G.; Romitelli, A.; Pir, P.; Dassi, E.; Conticello, S. G.; Aguilo, F.; Bujnicki, J. M., MODOMICS: a database of RNA modification pathways. 2021 update. *Nucleic Acids Res* **2022,** *50* (D1), D231-D235.

25. Koo, B. M.; Kritikos, G.; Farelli, J. D.; Todor, H.; Tong, K.; Kimsey, H.; Wapinski, I.; Galardini, M.; Cabal, A.; Peters, J. M.; Hachmann, A. B.; Rudner, D. Z.; Allen, K. N.;

Typas, A.; Gross, C. A., Construction and Analysis of Two Genome-Scale Deletion Libraries for Bacillus subtilis. *Cell Syst* **2017,** *4* (3), 291-305 e7.

26. Team, i. Handbook How to handle *Bacillus subtilis.*

27. Avcilar-Kucukgoze, I.; Gamper, H.; Hou, Y. M.; Kashina, A., Purification and use of tRNA for enzymatic post-translational addition of amino acids to proteins. *STAR Protoc* **2020,** *1* (3), 100207.

28. Yu, N.; Jora, M.; Solivio, B.; Thakur, P.; Acevedo-Rocha, C. G.; Randau, L.; de Crecy-Lagard, V.; Addepalli, B.; Limbach, P. A., tRNA modification profiles and codon-decoding strategies in *Methanocaldococcus jannaschii*. *J Bacteriol* **2019,** *201* (9).

29. Meyerdierks, A.; Kube, M.; Kostadinov, I.; Teeling, H.; Glockner, F. O.; Reinhardt, R.; Amann, R., Metagenome and mRNA expression analyses of anaerobic methanotrophic archaea of the ANME-1 group. *Environ Microbiol* **2010,** *12* (2), 422-439.

30. Arragain, S.; Handelman, S. K.; Forouhar, F.; Wei, F. Y.; Tomizawa, K.; Hunt, J. F.; Douki, T.; Fontecave, M.; Mulliez, E.; Atta, M., Identification of eukaryotic and prokaryotic methylthiotransferase for biosynthesis of 2-methylthio-N6-threonylcarbamoyladenosine in tRNA. *J Biol Chem* **2010,** *285* (37), 28425-28433.

31. Pomerantz, S. C.; McCloskey, J. A., Analysis of RNA hydrolyzates by liquid chromatography-mass spectrometry. *Methods Enzymol* **1990,** *193*, 796-824.

32. Noon, K. R.; Guymon, R.; Crain, P. F.; McCloskey, J. A.; Thomm, M.; Lim, J.; Cavicchioli, R., Influence of temperature on tRNA modification in archaea: *Methanococcoides burtonii* (optimum growth temperature [Topt], 23 degrees C) and *Stetteria hydrogenophila* (Topt, 95 degrees C). *J Bacteriol* **2003,** *185* (18), 5483-5490.